Norwegian University of Life Sciences
Faculty of Science and Technology

Philosophiae Doctor (PhD)
Thesis 2018:3

Rapid spectroscopic methods for predicting water-holding capacity in meat

Hurtige spektroskopiske målemetoder for prediksjon av vannbindingsevne i kjøtt

Petter Vejle Andersen

Rapid spectroscopic methods for predicting water-holding capacity in meat

Hurtige spektroskopiske målemetoder for prediksjon av vannbindingsevne i kjøtt

Philosophiae Doctor (PhD) Thesis

Petter Vejle Andersen

Norwegian University of Life Sciences
Faculty of Science and Technology

Ås (2017)

Thesis number 2018:3
ISSN 1894-6402
ISBN 978-82-575-1493-8

Table of Contents

ACKNOWLEDGEMENTS I

ABSTRACT II

SAMMENDRAG III

ABBREVIATIONS IV

LIST OF PAPERS V

1. INTRODUCTION 1

2. WATER-HOLDING CAPACITY 1

2.1 Muscle structure 2

2.2 Protein structure 4

2.3 Distribution of water in muscle 4

2.4 Muscle to meat and drip formation 5

2.5 Measuring WHC 9

3. SPECTROSCOPY 11

3.1 Near-infrared spectroscopy 11

3.2 Infrared spectroscopy 13

3.3 Raman spectroscopy 16

3.4 Fluorescence spectroscopy 19

4. DATA ANALYSIS 19

4.1 Pre-processing of spectral data 19

4.2 Unsupervised data analysis 20

4.3 Supervised data analysis 20

4.4 Validation of models 20

5. MAIN RESULTS AND DISCUSSION 22

5.1 Summary of papers 22

5.2 Methodological aspects 23

5.3 Spectroscopic analysis of pH and proteolysis 26

5.4 Spectroscopic analysis of WHC 29

6. CONCLUSION AND FUTURE PROSPECTS 30

7. REFERENCES 31

Papers I – III

Acknowledgements

I would like to thank the Foundation for Research Levy on Agricultural products, the Agricultural Agreement Research Fund of Norway and the industry partners for funding this work.

My sincerest thanks and gratitude goes to my supervisors Eva Veiseth-Kent and Jens Petter Wold. Thank you for sharing your knowledge and insight, and for always being enthusiastic, including and encouraging through all our discussions. I earnestly thank my supervisor at the Norwegian University of Life Sciences, Achim Kohler, for guiding me on the right path at the very beginning of these studies and for keeping up over the past years.

I would also like to thank Tormod Næs, Nils Kristian Afseth, Ragni Ofstad, Ulrike Böcker, Eli Gjerlaug-Enger and Kristian Liland for their generous contributions to this thesis by discussing approaches to experiment design, answering more or less dumb questions and reviewing the papers. Special thanks goes to Bjørg Narum and Karen Wahlstrøm Sanden for their efforts during analyses for experiments and for the nice trips to abattoirs. Vibeke Høst and Lene Øverby are thanked for their terrific help regarding data collection.

All the other colleagues, PhD students and Nofima runners I have had the pleasure of encountering are thanked for contributing to the welcoming and inspiring working environment at Nofima.

I would especially like to thank my family. My significant other Cecilia, for always being there for me, for believing in me and encouraging me to push on. My daughter Vida, for just being awesome. My parents and brothers for supporting me all this time. Could not have done it without you all!

Ås, Norway, November 2017

Petter Vejle Andersen

Abstract

Water-holding capacity (WHC) is one of the most important quality traits in meat, and the main aim of this thesis was to examine the potential for rapid spectroscopic techniques to predict WHC in meat. A secondary aim was to examine the potential for spectroscopic techniques to analyze pH and proteolysis; mechanisms known to affect WHC of meat.

A model system consisting of isolated myofibrils from pork was used to investigate if spectroscopic techniques have potential to identify changes in samples with different pH or degree of protein degradation. Raman, Fourier transform-infrared (FT-IR), near-infrared (NIR) and fluorescence spectroscopy were used for analyses. Raman and FT-IR spectroscopy performed very well in the pH- and proteolysis experiment. Changes in protein secondary structure and protonation of carboxylic acid side chains of amino acids were affected by changes in pH. Degree of protein degradation affected spectral regions related to breakage of peptide bonds, such as CN-vibrations and carboxylic acid vibration caused by C-terminal formation, as well as changes in protein secondary structure. NIR performed poorly in the pH experiment, but performed reasonably well for dried samples in the proteolysis experiment, attributing this to an increased ability to form protein gels at low degrees of protein degradation. Fluorescence spectroscopy performed worse in the proteolysis experiment than in the pH experiment, attributing the performance in the pH experiment to a pH-related shift caused by changes in the microenvironment of tryptophan.

A study analyzing 122 samples from *longissimus lumborum* of *Norwegian landrace* boars was conducted to investigate if spectroscopic techniques have the potential to predict WHC and estimate ultimate pH in pork. WHC was measured as EZ-DripLoss and drip loss formed during eight days of vacuum storage. Assessment of results from partial least squares regression (PLSR) analyses from spectroscopy and reference measurements showed that Raman spectroscopy performed the best, followed by NIR and at last, fluorescence. PLSR models from Raman spectroscopy gave coefficient of correlation from cross validation (R^2_{cv}) of 0.51, 0.41 and 0.49 and root mean square error of cross validation (RMSECV) of 1.2, 0.82 and 0.06 for EZ-DripLoss, vacuum drip loss and pH, respectively. In comparison, NIR yielded PLSR models with R^2_{cv} of 0.27, 0.16 and 0.29 and RMSECV of 1.5, 0.97 and 0.07 for EZ-DripLoss, vacuum drip loss and pH, respectively. Regarding pH in meat, changes in Raman spectra related to protein secondary structure were similar in the model system and in meat. Changes in carboxylic acid protonation were not detected in meat, but signals from molecules related to metabolism were identified.

In conclusion, this highly encourages more research using Raman spectroscopy for analysis of meat quality.

Sammendrag

Vannbindingsevne (VBE) er en av de viktigste kvalitetsegenskapene i kjøtt, og hovedmålet med denne avhandlingen var å undersøke potensialet for bruk av hurtige spektroskopiske metoder til prediksjon av VBE i kjøtt. Et sekundært mål var å undersøke potensialet for spektroskopiske metoder til analyse av pH og proteinnedbryting (proteolyse); mekanismer som er kjent å kunne påvirke VBE.

Et modellsystem bestående av isolerte myofibriller fra svinekjøtt ble brukt til å undersøke om spektroskopiske teknikker kan identifisere endringer i prøver som følge av pH-forandringer eller ulik grad av proteinnedbrytning. Raman-, Fourier transform-infrarød- (FT-IR), nær-infrarød- (NIR) og fluorescensspektroskopi ble brukt i analysene. Raman- og FT-IR-spektroskopi viste gode evner til å analysere prøvene fra pH- og proteolyseforsøkene. Endringer i proteinenes sekundærstruktur og protonering av karboksylsyregruppen i sidekjedene til aminosyrer ble påvirket av endring i pH. Grad av proteinnedbrytning påvirket områder i spektrene knyttet til brudd av peptidbånd, som CN-vibrasjoner og karboksylsyrevibrasjoner forårsaket av dannelsen av nye C-terminaler, i tillegg til endringer i proteinenes sekundærstruktur. NIR viste begrenset evne til å identifisere endringer som følge av pH-forandring, men viste rimelig god evne til å identifisere tørkede prøver med ulik grad av proteinnedbrytning, som ble tilskrevet spektrale områder relatert til proteinenes evne til å danne gel. Fluorescens viste bedre evne til å beskrive prøver fra pH-forsøket enn fra proteolyseforsøket, hvor dette ble tilskrevet et skift i spektrene forårsaket av endring i mikromiljøet rundt aminosyren tryptofan.

For å undersøke potensialet spektroskopiske metoder har for prediksjon av VBE og estimering av slutt-pH, ble en studie gjennomført hvor 122 prøver fra *longissimus lumborum* fra *Norske landsvin* råner analysert. VBE ble målt som EZ-DripLoss og som væskeslipp i vakuumposer etter åtte dagers lagring. Vurdering av resultater fra partial least squares regression (PLSR) av spektroskopi og referanseanalyser viste at Raman ga best resultat, etterfulgt av NIR, med fluorescens til slutt. PLSR-modellen fra Raman ga en korrelasjonskoeffisient fra kryssvalidering (R^2_{cv}) på 0.51, 0.41 og 0.49 og root mean square error of cross validation (RMSECV) på 1.2, 0.82 og 0.06 for henholdsvis EZ-DripLoss, vakuumdrypptap og pH. Til sammenligning ga NIR PLSR-modeller med R^2_{cv} på 0.27, 0.16 og 0.29, og RMSECV på 1.5, 0.97 og 0.07 for henholdsvis EZ-DripLoss, vakuumdrypptap and pH. Endringer i Ramanspektrene som følge av forskjeller i pH var like for protein sekundærstruktur i modellsystemet og i kjøtt. Spektroskopiske endringer i karboksylsyreprotonering ble ikke oppdaget i kjøtt, men endringer knyttet til metabolske molekyler ble avdekket.

Resultatene fra denne avhandlingen viser at videre forskning knyttet til bruken av Ramanspektroskopi for analyse av kjøttkvalitet bør prioriteres.

Abbreviations

ATR	Attenuated total reflection
DFD	Dark, firm and dry
FT-IR	Fourier transform-infrared
IMF	Intramuscular fat
IR	Infrared
MHC	Myosin heavy chain
NIR	Near-infrared
NMR	Nuclear magnetic resonance
PCA	Principal component analysis
PLSR	Partial least squares regression
PSE	Pale, soft and exudative
R	Correlation coefficient
RMSECV	Root mean square error of cross validation
RMSEP	Root mean square error of prediction
SEP	Standard error of prediction
WHC	Water-holding capacity

List of papers

I. Andersen, P. V., Veiseth-Kent, E., & Wold, J. P. (2017). Analyzing pH-induced changes in a myofibril model system with vibrational and fluorescence spectroscopy. Meat Sci, 125, 1-9. doi: 10.1016/j.meatsci.2016.11.005

II. Andersen, P. V., Wold, J. P., Veiseth-Kent, E. Analyzing μ-Calpain induced proteolysis in a myofibril model system with vibrational and fluorescence spectroscopy. (Submitted for publication in *Meat Science*)

III. Andersen, P. V., Wold, J. P., Gjerlaug-Enger, E., Veiseth-Kent, E. Predicting post-mortem meat quality of porcine longissimus lumborum using Raman, Near Infrared and Fluorescence spectroscopy (Manuscript prepared for submission to Meat Science)

1. Introduction

Consumption of meat has been an important part of the human diet for ages, and it still is today, but there is an increasing focus on decreasing the daily consumption of meat because of environmental and ethical considerations related to livestock production. Nevertheless, as we keep consuming meat it is essential that the meat we eat is of a high quality, to avoid wasting food and to preserve the nutrients in the meat. Ultimately, there are many factors that affect meat quality, such as pre-slaughter handling (Vermeulen et al., 2015), stunning (Channon, Payne, & Warner, 2000) and chilling of carcasses (Rybarczyk, Karamucki, Pietruszka, Rybak, & Matysiak, 2015), and all the mechanisms involved are not completely understood. One of the most important characteristics for pork quality is water-holding capacity (WHC), which can be defined as "the ability of meat to retain both inherent water and added water" (Cheng & Sun, 2008), affecting both technological and economic aspects of meat production. Current methods for measuring WHC is based on passive (gravimetric) or forced measurements (centrifugation or filter paper press), all of which are time consuming and invasive, making them unsuitable for process control in meat production. Conversely, spectroscopic techniques, such as near infrared (NIR), Raman, Infrared (IR) and fluorescence spectroscopy, are fast and non-invasive candidate techniques for analyzing post-mortem meat quality in the meat processing plant.

The main objectives of this work was to investigate the possibility for rapid spectroscopic measurements of mechanisms affecting WHC, primarily pH and proteolysis, as well as rapid measurements of actual WHC of fresh pork. Two approaches were used to study these issues:

1. A model system using myofibrils isolated from pig muscle was used to study the effects of different pH and degree of proteolysis on spectroscopic outputs.
2. Meat quality and spectroscopic measurements of fresh pork.

2. Water-holding capacity

Water-holding capacity is recognized as one of the most important quality characteristics of meat, affecting diverse meat attributes such as overall yield from a carcass, nutritional value (Savage, Warriss, & Jolley, 1990), shelf life (Blixt & Borch, 2002), processing properties (Torley, D'Arcy, & Trout, 2000) and sensory attributes (e.g. juiciness) (Hughes, Oiseth, Purslow, & Warner, 2014). The ability of meat to retain water is obviously important for the direct relationship with amount of sellable product from slaughter to meat processors or consumers. Drip formed before meat is processed results in a net loss of value to the abattoir because they have less product to sell to processors or they have less raw material to use in their own products. It has been estimated that as much as 50% of all produced pork has unacceptable high drip loss caused by low WHC (Huff-

Lonergan & Lonergan, 2005). Drip from pork can exceed 15% of initial muscle weight (Purslow et al., 2008), and this can influence consumer satisfaction negatively and increase waste, as products remain unsold because of perceived quality defects. Since the prevalence of high drip loss meat is high and the overall quality of this meat is inferior to normal meat, there have been some efforts to make use of this pork in processed products, such as sausages and hams, giving an acceptable quality when the mix contains 50% high drip meat and 50% normal meat (Kuo & Chu, 2003; Motzer, Carpenter, Reynolds, & Lyon, 1998; Schilling, Mink, Gochenour, Marriott, & Alvarado, 2003). To understand the process of drip formation, it is important to understand the physiology of muscle structure and what happens to muscles when they transform into meat post-mortem.

2.1 Muscle structure

Skeletal muscle tissue is primarily made up of muscle fibers and connective tissue (Fig. 1), organized in a systematic and similar manner for all skeletal muscles. Enclosing the entirety of the muscle is an outer layer of connective tissue named epimysium, which also anchors the muscle to the bones. Inside, there are several smaller compartments, named fasciculi, containing a large number of individual muscle fibers. The fasciculi is covered by a connective tissue named perimysium, and the individual muscle fibers by endomysium. A membrane, the sarcolemma, covers the individual muscle fibers and is the barrier between individual muscle fibers and their surroundings, responsible for transport of water and other substances in and out of the muscle fiber (OpenStax, 2013).

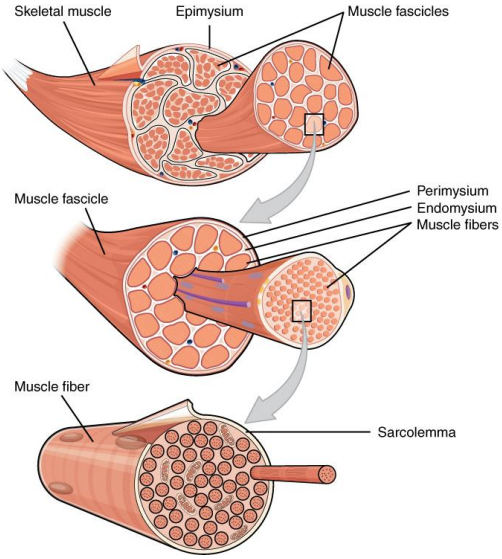

***Figure 1**. Overview of skeletal muscle organization. (OpenStax, 2013)*

Muscle fibers themselves are long, cylindrical and multi-nucleated cells containing myofibrils, which are responsible for muscle contraction (Fig. 2). The cytoplasm of a muscle fiber is called sarcoplasm, and this is where the muscle cells powerhouse, the mitochondria resides. The mitochondria supplies the myofibrils with the energy needed to contract by producing ATP via respiration. Another important organelle for controlling contraction is the sarcoplasmic reticulum;

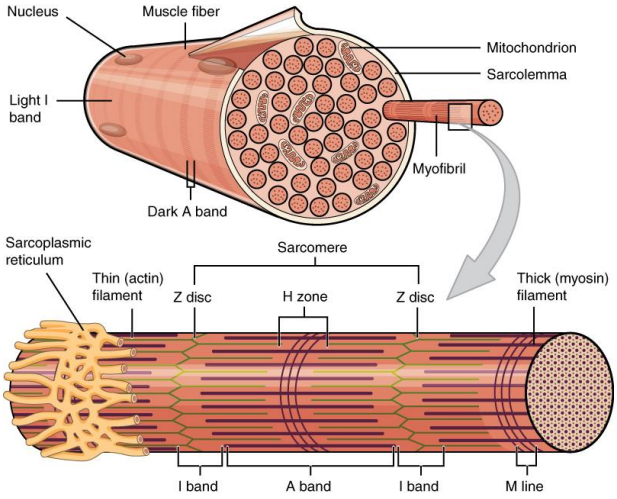

***Figure 2**. Overview of skeletal muscle fiber structure. (OpenStax, 2013)*

it covers the myofibril in a pipe-like system, and is used for controlling the Ca^{2+} concentration needed for contraction. The main components of myofibrils are the proteins myosin (thick filament) and actin (thin filament), which have a highly organized structure of alternating repeating units, accounting for approximately 60% (w/w) of proteins in muscle. The remaining bulk of proteins are water-soluble sarcoplasmic proteins (approx. 20% w/w) and water-insoluble stroma proteins (approx. 10% w/w) (OpenStax, 2013).

The interaction between myosin and actin filaments is what in fact causes skeletal muscles to contract (Fig. 3). Simply explained, a nerve impulse causes an opening of channels in the sarcoplasmic reticulum initiating an influx of Ca^{2+} into the cell, enabling the myosin head to link to the actin filament. The myosin head moves such that the entire sarcomere shortens, this happens across the entire myofibril as the muscle contracts and shortens. This process requires energy in the form of ATP to both move the myosin heads and to loosen the myosin head for a new stroke or relaxation of the myofibril, and it needs sufficient concentrations of Ca^{2+} for successful linkage of myosin and actin. An ATP-requiring pump transports Ca^{2+} back into the sarcoplasmic reticulum after the nerve signal ends (OpenStax, 2013).

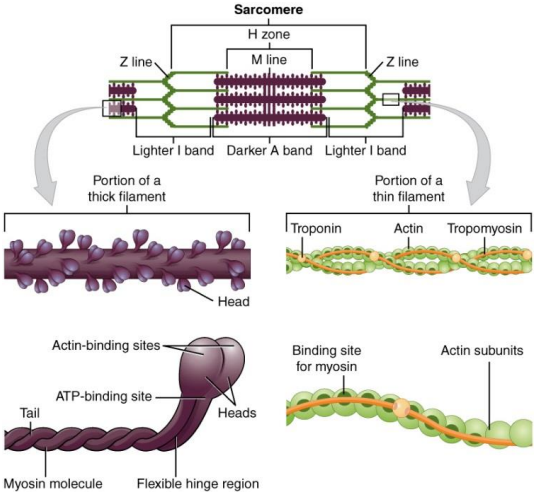

***Figure 3**. Overview of sarcomere structure. (OpenStax, 2013)*

2.2 Protein structure

Protein structure is important for the functional properties of proteins and the structure is prone to modifications following changes in the cellular environment, e.g. changes in pH and temperature. Protein structure is divided in four levels, primary, secondary, tertiary and quaternary structures. Primary structure refers to the order of amino acids in a protein, secondary structure refers to the arrangement of amino acids in α-helices and β-sheets (parallel or antiparallel), tertiary structure refers to the three dimensional arrangement of α-helices and β-sheets in one peptide, while quaternary structure refers to the assembly of two or more peptide strands in one functional unit (Fig. 4) (Mathews, Van Holde, & Ahern, 2000). To form the tertiary structure additional structural elements are needed, such as turns in the peptide chain and irregularly structured regions (sometimes referred to as random coil structure), as seen in the regions between α-helices and β-sheets in figure 4. Protein structure is one of the features spectroscopy can provide details about, especially secondary structure, as detailed in later chapters.

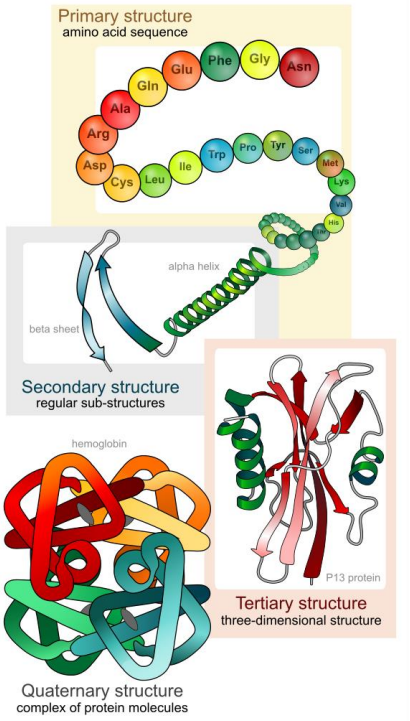

Figure 4. Overview of main protein structure levels.

2.3 Distribution of water in muscle

Muscle contains approximately 75% water, 20% protein, 5% fat, 1% carbohydrates and 1% vitamins and minerals. About 85% of the water in muscles is located inside the myofibrils (intra-myofibrillar water), while the remaining 15% is in extra-myofibrillar spaces and is found as inter-myofibrillar, inter-fascicular and extra-fascicular water. This water can be categorized in three different fractions: 1) protein-associated water, 2) immobilized water and 3) free water (Pearce, Rosenvold, Andersen, & Hopkins, 2011). 1) Protein associated water: water is a dipolar molecule, which makes it possible to bind tightly to charged proteins, making the link between water and proteins robust, so that the water does not move to other compartments even when external forces are applied. This fraction accounts for less than 10% of the total water in muscle. 2) Immobilized water is found within the thick filaments and between thick and thin filaments within the myofibril, and is bound

by steric effects between the filaments or by hydrogen bonding to proteins or other macromolecules. Immobilized water makes up the bulk of water in muscle, and accounts for approximately 85% of water in muscle. This water can be mobilized during conversion from muscle to meat because of changes in muscle cell structure and pH, and is thought to be the major contributor to reduced WHC and drip formation in meat (Huff-Lonergan & Lonergan, 2005). 3) Free water is held in place by weak surface forces within the sarcoplasmic area, and this fraction can flow from the tissue unimpeded. Free water accounts for approximately 5% of water in muscle.

2.4 Muscle to meat and drip formation

To understand how drip is formed and what mechanisms that are known to impact drip, it is crucial to examine the ante-mortem and post-mortem processes relevant for WHC taking place in the slaughterhouse and when muscle is converted to meat. Many factors are known to affect WHC, e.g. genetics, feeding, pre-slaughter treatment, stunning and slaughter procedures (Rosenvold & Andersen, 2003), but only properties of post-mortem meat will be considered in this chapter.

2.4.1 Muscle pH post-mortem

When the blood is removed and the animal is dead, blood circulatory system failure is imminent, which means that the cells in the body will not be supplied with oxygen. This has major implications for muscle tissue because when oxygen diminishes, the cells convert to anaerobic respiration, which produces lactic acid and results in a pH drop in the muscles from about 7.1 to 5.5 within the first 24 hours post-mortem. The accumulation of lactic acid makes proteins liable to denature and decreases their ability to withhold water, an effect which is exaggerated when the temperature is high post-mortem (Offer, 1991). The drop in pH also causes the main proteins in meat to approach their isoelectric point (myosin isoelectric point = 5.4), resulting in a laterally tighter packed protein matrix because the protein net charge approaches zero, thus expelling water from the protein network (Huff-Lonergan & Lonergan, 2005). Amount of available energy at time of death, both in the blood stream and as stored glycogen, influences pH development and ultimate pH (pH_u).

There are two common causes of deviating post-mortem energy reservoirs, long-term exhaustion and short-term stress, as noted in the previous part. Long-term exhaustion results in a high pH_u because there is not enough glycogen left in the animal to maintain anaerobic respiration, and this is the cause of undesirable meat known as dark, firm and dry (DFD) meat (Bendall, 1973). Short-term exhaustion leads to elevated blood glucose levels, higher concentration of lactic acid in muscles at time of slaughter and higher body temperature, which leads to rapid pH-decline and increased protein denaturation, often causing inferior meat quality known as pale, soft and exudative (PSE) meat (Briskey, 1964). Warner, Kauffman, and Greaser (1997) defined DFD as meat

having $pH_u \geq 6.0$, drip < 5% and L* < 42, while PSE was defined as having $pH_u < 6.0$, drip > 5% and L* > 50, where higher L* values corresponds to paler meat (measured with a chroma meter) and drip was measured by the bag method (Honikel, 1998). Desired meat quality was defined as having $pH_u < 6.0$, drip < 5% and 42 < L* < 50, and this quality is usually named reddish-pink, firm and non-exudative meat (Warner et al., 1997). The prevalence of PSE is generally higher than DFD in pig meat, evidenced by two European studies where prevalence of PSE was from 25% to 30% and DFD was from 0.5% to 10% (O'Neill, Lynch, Troy, Buckley, & Kerry, 2003; Santos, Roseiro, Goncalves, & Melo, 1994).

The effect of pH on drip formation is more nuanced than the categorization of PSE and DFD meat, and it is still in general established that higher pH gives less drip loss. This was documented by Warriss and Brown (1987) when they examined the relationship between pH at 45 min post-mortem (pH_{45}) and pH_u and drip loss in over 700 pork loins, shown in figure 5. A study by Gardner, Huff Lonergan, and Lonergan (2005) confirmed this relationship, and found that the correlation between pH and drip loss was even stronger when pH was measured at 4h or 6h post-mortem, giving correlations as high as −0.60 for drip and pH at 4h and 6h compared to −0.45 for pH_u. Taken together, this indicates that there might be an optimal time post-mortem to measure pH, but that the overall relationship between pH and drip formation is time independent.

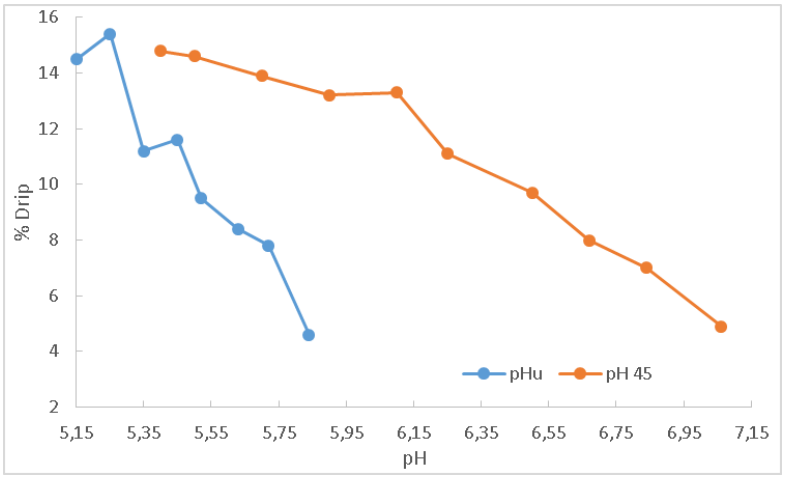

Figure 5. *Relationship between pH and drip loss in pork loins. Adapted from Warriss and Brown (1987).*

It should be mentioned that animals carrying certain versions of the Halothane or Rendement Napole gene are predisposed to produce PSE meat, but the genetics of pigs is beyond the scope of this thesis, and readers interested in genetic aspects of pig production are referred to publications by Hamilton, Ellis, Miller, McKeith, and Parrett (2000) and Salas and Mingala (2017).

2.4.2 Rigor mortis

Another major event in the early stages post-mortem is the onset of rigor mortis, a process in which the muscles become inextensible and stiff. Rigor starts when muscle ATP diminishes and actin and myosin forms rigid chains of actomyosin, which is facilitated by the influx of calcium ions from leakages in sarcoplasmic reticulum. The rigor state is maintained by the inability of the cell to break the linkage between actin and myosin because of lack of ATP. This leads to longitudinal shrinkage of sarcomeres and in the interplay with lateral shrinkage caused by pH-decline, this makes a milieu within the myofibril advantageous for repulsion of water (Pearce et al., 2011). Shortening is manifested across the entire myofibril and this makes the entire muscle fiber shorten in the same way, when this happens, gaps for water migration are formed between muscle fibers resulting in water migrating to the perimysial and endomysial spaces, and finally the water can escape the muscle as drip (Offer & Cousins, 1992).

2.4.3 Proteolysis

Proteolysis is defined as the breakdown of proteins into smaller polypeptides or amino acids, which involves breakage of CN bonds in the protein backbone, thus creating new N- and C-terminals and disruption of protein structure. Post-mortem proteolysis by the Calpain-system is known to play a key role in tenderization through the weakening of structural integrity of the meat (Huff Lonergan, Zhang, & Lonergan, 2010; Koohmaraie, 1992). The link between proteolysis and WHC is more complex, but it involves the same proteolytic system as the one responsible for meat tenderization. The Calpain-system consists of three major players; the Ca^{2+}-requiring cysteine proteases μ-Calpain and m-Calpain, and the calpain-specific inhibitor Calpastatin (Goll, Thompson, Li, Wei, & Cong, 2003). The prefix before the calpains refers to the amount of Ca^{2+} needed for activation, where μ-Calpain and m-Calpain needs 3-50 μM and 400-800 μM Ca^{2+}, respectively, for half maximum activity. Calpastatin also requires Ca^{2+} to bind to the calpains, and the concentration needed is dependent on which calpain it binds to. As pointed out earlier, there is an influx of Ca^{2+} into myofibrils post-mortem, which facilitates the activation of calpains. Furthermore, calpains have been shown to be active in meat at the low temperatures (4°C) and low pH (pH = 5.5) normally seen during post-mortem storage of meat (Koohmaraie, Schollmeyer, & Dutson, 1986), even though optimal pH for calpains are 7.2 to 8.2 (Goll et al., 2003). However, the extent of proteolysis seem to partly depend on pH development post-mortem, where high pH correlates with greater

amount of proteolysis (Bee, Anderson, Lonergan, & Huff-Lonergan, 2007). Calpains are known to degrade a wide range of proteins, including troponin-T, actin, desmin, myosin heavy chain and myosin light chain (Lametsch, Roepstorff, Moller, & Bendixen, 2004).

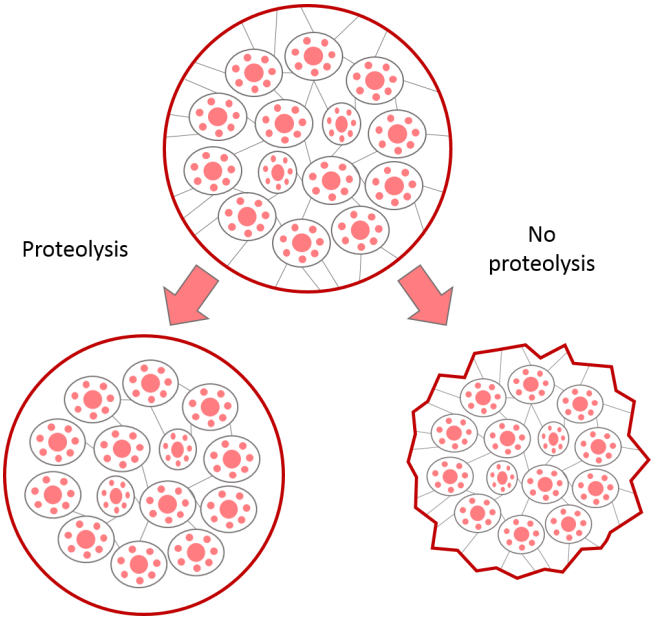

Figure 6. *Schematic overview of potential changes to a muscle fiber with and without proteolysis post-mortem. Adapted from Huff-Lonergan and Lonergan (2005).*

The main hypothesis for how proteolysis affects WHC is related to shrinkage of muscle fibers post-mortem (Huff-Lonergan & Lonergan, 2005; Zeng, Li, & Ertbjerg, 2017). As noted previously, because of rigor development and pH-decline post-mortem, myofibril proteins are more tightly packed, and this translates to an overall shrinkage of the muscle fiber. The important candidate proteins in this regard is the cytoskeletal proteins ensuring the integrity of the muscle fiber, such as desmin, talin and vinculin (Kristensen & Purslow, 2001). Figure 6 shows the theoretical extreme end results of proteolysis and no proteolysis, where it is apparent that the muscle fiber with proteolysis has more potential to keep the water within the endomysium, while the muscle fiber with no proteolysis has less room to maintain the water and it can be expelled from the fiber (Huff-Lonergan & Lonergan, 2005). To affect this development, proteolysis must start early post-mortem because the pH declines and rigor starts developing within hours, and it has been shown that desmin degradation starts as early as 45 min post-mortem in some muscles (Melody et al., 2004).

2.5 Measuring WHC

As noted earlier, the definition of WHC is independent on how and when the drip is formed, and it encompasses all stages where water can escape the muscles. There is no surprise then that there are numerous different approaches to measuring WHC, but most of the methods developed are based on passive, forced or heat treatment of defined meat samples. The different approaches are not entirely correlated, meaning that a sample with low drip in a passive measurement can have disproportional high drip in a forced measurement (Van Oeckel, Warnants, & Boucque, 1999), thus one need to take this into account when choosing a method for measuring WHC. To give an example, if one is interested in minimizing drip formation for modified atmosphere consumer packed meat it would be most appropriate to choose a method based on passive measurements of WHC to mimic the actual circumstances where drip is formed. Passive methods for measuring WHC include EZ-DripLoss method, the bag method and purge loss in consumer packages, and these methods will be described in detail in the next paragraphs. Forced measurements are usually performed using a filter press to drive the water out of the meat (Van Oeckel et al., 1999) or by centrifugation to force water out (Kristensen & Purslow, 2001). Heat treatment measurements of WHC can be performed by keeping the meat in a plastic bag in boiling water until a certain core temperature is reached, and water loss is calculated by the difference in weight before and after heat treatment (Honikel, 1998).

The EZ-DripLoss method has gained traction the last decade or so, thanks to its relative simplicity and that it conveniently need less space to carry out the measurements than for instance the bag method. The EZ-DripLoss method was first described by Rasmussen and Andersson (1996), and an overview of sampling procedure is shown in figure 7. The procedure starts by cutting a slice of a predetermined thickness of the muscle in question and then cutting out two to three cylindrical tubes from this slice. The cylindrical meat sample is then placed in a sample holder, which is weighed before insertion of sample, then it is weighed again with the sample inside and finally it is weighed without the sample after storage at 1-5°C for 24h, only containing the drip, to finally determine the percentage drip formed. As one can see, this is an invasive measurement, and the results are probably dependent on the person performing the measurement, because a change in force applied or location when making the cylindrical samples can affect the results. It has been documented that there is differences in drip loss both when changing the transverse and longitudinal location of the sample taken (L. B. Christensen, 2003), therefore it is very important to keep the location the same and that the procedure is performed by the same staff when sampling over longer time periods.

The bag method was proposed as the reference method for measuring WHC by Honikel (1998). In this method, a muscle slice of predefined size is trimmed of all outer connective tissue and fat, before it is weighed and placed within a netting bag, which is then placed in a plastic bag or container, without direct contact with the walls of the container. The sample is stored at 1-5°C for 24h, before it is gently blotted and weighed again for determination of drip loss. The analysis should be carried out in duplicate or triplicate from the same muscle, and because this method uses an entire slice of the studied muscle to determine drip loss, it requires a lot of sample for one complete measurement. The bag method also needs more space for the measurements because of larger storage containers, and when correlation to EZ-DripLoss is relatively high (L. B. Christensen, 2003; Otto, Roehe, Looft, Thoelking, & Kalm, 2004; Torres, Cazedey, Fontes, Ramos, & Ramos, 2017), it is easy to see why this method might be falling out of favor when conducting large scale experiments.

Figure 7. *Set-up for EZ-DripLoss measurement showing sampling of cylindrical meat pieces and the storage containers for meat samples. Photo: Danish Meat Research Institute.*

Another approach for studying the properties of water in meat is by utilizing proton nuclear magnetic resonance (NMR). NMR is capable of identifying the compartmentalization and distribution of water in meat, which in turn can estimate the amount of water that is susceptible to be lost as drip (Bertram & Andersen, 2007). This relationship was established on the basis of three different NMR relaxation decays corresponding to different water states in muscle, where the shortest relaxation time (T_{2B}) corresponds to protein-associated water, the middle relaxation time (T_{21}) corresponds to immobilized myofibrillar water and the longest relaxation time (T_{22}) corresponds to extra-myofibrillar water (Bertram, Donstrup, Karlsson, & Andersen, 2002).

3. Spectroscopy

Spectroscopy is defined as “the production, measurement, and interpretation of spectra arising from the interaction of electromagnetic radiation with matter” (Penner, 2010). Such data can then be used to, directly or indirectly, describe chemical or physical features of a given sample. Many of the spectroscopic techniques are considered non-invasive and rapid methods of analysis, and some of the techniques require little to no sample preparation. This chapter will describe the different spectroscopic techniques utilized in the work of the current thesis; Near-infrared (NIR), infrared (IR), Raman and fluorescence spectroscopy, with emphasis on possible applications for determining WHC and related quality parameters in the meat industry.

3.1 Near-infrared spectroscopy

Near-infrared (NIR) spectroscopy refers to absorption of electromagnetic radiation starting just above visible light and moving into IR, referring to wavelengths from 780 nm to 2500 nm. In this range, there are overtones and combination bands from C-H, O-H and N-H vibrations, which give broad bands consisting of absorptions in overlapping wavelengths (Blanco & Villarroya, 2002). Figure 8 shows typical NIR reflectance spectra from pork, where the visible (VIS) range from 400 nm to 780 nm also is included. The resulting absorption spectrum from NIR acts as a “fingerprint” from the analyzed sample, and contains information about chemical and physical composition of the sample (Prieto, Pawluczyk, Dugan, & Aalhus, 2017).

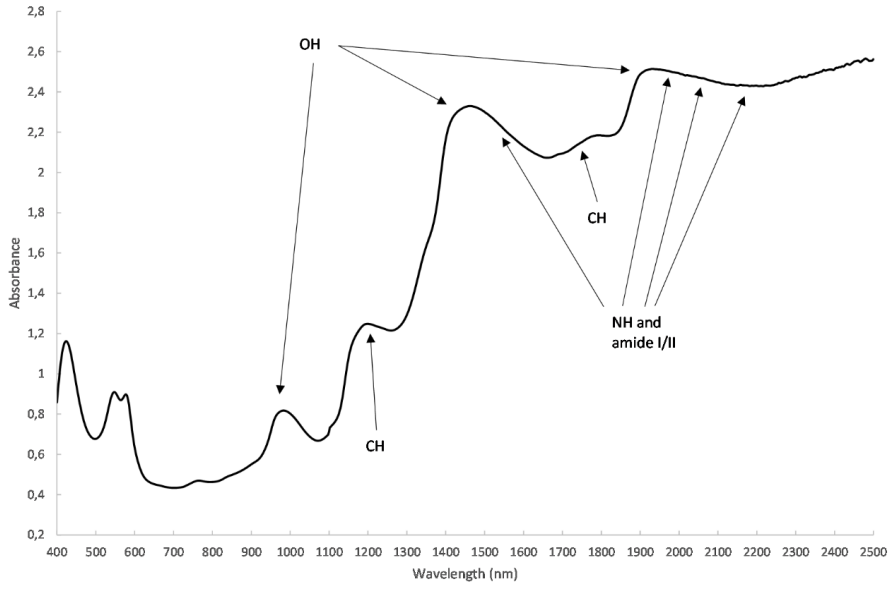

Figure 8. *NIR spectrum from pork, including assignment of some peaks in accordance with Li-Chan, Ismail, Sedman, and van de Voort (2002).*

NIR spectroscopy has many known advantages, including low operational costs, rapid, non-destructive, non-contact and non-invasive measurements, it is chemical-free, it requires minimal to no sample preparation and acquisition of one spectrum allows for determination of multiple parameters (Blanco & Villarroya, 2002). However, there are some drawbacks when analyzing intact meat, such as problems with the heterogeneity of meat when measuring small sample areas and the relatively high absorption of water in the IR region (Prieto et al., 2017). There is no direct link between NIR spectroscopy and WHC or pH, meaning that the ability of NIR to predict these parameters has to rely on indirect relationships between physical or chemical traits related to them (e.g. light transmittance and water characteristics).

There have been numerous studies performed to analyze WHC and pH using NIR spectroscopy, but there are still no successful procedures in use at slaughterhouses or meat processors for these applications. One of the first published attempts of measuring drip loss with NIR was conducted by Forrest et al. (2000), where an insertion probe was used to collect NIR spectra in the range of 900 nm to 1800 nm for 6 min in the *longissimus* muscle 30 min post-mortem at the slaughter line. Their results were promising, yielding models for drip loss with R of 0.84 and RMSEP of 1.8%, which should be good enough for differentiation in quality classes. The procedure was neither rapid nor non-invasive, but it showed promise for analyzing rather complex quality parameters using NIR spectroscopy. Brondum et al. (2000) used a laboratory NIR instrument, recording NIR reflectance in the range from 802 nm to 2500 nm, to model drip loss in loin and ham muscles. Their results was not as promising as those of Forrest et al. (2000), yielding an R of 0.64 and a SEP of 2.43, but it showed some potential for analyzing WHC without having to insert a probe into the meat. Despite the promising initial attempts of measuring WHC in pork and the continued improvement of NIR technology, no studies have shown any better utilization of NIR than to carry out rough screening of WHC at best in recent years (Candek-Potokar, Prevolnik, & Skrlep, 2006; Geesink et al., 2003; Kapper, Klont, Verdonk, & Urlings, 2012; Kapper, Klont, Verdonk, Williams, & Urlings, 2012; Prieto et al., 2017; Weeranantanaphan, Downey, Allen, & Sun, 2011). The main reasons cited for this lack of correlation between WHC and NIR spectroscopy is the heterogeneity of meat and the low repeatability of measured WHC (Prieto et al., 2017).

Studies have also been conducted to investigate if NIR spectroscopy is able to analyze pH in pork. Liao, Fan, and Cheng (2010) used VIS-NIR, recording wavelengths between 450 nm and 910 nm, set up for online measurements to analyze pork *longissimus* pH_u, yielding a PLS model with R_{CV} of 0.82 and RMSECV of 0.10. In a more recent study by Balage, Silva, Gomide, Bonin, and Figueira (2015) similar results were obtained when analyzing pork samples in the wavelength range from 400 nm to 1495 nm, yielding a R_{CV} of 0.70 and SECV of 0.11. Both of these studies gave results good enough

for routine screening of pH_u in pork. While these two studies show promise for routine pH measurements conducted by NIR, there are numerous studies showing limited connection between NIR and pH (Candek-Potokar et al., 2006; Kapper, Klont, Verdonk, & Urlings, 2012; Kapper, Klont, Verdonk, Williams, et al., 2012; Savenije, Geesink, van der Palen, & Hemke, 2006). One strategy to overcome some of the heterogeneity in meat is to scan a larger area of the meat surface, thus accounting for the transversal heterogeneity of the sample, known as hyperspectral spectroscopy (Xiong, Sun, Zeng, & Xie, 2014). The procedure is usually more time consuming than simpler point measurements, but still much faster than traditional measurements of WHC, and the scanning time could be significantly reduced by developing specific instruments for meat analysis. Hyperspectral NIR spectroscopy has been used to study both WHC and pH in pork, yielding promising models with R_{cv} of 0.83 and 0.87 with a RMSECV of 1.11% and 0.11 for WHC and pH_u, respectively (Barbin, ElMasry, Sun, & Allen, 2012). Similar results have been obtained when analyzing meat from beef, which resulted in R_{cv} of 0.89 and 0.73 with a SECV of 0.26% and RMSECV of 0.06 for WHC and pH_u, respectively (ElMasry, Sun, & Allen, 2011, 2012). This shows great promise for improvement when determining WHC by scanning a larger area, while it does not help significantly in linking pH and NIR spectroscopy.

There are examples of successful implementations of NIR spectroscopy in the meat industry for other parameters than WHC and pH. The first example of studies transferred to industrial use is the utilization of NIR spectroscopy for on-line measurement of fat, moisture and protein in ground beef (Isaksson, Nilsen, Togersen, Hammond, & Hildrum, 1996), and today there are several commercially available instruments for on-line or at-line analysis of fresh and ground meat (Bruker, 2017; FOSS, 2017; Prediktor, 2017; TOMRA, 2017).

3.2 Infrared spectroscopy

The infrared (IR) region usually refers to a continuation of the wavelengths from NIR, ranging from 2500 nm to 50000 nm, while IR spectra are usually reported in wavenumbers, corresponding to the range from 4000 to 200 cm^{-1}. Stretching and bending vibrational frequencies of bonds in most covalent molecules corresponds to radiation in this range. When a molecule absorbs IR radiation matching its natural vibrational frequencies, the energy is used to increase the amplitude of the vibrational motions of the bonds in the molecule (Pavia, Lampman, & Kriz, 2001). To be IR active, the bond must have a dipole moment that changes as a function of time, which mostly excludes symmetric bonds and symmetric molecules (e.g. H_2 and ethylene).

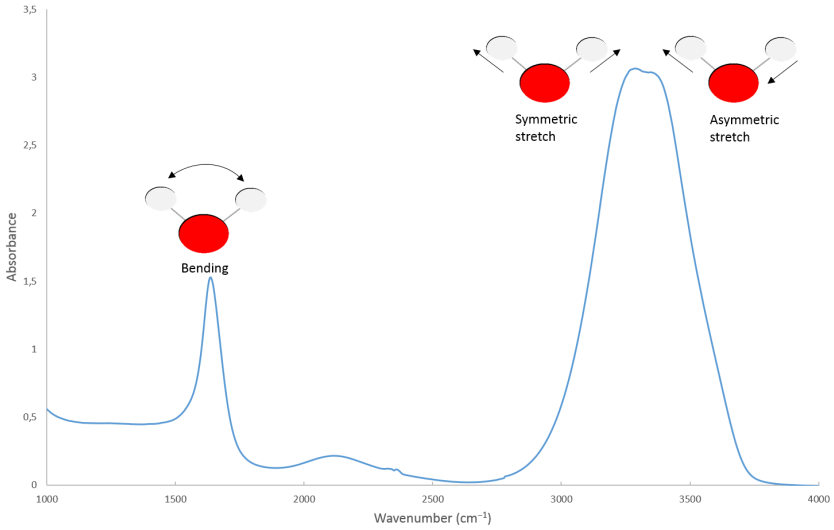

Figure 9. *Water IR absorption spectra in the range from 1000 to 4000 cm^{-1}, showing the vibrational modes contributing to each peak.*

To illustrate what happens to a molecule when it absorbs IR radiation, it is convenient to examine H_2O, which is a relatively simple molecule with only 3 vibrational modes, symmetric stretch, asymmetric stretch and bending (Fig. 9). Bending occurs when the water absorbs IR radiation at approx. 1640 cm^{-1} and gives rise to one distinct peak. Even though symmetric stretch requires less energy than the asymmetric stretch, the two stretching vibrations are so close in required energy for absorption that they appear as one peak in the IR absorption spectrum at approx. 3400 cm^{-1}. The nature of these peaks can then be used to discern chemical information about the analyzed sample, but one needs to be cautious when analyzing complex samples because spectrums often are complicated by weak overtones, difference and combination bands.

For analysis of meat, it is advantageous that IR radiation corresponds with protein backbone vibrations, the amide bands, which have been useful for analyzing secondary structure of peptides and proteins. There are nine amide bands, amide A, amide B and amides I-VII, where amides I-III are of special interest for protein structure analysis (Table 1). The amide I band is most widely used for protein secondary structure analysis, since it is relatively unaffected by amino acid side chain vibrations. Assignment of infrared band locations for secondary structure analysis is summarized in table 2. IR spectroscopy can provide information about amino acid side chains, which is useful for studying mechanisms of protein reactions and provide insight into protonation state, conformational freedom and charge of the side chain (Barth, 2000). Figure 10 shows an IR spectra of dried myofibrils, where vibrations of amides I-III and amino acid side chains of aspartic acid (Asp)

and glutamic acid (Glu) are indicated. IR spectra also contain information about fats and carbohydrates (Li-Chan et al., 2002), meaning that all major components in meat can be examined to some degree by this technique.

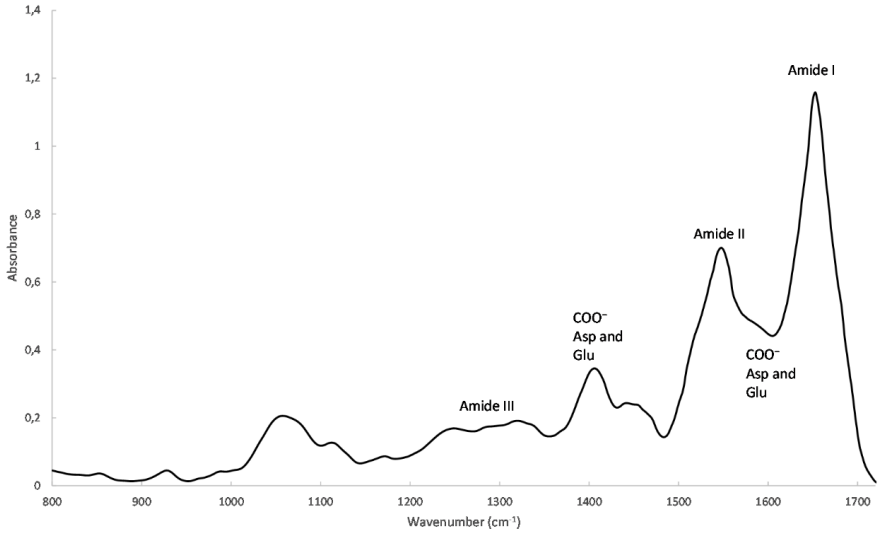

Figure 10. *Example IR spectrum in the range from 800 to 1720 cm^{-1} derived from dried myofibrils. Assignment of amino acid side chain and amide I-III vibrations in accordance with Barth (2007).*

Table 1. Characteristics of amides I-III bands in IR spectroscopy (Barth, 2007).

Nomenclature	**Band position (cm^{-1})**	**Vibrational modes**
Amide I	~ 1650	C=O stretching, CN stretching, CCN deformation and NH in plane bend.
Amide II	~ 1550	Combination of NH in plane bend and CN stretching, CO in-plane bend, CC stretching and NC stretching.
Amide III	$\sim 1400 - 1200$	In-phase combination of NH bend and CN stretching, CO in plane bending and CC stretching.

Table 2. Assignment of secondary structure from amide I band positions for IR (Barth, 2007) and Raman spectroscopy (Li-Chan, 1996).

Secondary structure	IR band position (extremes)	Raman band position
α-helix	1654 (1648-1657)	1655 (±5)
β-sheet	1633 (1623-1641)	
	1684 (1674-1695)	1679 (±3)
Turns	1672 (1662-1686)	
Disordered	1654 (1642-1657)	1665 (±3), solvated
		1685, non-hydrogen bonded

There are very few studies investigating the relationship between IR spectroscopy and meat quality, but there is one study by Pedersen, Morel, Andersen, and Balling Engelsen (2003) using IR to predict WHC in pork. They used an ATR approach to analyze meat samples in the laboratory and close to the slaughter line in an abattoir. Results were better for laboratory samples (R_{cv} of 0.89 and RMSECV of 0.85) than for samples analyzed at the slaughter line (R_{cv} of 0.79 and RMSECV of 1.06), but both results show promise for IR to analyze meat quality. The lack of further research in this area might be caused by the difficulties in implementing IR spectroscopy in the abattoir, because of sensitivity to changing temperatures and humidity and the lack of good optical fibers for the IR region (Pedersen et al., 2003). Consequently there are no commercially available IR instruments used in the meat processing industry.

3.3 Raman spectroscopy

Raman spectroscopy is similar to IR spectroscopy in that both methods analyzes molecular vibrations. The main difference between the two methods is that Raman deals with scattered photons while IR deals with absorption of light. Raman scattering happens when incident light interacts with a molecule and polarizes the electron cloud surrounding the nuclei, forming a short-lived virtual state, before quickly re-emitting a photon (Smith & Dent, 2013). Most scattered photons will stay relatively unchanged compared to the incident light, because only the electron cloud is distorted; this phenomenon is called Rayleigh scattering. However, if nuclear motion is induced in this process, the emitted photon will be of a higher or lower energy level than the incident light, and the emitted photons from this process is what is detected in Raman spectroscopy. This process is inherently weak, only occurring in one out of 10^6-10^8 photons. A

molecule needs to be polarizable to be Raman active, as opposed to a change in dipole moment to be IR active. This means that Raman and IR spectroscopy detects fundamentally different vibrational modes, but they may still be able to analyze many of the same compounds because of the multiple vibrational modes exhibited in complex molecules. This can be illustrated by examining the vibrational modes of carbon dioxide, where the symmetrical stretch is Raman active while the asymmetrical stretch is IR active (Fig. 11). Water has a relatively weak Raman signal, which is very advantageous for Raman spectroscopy when analyzing biological systems, as they usually contain high amounts of water.

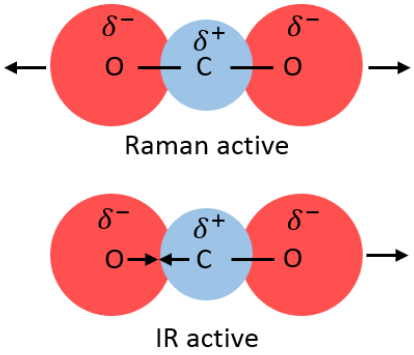

Figure 11. *Electron cloud model of carbon dioxide showing a Raman and an IR active vibration. Adapted from Smith and Dent (2013).*

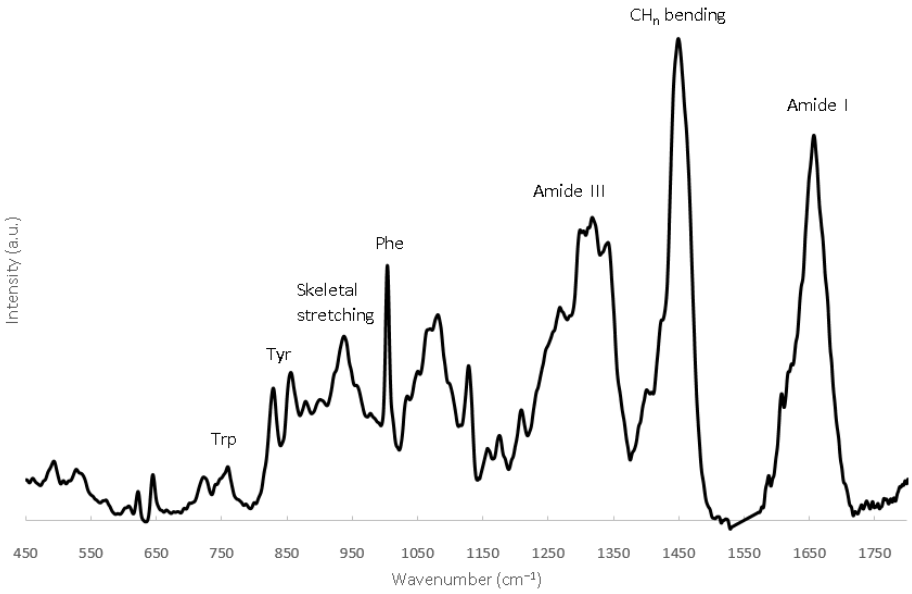

Figure 12. *Baseline corrected Raman spectrum from pork. Assignment of amide I and III and amino acid side chain vibrations in accordance with Herrero (2008).*

Raman spectroscopy can, like IR spectroscopy, provide insight into protein secondary structure mostly through amide I (Table 2) at approx. 1650 cm^{-1} and amide III vibrations at 1200 to 1400 cm^{-1}, but also from a characteristic skeletal stretching mode at 880 to 960 cm^{-1} (Krimm &

Bandekar, 1986). The amide II vibration exhibits little change in polarization, and is therefore weak or absent in Raman spectroscopy. Amino acid side chain vibrations are also detectable in Raman spectra, where especially aromatic side chain vibrations of phenylalanine (Phe), tyrosine (Tyr) and tryptophan (Trp) give rise to very intense Raman lines (Lord & Yu, 1970). Figure 12 shows an example spectra from meat where amide and amino acid vibrations are indicated. Raman can, as IR spectroscopy, be used to analyze fats and carbohydrates (Li-Chan et al., 2002).

The first attempt at predicting WHC in pork using Raman spectroscopy was conducted by Pedersen et al. (2003), with unrealistic good results according to the authors, where the models yielded R of 0.98 and RMSECV of 0.23% for the best models. Only 14 samples were analyzed by Raman spectroscopy in the study, so there was indeed a need to conduct more extensive experiments to incorporate more samples/variation in the models. There was not much activity following this study until the development of a handheld Raman instrument for meat analysis reinvigorated the field (Schmidt, Sowoidnich, & Kronfeldt, 2010), resulting in numerous experiments investigating pH and WHC in pork by the German research group. Their results for prediction of drip loss have been encouraging, resulting in an R_{CV} of 0.73 and RMSECV of 1.0% in their first study (Scheier, Bauer, & Schmidt, 2014) and R_{CV} of 0.52 and RMSECV of 0.6% in their second trial (Scheier, Scheeder, & Schmidt, 2015).

Table 3. Prediction of pH from Raman spectroscopy recorded 1-2 h and 24 h post-mortem. Adapted from Nache, Hinrichs, Scheier, Schmidt, and Hitzmann (2016).

	Pre-rigor dataset		Post-rigor dataset	
	pH_{45}	pH_{24}	pH_{45}	pH_{24}
RMSECV	0.18	0.13	0.19	0.10
R	0.95	0.80	0.83	0.87

Regarding the feasibility of pH-measurements, they have conducted a series of experiments following the development of post-mortem pH and related muscle chemicals (e.g. lactate) to predict pH with very good accuracy (Nache, Scheier, Schmidt, & Hitzmann, 2015; Scheier & Schmidt, 2013). This approach is not suitable for use in an abattoir, so the feasibility studies was followed up with a recent experiment where Raman spectra were recorded at 1-2 h and 24 h post-mortem and pH was measured at 45 min and 24 h post-mortem, results are summarized in Table 3 (Nache et al., 2016). This experiment shows that the Raman spectra contain information about both early and late pH regardless of when the spectra are recorded, but that the connection is stronger when the spectrum is recorded close to the pH measurement. Taken together, these

experiments show great promise for using Raman spectroscopy for meat quality assessment, but that development of robust equipment and procedures needs to be emphasized.

3.4 Fluorescence spectroscopy

Fluorescence is a three-stage process that occurs in molecules named fluorophores, which can be summarized as the fluorophore being excited to an electronic singlet state by absorption of an external photon, then interacting with the molecular environment and undergoing conformational changes, before a photon is emitted at a longer wavelength than the external photon and the fluorophore returns to its ground state (J. Christensen, Norgaard, Bro, & Engelsen, 2006). Since each electronic state in fluorophores has several vibrational levels, the excitation and emission spectra are distributed over numerous wavelengths, which can be visualized in fluorescence landscapes. The fluorescence process happens within nanoseconds, making fluorescence spectroscopy potentially a very fast technique for food analysis. Only specific molecules act as fluorophores, and for organic compounds, it is most often found when a rigid molecular skeleton is present, such as for polyaromatic hydrocarbons and heterocycles. Some fluorophores of interest in meat include the aromatic amino acids phenylalanine, tyrosine and tryptophan, in addition to different types of collagen and NADH. Because the molecular environment can affect the fluorescence spectra, e.g. due to changes in pH or exposure of fluorophores to the surrounding environment, it is plausible that fluorescence spectroscopy can be linked to meat quality.

Brondum et al. (2000) was the first to publish a promising experiment regarding a link between fluorescence spectroscopy and WHC in pork, resulting in an R of 0.68 and SEP of 2.27, citing a need for more research in the area to establish its feasibility as a rapid method for meat quality assessment.

4. Data analysis

Data obtained from spectroscopic techniques usually contain thousands of variables, often outnumbering samples analyzed by orders of magnitude. A consequence of this is that traditional statistical methods to find relationships between reference measurements (**Y**) and spectra (**X**), such as linear regression, have limited applicability. Many variables from spectroscopy are collinear, making techniques for variable reduction viable for interpretation of the data. Such methods are colloquially known as multivariate data analysis (e.g. principal component analysis (PCA) and partial least squares regression (PLSR)), and is widely used for detailed analysis of spectroscopic data.

4.1 Pre-processing of spectral data

Pre-processing of spectra is carried out to remove artifacts from the spectra, aiming to preserve chemical and physical information. Extensive multiplicative scattering correction (EMSC) is applied

to spectra to correct for additive baseline effects, multiplicative scaling effects and interference effects by using a mean spectrum (Afseth & Kohler, 2012), giving comparable spectra suitable for further data analysis. Standard normal variate (SNV) does not use a mean spectrum, but uses data from each individual spectrum by centering based on mean values for each variable and scaling using the sample variance (Barnes, Dhanoa, & Lister, 1989). 2nd derivative is used to emphasize band position and separations in addition to removing or reducing background effects, rather than intensity of the bands (DeNoyer & Dodd, 2001).

4.2 Unsupervised data analysis

Principal component analysis (PCA) is used to reveal if there are systematic patterns of variation between samples, which is computed from a single input matrix **X** (e.g. data from spectroscopy) (H. Martens & Martens, 2001). This means that PCA is an unsupervised method of data analysis, meaning that the data creates structures unaffected by other responses, and is consequently useful for studying inherent grouping in datasets.

4.3 Supervised data analysis

Partial least squares regression (PLSR) is a method for determining relationships between two data matrices, **Y** (e.g. pH measurement) and **X** (e.g. spectrum from NIR), where the modelling of **X** and **Y** is done simultaneously to ensure that important information for **Y** is extracted from **X** (H. Martens & Martens, 2001). PLSR is consequently a supervised method for data analysis, useful for making prediction models from data matrices.

4.4 Validation of models

Validation of models is performed to estimate the reliability of the models. There are two important measures for this, the predictive ability and the parameter stability. Predictive ability refers to how good the model can predict **Y** from **X** for independent samples, while parameter stability concerns the precision of the model's parameter values (e.g. β coefficients) (H. Martens & Martens, 2001). An established method for validation of models is cross-validation. In cross-validation, a sub-set of samples is left out of the model and used as separate test samples, and this process is repeated until all samples have been left out once. The sub-model predicts the **Y-value** of samples left out and the error of this prediction is used to calculate the performance of the model, which is called the root mean square error of cross-validation (RMSECV). The aim is always for the RMSECV-value to be as low as possible, but it needs to be considered in relation to the scale on which **Y** is recorded and the variance in **Y**. This is a way of testing the validity of a model without needing a separate test-set.

An uncertainty test, which is based on a modified jack-knifing procedure, is conducted when making a PLSR model to give information about important variables in a model (H. Martens & Martens, 2000). The uncertainty test determines which variables are important by comparing all β-coefficients from sub-models made in cross-validation, and subsequently analyzes which variables are stable across these sub-models. These variables can then be used to make a new model, which often is more stable than the one including all the variables.

5. Main results and discussion

The first part of this chapter summarizes results from the three studies performed, followed by a discussion regarding choice of methodology and the use of spectroscopic analyses of pH, proteolysis and WHC in a model system and intact meat.

5.1 Summary of papers

In **paper I** and **II** the objective was to investigate if chosen spectroscopic techniques could provide specific information related to muscle proteins when only one factor was changed in a model system containing isolated myofibrils from pork muscle. In **paper I**, the chosen factor was pH, and in **paper II**, the chosen factor was proteolysis. In **paper III**, three of the spectroscopic methods were used to analyze intact meat, with an aim to recognize some of the effects discovered in **paper I** and **II** and at the same time investigate their potential for prediction of drip loss.

The range of pH studied in **paper I** was chosen to encompass the variation normally encountered in pork post-mortem, therefore, the chosen pH-levels were 5.3, 5.8 and 6.3. This experiment was conducted mainly to identify what spectral regions changed following changes in pH, and to establish if these regions possibly can be used for quantitative pH determination. Samples for Fourier transform-infrared (FT-IR) and Raman spectroscopy were dried prior to analysis, while fluorescence and NIR spectroscopy samples were analyzed in liquid form. The main result from the experiment was the good performance of FT-IR and Raman spectroscopy, both qualitatively and quantitatively, and that results from both methods confirmed each other. The affected regions from FT-IR and Raman spectroscopy were related to changes in protein secondary structure, mainly an increase in α-helical structures, a decrease in β-sheets and an increase in deprotonated carboxylic acid as pH increased. Fluorescence spectroscopy performed reasonably well, attributing the change in Trp fluorescence to a change in the microenvironment surrounding this amino acid side chain. NIR spectroscopy did not perform well, most likely caused by the relatively low protein concentration in the samples.

To induce proteolysis in the experiment for **paper II**, the isolated myofibrils were incubated with μ-calpain for 15 or 45 min, while the control was not incubated. Once again, FT-IR and Raman spectroscopy proved to be excellent tools for distinguishing samples with different degree of protein degradation on dried samples. Affected regions were related to changes in protein secondary structure and carboxylic acid in this experiment; an increase in α-helical structures, a decrease in β-sheets and an increase in deprotonated carboxylic acid were detected as degree of protein degradation increased. NIR spectroscopy predicted degree of protein degradation reasonably well in dried samples, and this was attributed to gelling properties of the myofibril isolates. Fluorescence

and NIR spectroscopy did not provide useful information for interpreting changes following protein degradation in viscous samples, nor did they make good models for protein degradation.

The aim in **paper III** was to measure drip loss in pork using the spectroscopic techniques employed previously, with additional aims to measure pH and IMF. Samples in the study were analyzed with Raman, NIR and fluorescence spectroscopy, while IR spectroscopy was left out because of shortcomings in instrumentation and the inconvenience of using IR spectroscopy as an on-line method. The reference measurements of EZ-drip loss, pH_u and IMF were conducted at a meat research facility at 4-5 days post-mortem, while vacuum drip loss after further eight days of storage was measured in-house. Raman spectroscopy proved to be the most promising technique for analysis of all quality traits (Table 4), assigning important regions from PLSR for drip loss and pH to signals from post-mortem metabolites and changes in protein secondary structure. PLSR for IMF relied predominantly on characteristic fat peaks. In addition, Raman spectroscopy could be used to sort samples in rough batches according to their predicted drip loss from PLSR. NIR spectroscopy performed reasonably well for pH and IMF, but was unreliable for drip loss measurements. This supports the notion that NIR spectroscopy is better suited to analyze innate physical traits (e.g. IMF) than predicting changes happening over time (e.g. drip loss). PLSR models from fluorescence spectroscopy did not perform very well, despite the promising results for pH measurements in **paper I**. It seems that the fluorescence from meat is too complex to give practical models from excitation at only one wavelength.

5.2 Methodological aspects

Important considerations regarding methodology in the current thesis was what kind of samples to analyze, which mechanisms and quality parameters to focus on and which spectroscopic techniques to use for different samples and mechanisms.

5.2.1 Samples and mechanisms

Since many of the mechanisms affecting WHC are dependent on each other (e.g. pH and proteolysis), it would be convenient to be able to analyze these factors in isolation. This led to a realization that there was a need for a simplified model system, which could easily be manipulated and analyzed, by both reference methods and spectroscopic analyses. Thus, a model system consisting of myofibrils isolated from pork *longissimus thoracis et lumborum* was developed. The samples were prepared by homogenizing and filtering muscle pieces, followed by washing and subsequently freezing them with glycerol for later use in experiments. Thawed samples were washed and suspended in buffers appropriate for the different experiments. By isolating myofibrils, many of the different proteins in muscle are retained in the samples, while other muscle constituents, such as fat and connective

tissue, are removed. The reason for analyzing myofibrils is that most of the post-mortem modifications in muscle tissue are manifested in proteins, such as proteolysis, rigor development and protein attraction caused by changes in pH. Other advantages for such a model system is that it is relatively easy to obtain similar parallels in experiments, and the samples can be prepared at any time and still be comparable to samples from other experiments. However, there are some disadvantages to this system, the most important being that there is no information about the significance of muscle structure on the parameters in question. Other disadvantages include not knowing if the isolation procedure changes some of the properties of proteins, lower concentration of proteins compared to meat (about a tenfold decrease in the model system) and how freeze/thaw cycles affect the samples in general.

In the first experiment utilizing the model system, pH was altered to reflect that of post-mortem meat and samples were analyzed with spectroscopy. This parameter was primarily chosen because there is a lot of evidence linking pH to WHC (see chapter 2.4.1) and it is plausible that spectroscopy can identify pH-related changes in proteins. The secondary reason pH was chosen was because it is a parameter that is easy to modify in a model system, thus serving as an experiment to determine if the model system could be used for spectroscopic analyses. A rapid method for measuring pH is also desirable for the meat industry, because todays methods of measuring pH by insertion electrodes are time consuming and invasive and are mostly used for screening purposes.

Degree of proteolysis was the second parameter studied in the model system. Proteolysis is also linked to WHC (see chapter 2.4.3), but the direct relationship is not as strong as for pH. There is commercially available calpain isolated from pigs, which makes it possible to conduct experiments closely mimicking real-life events in meat. Since the model system contains dispersed and broken down myofibrils it is possible that these myofibrils are more easily degraded by calpains than myofibrils would be in intact muscle, meaning that the degradation products in the model system can be different from that of meat. However, the model system will still serve as a reasonable test if spectroscopy is at all able to detect differences in protein degradation in myofibrils.

The last experiment was conducted in collaboration with a Norwegian pig breeding facility. Reference measurements were carried out at their testing facility, while spectroscopic analysis and an additional purge measurement was carried out in-house. Reference measurements included pH_u, EZ drip loss and intramuscular fat (IMF). All pigs in the experiment were Norwegian landrace boars, known for their relatively high drip loss and low amounts of IMF, which makes these animals suitable for studies involving spectroscopy because many spectroscopic techniques are sensitive to fat. An additional aim of the experiment was to investigate if the results from the model system experiments could help explain or interpret results from intact meat samples.

5.2.2 Spectroscopic techniques

There are a multitude of spectroscopic techniques available, and a need to narrow down which techniques to focus on emerged early. The different techniques utilized in the current thesis are explained in more detail in **chapter 3**, therefore, the focus of this part is on the comparison of methods included in the current thesis.

There were several criteria for including a spectroscopic technique in the present thesis, these included:

1. Rapid measurement
2. Non-destructive, and preferably non-contacting
3. Potential for on-line or at-line implementation in the abattoir
4. Contain information about meat components

IR spectroscopy is the most questionable technique used regarding potential for online implementation, as it is currently reliant on the ATR technology for measurements on intact meat. This means that the relatively large ATR crystal needs to stay in contact with the meat sample when conducting the measurement, creating a need for cleaning in-between each measurement, making it more cumbersome and time-consuming than just making individual measurements. There are also uncertainties related to whether instruments can be manufactured with sufficient robustness to be installed in an abattoir. On the other hand, IR spectroscopy has proven to be an excellent tool for characterizing meat properties and meat components, by e.g. cryo-sectioning before microspectroscopic analysis (Perisic, Afseth, Ofstad, & Kohler, 2011; Wu et al., 2006)), and it is very useful for research purposes. Thus, IR spectroscopy was included for analysis of samples from the model system, using the FT-IR spectroscopy technique (for details see Perkins (1986, 1987a, 1987b)).

Raman spectroscopy checks all the boxes of criteria, except for the fact that it is not an exceptionally rapid technique with the present technology. This is mainly caused by the inherent low intensity of Raman scattering, resulting in lengthy accumulation of signal for representative spectra. It is possible that this can be overcome by development of instruments specifically for meat analysis (e.g. optimal laser configurations and selective detectors). A hand-held contact Raman instrument has already been developed, and it should be possible to develop an instrument where meat is transported through a dark chamber where the Raman analysis is conducted, thus creating a non-contact environment for the analysis.

NIR spectroscopy also fulfills nearly all the criteria, but this method is limited by its low selectivity and specificity. In fact, one of the main reasons for including NIR in the thesis is that commercially instruments for use in the meat industry are already available, meaning that if experiments were

successful, the method could relatively easily be tested for on-line applications. Because NIR can be used to analyze liquid samples, the samples for **paper I** in the model system were only analyzed in liquid form, however, this gave inadequate signals from myofibrils. This led to the inclusion of dried samples in addition to liquid samples for experiments in **paper II** in order to increase protein absorption.

Fluorescence spectroscopy is relatively unexplored as a method for meat quality analysis, but it also fulfills all the criteria listed above. The question is mainly whether the information contained in the fluorescence spectra correlates to mechanisms related to meat quality, as it is rather limited when studying myofibrils and intact meat (e.g. only containing information about three amino acids).

5.3 Spectroscopic analysis of pH and proteolysis

PLSR models from Raman and FT-IR spectroscopy gave high correlations for pH and degree of protein degradation in the model system (Table 4). Many of the same responses were identified as important for both spectroscopic methods, in a way serving as validation for one another. PLSR models for Raman spectroscopy and pH had higher correlation in the model system than compared to that of intact meat. A comparison between model system and intact meat for Raman spectroscopy and pH revealed some of the same affected spectral regions (e.g. changes in protein secondary structure), which strengthens the findings in both these studies. However, the most important region from the model system, the region attributed to carboxylic acid residues at approx. 1400 cm^{-1}, was not identified as important for PLSR model of intact meat, indicating that this region is not as prominent in the complex meat spectra as for isolated myofibrils. The range of measured pH was 0.37 pH units in intact meat and 1.22 pH units in the model system, possibly contributing to the reduced importance of the carboxylic acid residues for intact meat. Signals from metabolic molecules, such as phosphates and lactate, have been linked to prediction of pH (Scheier, Bauer, et al., 2014; Scheier, Kohler, & Schmidt, 2014; Scheier et al., 2015), and these molecules were important for the PLSR model of pH from intact meat in the current thesis as well. Raman signals from these molecules were not included in the final PLSR model from the model system, most likely caused by removal of many of the metabolic molecules in the myofibril isolation process. Results presented in the current thesis did not show improved capability of estimating pH with Raman spectroscopy, nevertheless, results from Raman spectroscopy in **paper III** can be seen as an independent validation of the regions in the Raman spectra affected by changes in pH identified by others (Nache et al., 2016; Scheier, Bauer, et al., 2014; Scheier & Schmidt, 2013).

PLSR models from NIR spectroscopy performed poorly for liquid samples when analyzing pH and proteolysis, but performed much better when analyzing dried samples from the proteolysis model

experiment. In hindsight, one can imagine that NIR analysis of dried samples in the pH model experiment would have improved the results. PLSR models from NIR and pH showed that NIR had higher correlation for intact meat than in the model system. It is difficult to identify what could have caused this, but the main assumption is that the low protein concentration in the model system caused too low absorption from proteins. Another factor could be that color of meat correlates with pH (Joo, Kauffman, Kim, & Park, 1999), an effect which is more pronounced in intact meat than in the model system. The VIS range was not important for the PLSR model from the myofibrill model system, while it was the most important region for the PLSR model for pH from the intact meat samples. Results from NIR spectroscopy in the current thesis did not demonstrate improved performance for estimating pH compared to other studies (Balage et al., 2015; Liao et al., 2010).

Fluorescence spectroscopy was sensitive enough to analyze liquid samples in the model system. PLSR models for pH gave relatively good correlations in the model system, but the same responses were not detected for intact meat, resulting in poor PLSR models. It is likely that the minute changes in the model system is not present in intact meat, caused by rigid structure of intact meat compared to the model system.

Proteolysis was not analyzed for intact meat in the experiment with meat, making it impossible to compare the model system with intact meat. Nevertheless, the results showed that the affected regions from Raman and IR spectroscopy were related to universal changes following proteolysis (e.g. peptide bond breakage and formation of new C-terminals) and these changes can possibly be detected in intact meat. The changes in the spectra are also unrelated to the specific enzyme system causing the protein degradation, as the same changes were shown when using FT-IR to analyze proteins degraded by alcalase (Bocker, Wubshet, Lindberg, & Afseth, 2017; Wubshet et al., 2017). Further research is needed to establish the connections between spectroscopy and proteolysis.

In summary, the model system served as a good indicator of the possibilities for spectroscopic techniques to analyze specific mechanisms affecting WHC in meat. However, the experiment analyzing intact meat shows that it is very important to verify if the spectroscopic responses seen in a model system are present in samples that are more complex.

Table 4. Summary of spectroscopy PLSR model performance from **paper I-III**.

	pH		Degree of proteolysis		pH		EZ-DripLoss		Vacuum drip loss		IMF	
	Model system		Model system		Intact meat		Intact meat		Intact meat		Intact meat	
Method	r_{cv}^2	RMSECV	r_{cv}^2	RMSECV	r_{cv}^2	RMSECV	r_{cv}^2	RMSECV	r_{cv}^2	RMSECV	r_{cv}^2	RMSECV
Raman	0.95	0.10	0.83	1.07	0.49	0.06	0.51	1.2	0.41	0.82	0.73	0.09
FT-IR	0.94	0.11	0.92	0.78								
NIR (liquid)	0.14	0.42	0.10	2.61								
NIR (dried)			0.74	1.42								
NIR					0.29	0.07	0.27	1.5	0.16	0.97	0.51	0.12
Fluorescence	0.84	0.18	0.25	2.27	0.02	0.08	0.18	1.6	0.02	1.1	0.12	0.17

5.4 Spectroscopic analysis of WHC

The results presented in **paper III** shows that Raman spectroscopy has potential for prediction of WHC in intact meat, while NIR and fluorescence showed limited applicability for WHC prediction (Table 4). The model from Raman spectroscopy performed on a similar level as results from other studies (Scheier, Bauer, et al., 2014; Scheier et al., 2015), while NIR performed worse than other studies (Candek-Potokar et al., 2006; Kapper, Klont, Verdonk, & Urlings, 2012; Kapper, Klont, Verdonk, Williams, et al., 2012). The reason for the better performance of Raman spectroscopy compared to NIR in the current thesis is believed to be caused by the greater level of molecular details provided in the Raman spectra compared to NIR and fluorescence spectra. Even though the PLSR model from Raman spectroscopy was not good enough for screening purposes on a sample level, the model can be used to make batches of samples with significantly higher drip loss according to the predicted drip loss from the PLSR model. Thus, it is possible to eliminate the majority of meat with poor quality and use it in alternative products where WHC is of less importance.

Analysis of WHC is not an exact science; there is no consensus best method for measuring WHC and results might vary considerably based on sample handling. It is also difficult to obtain margins of error for the measurement, as there is no way of measuring the same sample multiple times. This results in a quality parameter that has a high degree of uncertainty associated with it, and consequently makes it difficult to make models from spectroscopy with small errors. Another limiting factor for determination of drip loss by spectroscopic techniques is that there is a delay between spectroscopic analysis and measurement of drip loss, meaning that spectroscopy has to measures the potential for drip formation. When collecting spectra at e.g. 24 h post-mortem and measurements of drip loss are conducted after 48-72 h post-mortem or eight days (as for VD in the current thesis), it is unlikely that the spectroscopic measurement accurately can account for all the changes happening over that extended time. This can indeed be a reason why the Raman PLSR model for VD was weaker than for EZ-DripLoss, since drip loss was measured eight or one day after the spectroscopic measurements, respectively.

6. Conclusion and future prospects

The work presented in this thesis showed that spectroscopic techniques have a potential to predict WHC in meat, as well as estimate pH and proteolysis in isolated myofibrils.

Both Raman and FT-IR proved to be excellent tools for analyzing samples from isolated myofibrils, providing detailed information about protein structure and amino acid side chain properties for different pH and degree of proteolysis. Findings regarding protein secondary structure were also present in Raman spectra from intact meat, showing that some of the information was preserved in the model system. Conversely, the amino acid side chain vibrations were not important for models from intact meat, indicating that results from the model system must be validated in intact meat. Raman spectroscopy was the most promising technique for analysis of meat quality, as it showed the best ability to predict drip loss and measure pH and IMF in intact meat. NIR and fluorescence spectroscopy did not show much promise for analyzing meat quality. Taken together, this highly encourages more research using Raman spectroscopy for analysis of meat quality.

In my opinion, what should be prioritized is to investigate the potential for Raman spectroscopy to predict drip loss without the confounding factors at an abattoir. An interesting strategy to achieve this can be to measure spectra of the exact same samples used in EZ-DripLoss measurement. These samples are relatively small, so it is possible to scan most of the surface area, thus eliminating much of the differences in sampling location and sample area for spectroscopy vs. drip loss measurements. Such a set-up will allow samples to be analyzed by spectroscopy at different times after sample preparation, and possibly establish at what time it is best to acquire spectra for analyses of meat quality. Even though sampling was done at 4-5 days post-mortem in the current thesis, there is nothing preventing sampling at earlier time points post-mortem, e.g. at 30 min post-mortem, for simultaneous EZ-DripLoss and spectroscopic analyses. To be able to better assess models for prediction of drip loss, error of the reference method should be examined, as a spectroscopic model cannot be expected to perform better than the reference measurement.

In the future, it would be interesting to investigate the potential for on-line and non-contact assessment of meat quality with Raman spectroscopy, since this technique could be used to analyze several parameters simultaneously, e.g. WHC and IMF. In order to facilitate this, the acquisition time for Raman spectra needs to be reduced to enable measurements on the fast product flow during meat processing. In addition, development of new instruments operational in the humid and cold air conditions of the abattoir is required, but the development of a hand-held Raman sensor (Schmidt et al., 2010) shows that it is possible for a Raman instrument to be operational under such conditions.

7. References

Afseth, N. K., & Kohler, A. (2012). Extended multiplicative signal correction in vibrational spectroscopy, a tutorial. *Chemometrics and Intelligent Laboratory Systems, 117*, 92-99. doi: 10.1016/j.chemolab.2012.03.004

Balage, J. M., Silva, S. D. E., Gomide, C. A., Bonin, M. D., & Figueira, A. C. (2015). Predicting pork quality using Vis/NIR spectroscopy. *Meat Sci, 108*, 37-43. doi: 10.1016/j.meatsci.2015.04.018

Barbin, D. F., ElMasry, G., Sun, D. W., & Allen, P. (2012). Predicting quality and sensory attributes of pork using near-infrared hyperspectral imaging. *Analytica Chimica Acta, 719*, 30-42. doi: DOI 10.1016/j.aca.2012.01.004

Barnes, R. J., Dhanoa, M. S., & Lister, S. J. (1989). Standard Normal Variate Transformation and De-Trending of near-Infrared Diffuse Reflectance Spectra. *Applied Spectroscopy, 43*(5), 772-777. doi: Doi 10.1366/0003702894202201

Barth, A. (2000). The infrared absorption of amino acid side chains. *Prog Biophys Mol Biol, 74*(3-5), 141-173.

Barth, A. (2007). Infrared spectroscopy of proteins. *Biochim Biophys Acta, 1767*(9), 1073-1101. doi: 10.1016/j.bbabio.2007.06.004

Bee, G., Anderson, A. L., Lonergan, S. M., & Huff-Lonergan, E. (2007). Rate and extent of pH decline affect proteolysis of cytoskeletal proteins and water-holding capacity in pork. *Meat Sci, 76*(2), 359-365. doi: DOI 10.1016/j.meatsci.2006.12.004

Bendall, J. R. (1973). Postmortem changes in muscle. In G. Bourne (Ed.), *Structure and function of muscle* (pp. 243-309): Elsevier Science.

Bertram, H. C., & Andersen, H. J. (2007). NMR and the water-holding issue of pork. *Journal of Animal Breeding and Genetics, 124*, 35-42. doi: DOI 10.1111/j.1439-0388.2007.00685.x

Bertram, H. C., Donstrup, S., Karlsson, A. H., & Andersen, H. J. (2002). Continuous distribution analysis of T-2 relaxation in meat - an approach in the determination of water-holding capacity. *Meat Sci, 60*(3), 279-285. doi: Doi 10.1016/S0309-1740(01)00134-6

Blanco, M., & Villarroya, I. (2002). NIR spectroscopy: a rapid-response analytical tool. *Trac-Trends in Analytical Chemistry, 21*(4), 240-250. doi: Doi 10.1016/S0165-9936(02)00404-1

Blixt, Y., & Borch, E. (2002). Comparison of shelf life of vacuum-packed pork and beef. *Meat Sci, 60*(4), 371-378. doi: Doi 10.1016/S0309-1740(01)00145-0

Bocker, U., Wubshet, S. G., Lindberg, D., & Afseth, N. K. (2017). Fourier-transform infrared spectroscopy for characterization of protein chain reductions in enzymatic reactions. *Analyst, 142*(15), 2812-2818. doi: 10.1039/c7an00488e

Briskey, E. J. (1964). Etiological Status and Associated Studies of Pale, Soft, Exudative Porcine Musculature. *Adv Food Res, 13*, 89-178.

Brondum, J., Munck, L., Henckel, P., Karlsson, A., Tornberg, E., & Engelsen, S. B. (2000). Prediction of water-holding capacity and composition of porcine meat by comparative spectroscopy. *Meat Sci, 55*(2), 177-185.

Bruker. (2017). Solutions for the Meat Processing Industry. Retrieved 15 October, 2017, from https://www.bruker.com/applications/food-agriculture/food-quality/meat.html

Candek-Potokar, M., Prevolnik, M., & Skrlep, M. (2006). Ability of near infrared spectroscopy to predict pork technological traits. *Journal of near Infrared Spectroscopy, 14*(4), 269-277.

Channon, H. A., Payne, A. M., & Warner, R. D. (2000). Halothane genotype, pre-slaughter handling and stunning method all influence pork quality. *Meat Sci, 56*(3), 291-299. doi: Doi 10.1016/S0309-1740(00)00056-5

Cheng, Q., & Sun, D. W. (2008). Factors affecting the water holding capacity of red meat products: a review of recent research advances. *Crit Rev Food Sci Nutr, 48*(2), 137-159. doi: 10.1080/10408390601177647

Christensen, J., Norgaard, L., Bro, R., & Engelsen, S. B. (2006). Multivariate autofluorescence of intact food systems. *Chem Rev, 106*(6), 1979-1994. doi: 10.1021/cr050019q

Christensen, L. B. (2003). Drip loss sampling in porcine m. longissimus dorsi. *Meat Sci, 63*(4), 469-477.

DeNoyer, L. K., & Dodd, J. K. (2001). Smoothing and derivatives in spectroscopy. In J. M. C. a. P. R. Griffiths (Ed.), *Handbook of Vibrational Spectroscopy* (Vol. 3, pp. 2173-2183). Chichester, U.K.: John Wiley & Sons Ltd.

ElMasry, G., Sun, D. W., & Allen, P. (2011). Non-destructive determination of water-holding capacity in fresh beef by using NIR hyperspectral imaging. *Food Research International, 44*(9), 2624-2633. doi: DOI 10.1016/j.foodres.2011.05.001

ElMasry, G., Sun, D. W., & Allen, P. (2012). Near-infrared hyperspectral imaging for predicting colour, pH and tenderness of fresh beef. *Journal of Food Engineering, 110*(1), 127-140. doi: DOI 10.1016/j.jfoodeng.2011.11.028

Forrest, J. C., Morgan, M. T., Borggaard, C., Rasmussen, A. J., Jespersen, B. L., & Andersen, J. R. (2000). Development of technology for the early post mortem prediction of water holding capacity and drip loss in fresh pork. *Meat Sci, 55*(1), 115-122.

FOSS. (2017). FoodScan™ Meat Analyser. Retrieved 15 October, 2017, from https://www.fossanalytics.com/en/products/foodscan-meat-analyser

Gardner, M. A., Huff Lonergan, E., & Lonergan, S. M. (2005). *Prediction of fresh pork quality using indicators of protein degradation and calpain activation*. Paper presented at the 51st International Congress of Meat Science and Technology, Baltimaore, Maryland USA.

Geesink, G. H., Schreutelkamp, F. H., Frankhuizen, R., Vedder, H. W., Faber, N. M., Kranen, R. W., & Gerritzen, M. A. (2003). Prediction of pork quality attributes from near infrared reflectance spectra. *Meat Sci, 65*(1), 661-668. doi: 10.1016/S0309-1740(02)00269-3

Goll, D. E., Thompson, V. F., Li, H., Wei, W., & Cong, J. (2003). The calpain system. *Physiol Rev, 83*(3), 731-801. doi: 10.1152/physrev.00029.2002

Hamilton, D. N., Ellis, M., Miller, K. D., McKeith, F. K., & Parrett, D. F. (2000). The effect of the Halothane and Rendement Napole genes on carcass and meat quality characteristics of pigs. *J Anim Sci, 78*(11), 2862-2867.

Herrero, A. M. (2008). Raman spectroscopy a promising technique for quality assessment of meat and fish: A review. *Food Chemistry, 107*(4), 1642-1651. doi: DOI 10.1016/j.foodchem.2007.10.014

Honikel, K. O. (1998). Reference methods for the assessment of physical characteristics of meat. *Meat Sci, 49*(4), 447-457.

Huff-Lonergan, E., & Lonergan, S. M. (2005). Mechanisms of water-holding capacity of meat: The role of postmortem biochemical and structural changes. *Meat Sci, 71*(1), 194-204. doi: 10.1016/j.meatsci.2005.04.022

Huff Lonergan, E., Zhang, W., & Lonergan, S. M. (2010). Biochemistry of postmortem muscle - lessons on mechanisms of meat tenderization. *Meat Sci, 86*(1), 184-195. doi: 10.1016/j.meatsci.2010.05.004

Hughes, J. M., Oiseth, S. K., Purslow, P. P., & Warner, R. D. (2014). A structural approach to understanding the interactions between colour, water-holding capacity and tenderness. *Meat Sci, 98*(3), 520-532. doi: 10.1016/j.meatsci.2014.05.022

Isaksson, T., Nilsen, B. N., Togersen, G., Hammond, R. P., & Hildrum, K. I. (1996). On-line, proximate analysis of ground beef directly at a meat grinder outlet. *Meat Sci, 43*(3-4), 245-253. doi: Doi 10.1016/S0309-1740(96)00016-2

Joo, S. T., Kauffman, R. G., Kim, B. C., & Park, G. B. (1999). The relationship of sarcoplasmic and myofibrillar protein solubility to colour and water-holding capacity in porcine longissimus muscle. *Meat Sci, 52*(3), 291-297.

Kapper, C., Klont, R. E., Verdonk, J. M. A. J., & Urlings, H. A. P. (2012). Prediction of pork quality with near infrared spectroscopy (NIRS) 1. Feasibility and robustness of NIRS measurements at laboratory scale. *Meat Sci, 91*(3), 294-299. doi: DOI 10.1016/j.meatsci.2012.02.005

Kapper, C., Klont, R. E., Verdonk, J. M. A. J., Williams, P. C., & Urlings, H. A. P. (2012). Prediction of pork quality with near infrared spectroscopy (NIRS) 2. Feasibility and robustness of NIRS

measurements under production plant conditions. *Meat Sci, 91*(3), 300-305. doi: DOI 10.1016/j.meatsci.2012.02.006
Koohmaraie, M. (1992). The Role of Ca-2+-Dependent Proteases (Calpains) in Postmortem Proteolysis and Meat Tenderness. *Biochimie, 74*(3), 239-245. doi: Doi 10.1016/0300-9084(92)90122-U
Koohmaraie, M., Schollmeyer, J. E., & Dutson, T. R. (1986). Effect of Low-Calcium-Requiring Calcium Activated Factor on Myofibrils under Varying Ph and Temperature Conditions. *Journal of Food Science, 51*(1), 28-&. doi: DOI 10.1111/j.1365-2621.1986.tb10828.x
Krimm, S., & Bandekar, J. (1986). VIBRATIONAL SPECTROSCOPY AND CONFORMATION OF PEPTIDES, POLYPEPTIDES, AND PROTEINS. *Advances in Protein Chemistry, 38*, 181-364. doi: 10.1016/s0065-3233(08)60528-8
Kristensen, L., & Purslow, P. P. (2001). The effect of ageing on the water-holding capacity of pork: role of cytoskeletal proteins. *Meat Sci, 58*(1), 17-23. doi: Doi 10.1016/S0309-1740(00)00125-X
Kuo, C. C., & Chu, C. Y. (2003). Quality characteristics of Chinese sausages made from PSE pork. *Meat Sci, 64*(4), 441-449. doi: Doi 10.1016/S0309-1740(02)00213-9
Lametsch, R., Roepstorff, P., Moller, H. S., & Bendixen, E. (2004). Identification of myofibrillar substrates for mu-calpain. *Meat Sci, 68*(4), 515-521. doi: 10.1016/j.meatsci.2004.03.018
Li-Chan, E. C. Y. (1996). The applications of Raman spectroscopy in food science. *Trends in Food Science & Technology, 7*(11), 361-370. doi: 10.1016/s0924-2244(96)10037-6
Li-Chan, E. C. Y., Ismail, A. A., Sedman, J., & van de Voort, F. R. (2002). Vibrational Spectroscopy of Food and Food Products *Handbook of Vibrational Spectroscopy*: John Wiley & Sons, Ltd.
Liao, Y. T., Fan, Y. X., & Cheng, F. (2010). On-line prediction of fresh pork quality using visible/near-infrared reflectance spectroscopy. *Meat Sci, 86*(4), 901-907. doi: DOI 10.1016/j.meatsci.2010.07.011
Lord, R. C., & Yu, N. T. (1970). Laser-excited Raman spectroscopy of biomolecules. I. Native lysozyme and its constituent amino acids. *J Mol Biol, 50*(2), 509-524.
Martens, H., & Martens, M. (2000). Modified Jack-knife estimation of parameter uncertainty in bilinear modelling by partial least squares regression (PLSR). *Food Quality and Preference, 11*(1-2), 5-16. doi: Doi 10.1016/S0950-3293(99)00039-7
Martens, H., & Martens, M. (2001). *Introduction to multivariate data analysis for understanding quality*. Chichester, U.K.: John Wiley & Sons Ltd.
Mathews, C. K., Van Holde, K. E., & Ahern, K. G. (2000). *Biochemistry*: Benjamin Cummings.
Melody, J. L., Lonergan, S. M., Rowe, L. J., Huiatt, T. W., Mayes, M. S., & Huff-Lonergan, E. (2004). Early postmortem biochemical factors influence tenderness and water-holding capacity of three porcine muscles. *J Anim Sci, 82*(4), 1195-1205.
Motzer, E. A., Carpenter, J. A., Reynolds, A. E., & Lyon, C. E. (1998). Quality of restructured hams manufactured with PSE pork as affected by water binders. *Journal of Food Science, 63*(6), 1007-1011.
Nache, M., Hinrichs, J., Scheier, R., Schmidt, H., & Hitzmann, B. (2016). Prediction of the pH as indicator of porcine meat quality using Raman spectroscopy and metaheuristics. *Chemometrics and Intelligent Laboratory Systems, 154*, 45-51. doi: 10.1016/j.chemolab.2016.03.011
Nache, M., Scheier, R., Schmidt, H., & Hitzmann, B. (2015). Non-invasive lactate- and pH-monitoring in porcine meat using Raman spectroscopy and chemometrics. *Chemometrics and Intelligent Laboratory Systems, 142*, 197-205. doi: 10.1016/j.chemolab.2015.02.002
O'Neill, D. J., Lynch, P. B., Troy, D. J., Buckley, D. J., & Kerry, J. P. (2003). Influence of the time of year on the incidence of PSE and DFD in Irish pigmeat. *Meat Sci, 64*(2), 105-111.
Offer, G. (1991). Modelling of the formation of pale, soft and exudative meat: Effects of chilling regime and rate and extent of glycolysis. *Meat Sci, 30*(2), 157-184. doi: 10.1016/0309-1740(91)90005-B

Offer, G., & Cousins, T. (1992). The mechanism of drip production: Formation of two compartments of extracellular space in muscle Post mortem. *J. Sci. Food Agric., 58*, 107-116.
OpenStax. (2013). *Anatomy & Physiology.* Retrieved from https://openstax.org/details/anatomy-and-physiology
Otto, G., Roehe, R., Looft, H., Thoelking, L., & Kalm, E. (2004). Comparison of different methods for determination of drip loss and their relationships to meat quality and carcass characteristics in pigs. *Meat Sci, 68*(3), 401-409. doi: 10.1016/j.meatsci.2004.04.007
Pavia, D. L., Lampman, G. M., & Kriz, G. S. (2001). *Introduction to Spectroscopy: A Guide for Students of Organic Chemistry*: Harcourt College Publishers.
Pearce, K. L., Rosenvold, K., Andersen, H. J., & Hopkins, D. L. (2011). Water distribution and mobility in meat during the conversion of muscle to meat and ageing and the impacts on fresh meat quality attributes--a review. *Meat Sci, 89*(2), 111-124. doi: 10.1016/j.meatsci.2011.04.007
Pedersen, D. K., Morel, S., Andersen, H. J., & Balling Engelsen, S. (2003). Early prediction of water-holding capacity in meat by multivariate vibrational spectroscopy. *Meat Sci, 65*(1), 581-592. doi: 10.1016/S0309-1740(02)00251-6
Penner, M. H. (2010). Basic Principles of Spectroscopy *Food Analysis* (pp. 375-385). Boston, MA: Springer US.
Perisic, N., Afseth, N. K., Ofstad, R., & Kohler, A. (2011). Monitoring Protein Structural Changes and Hydration in Bovine Meat Tissue Due to Salt Substitutes by Fourier Transform Infrared (FTIR) Microspectroscopy. *J Agric Food Chem, 59*(18), 10052-10061. doi: 10.1021/jf201578b
Perkins, W. D. (1986). Fourier Transform-Infrared Spectroscopy .1. Instrumentation. *Journal of Chemical Education, 63*(1), A5-A10.
Perkins, W. D. (1987a). Fourier-Transform Infrared-Spectroscopy .2. Advantages of Ft-Ir. *Journal of Chemical Education, 64*(11), A269-A271.
Perkins, W. D. (1987b). Fourier-Transform Infrared-Spectroscopy .3. Applications. *Journal of Chemical Education, 64*(12), A296-&.
Prediktor. (2017). Meat. Retrieved 15 October, 2017, from http://www.prediktor.no/nb/instruments/industries/food/meat/#.WeMg0HkUmpo
Prieto, N., Pawluczyk, O., Dugan, M. E. R., & Aalhus, J. L. (2017). A Review of the Principles and Applications of Near-Infrared Spectroscopy to Characterize Meat, Fat, and Meat Products. *Applied Spectroscopy, 71*(7), 1403-1426. doi: 10.1177/0003702817709299
Purslow, P. P., Mandell, I. B., Widowski, T. M., Brown, J., Delange, C. F. M., Robinson, J. A. B., . . . VanderVoort, G. (2008). Modelling quality variations in commercial Ontario pork production. *Meat Sci, 80*(1), 123-131. doi: 10.1016/j.meatsci.2008.05.022
Rasmussen, A. J., & Andersson, M. (1996, 1-6 September). *New method for determination of drip loss in pork muscles.* Paper presented at the In Proceedings 42nd international congress of meat science and technology, Lillehammer, Norway.
Rosenvold, K., & Andersen, H. J. (2003). Factors of significance for pork quality-a review. *Meat Sci, 64*(3), 219-237. doi: 10.1016/S0309-1740(02)00186-9
Rybarczyk, A., Karamucki, T., Pietruszka, A., Rybak, K., & Matysiak, B. (2015). The effects of blast chilling on pork quality. *Meat Sci, 101*, 78-82. doi: 10.1016/j.meatsci.2014.11.006
Salas, R. C., & Mingala, C. N. (2017). Genetic Factors Affecting Pork Quality: Halothane and Rendement Napole Genes. *Anim Biotechnol, 28*(2), 148-155. doi: 10.1080/10495398.2016.1243550
Santos, C., Roseiro, L. C., Goncalves, H., & Melo, R. S. (1994). Incidence of different pork quality categories in a Portuguese slaughterhouse: A survey. *Meat Sci, 38*(2), 279-287. doi: 10.1016/0309-1740(94)90117-1
Savage, A. W., Warriss, P. D., & Jolley, P. D. (1990). The amount and composition of the proteins in drip from stored pig meat. *Meat Sci, 27*(4), 289-303. doi: 10.1016/0309-1740(90)90067-G

Savenije, B., Geesink, G. H., van der Palen, J. G. P., & Hemke, G. (2006). Prediction of pork quality using visible/near-infrared reflectance spectroscopy. *Meat Sci, 73*(1), 181-184. doi: 10.1016/j.meatsci.2005.11.006

Scheier, R., Bauer, A., & Schmidt, H. (2014). Early Postmortem Prediction of Meat Quality Traits of Porcine Semimembranosus Muscles Using a Portable Raman System. *Food and Bioprocess Technology, 7*(9), 2732-2741. doi: DOI 10.1007/s11947-013-1240-3

Scheier, R., Kohler, J., & Schmidt, H. (2014). Identification of the early postmortem metabolic state of porcine M. semimembranosus using Raman spectroscopy. *Vibrational Spectroscopy, 70*, 12-17. doi: DOI 10.1016/j.vibspec.2013.10.001

Scheier, R., Scheeder, M., & Schmidt, H. (2015). Prediction of pork quality at the slaughter line using a portable Raman device. *Meat Sci, 103*, 96-103. doi: 10.1016/j.meatsci.2015.01.009

Scheier, R., & Schmidt, H. (2013). Measurement of the pH value in pork meat early postmortem by Raman spectroscopy. *Applied Physics B-Lasers and Optics, 111*(2), 289-297. doi: DOI 10.1007/s00340-012-5332-y

Schilling, M. W., Mink, L. E., Gochenour, P. S., Marriott, N. G., & Alvarado, C. Z. (2003). Utilization of pork collagen for functionality improvement of boneless cured ham manufactured from pale, soft, and exudative pork. *Meat Sci, 65*(1), 547-553. doi: 10.1016/S0309-1740(02)00247-4

Schmidt, H., Sowoidnich, K., & Kronfeldt, H. D. (2010). A Prototype Hand-Held Raman Sensor for the in Situ Characterization of Meat Quality. *Applied Spectroscopy, 64*(8), 888-894.

Smith, E., & Dent, G. (2013). *Modern Raman Spectroscopy: A Practical Approach*: Wiley.

TOMRA. (2017). IN-LINE MEAT & SEAFOOD ANALYSIS BY TOMRA'S QVISION Retrieved 03 November, 2017, from https://www.tomra.com/en/sorting/food/process-analytics/qvision

Torley, P. J., D'Arcy, B. R., & Trout, G. R. (2000). The effect of ionic strength, polyphosphates type, pH, cooking temperature and preblending on the functional properties of normal and pale, soft, exudative (PSE) pork. *Meat Sci, 55*(4), 451-462. doi: Doi 10.1016/S0309-1740(00)00004-8

Torres, R. D., Cazedey, H. P., Fontes, P. R., Ramos, A. D. S., & Ramos, E. M. (2017). Drip Loss Assessment by Different Analytical Methods and Their Relationships with Pork Quality Classification. *Journal of Food Quality*, 1-8. doi: 10.1155/2017/9170768

Van Oeckel, M. J., Warnants, N., & Boucque, C. V. (1999). Comparison of different methods for measuring water holding capacity and juiciness of pork versus on-line screening methods. *Meat Sci, 51*(4), 313-320.

Vermeulen, L., de Perre, V. V., Permentier, L., De Bie, S., Verbeke, G., & Geers, R. (2015). Pre-slaughter handling and pork quality. *Meat Sci, 100*, 118-123. doi: 10.1016/j.meatsci.2014.09.148

Warner, R. D., Kauffman, R. G., & Greaser, M. L. (1997). Muscle protein changes post mortem in relation to pork quality traits. *Meat Sci, 45*(3), 339-352.

Warriss, P. D., & Brown, S. N. (1987). The relationships between initial pH, reflectance and exudation in pig muscle. *Meat Sci, 20*(1), 65-74. doi: 10.1016/0309-1740(87)90051-9

Weeranantanaphan, J., Downey, G., Allen, P., & Sun, D. W. (2011). A review of near infrared spectroscopy in muscle food analysis: 2005-2010. *Journal of near Infrared Spectroscopy, 19*(2), 61-104. doi: Doi 10.1255/Jnirs.924

Wu, Z. Y., Bertram, H. C., Kohler, A., Bocker, U., Ofstad, R., & Andersen, H. J. (2006). Influence of aging and salting on protein secondary structures and water distribution in uncooked and cooked pork. A combined FT-IR microspectroscopy and H-1 NMR relaxometry study. *J Agric Food Chem, 54*(22), 8589-8597. doi: 10.1021/jf061576w

Wubshet, S. G., Mage, I., Bocker, U., Lindberg, D., Knutsen, S. H., Rieder, A., . . . Afseth, N. K. (2017). FTIR as a rapid tool for monitoring molecular weight distribution during enzymatic protein hydrolysis of food processing by-products. *Analytical Methods, 9*(29), 4247-4254. doi: 10.1039/C7AY00865A

Xiong, Z. J., Sun, D. W., Zeng, X. A., & Xie, A. G. (2014). Recent developments of hyperspectral imaging systems and their applications in detecting quality attributes of red meats: A review. *Journal of Food Engineering, 132*, 1-13. doi: DOI 10.1016/j.jfoodeng.2014.02.004
Zeng, Z., Li, C., & Ertbjerg, P. (2017). Relationship between proteolysis and water-holding of myofibrils. *Meat Sci, 131*, 48-55. doi: 10.1016/j.meatsci.2017.04.232

PAPER I

Meat Science 125 (2017) 1–9

Contents lists available at ScienceDirect

Meat Science

journal homepage: www.elsevier.com/locate/meatsci

Analyzing pH-induced changes in a myofibril model system with vibrational and fluorescence spectroscopy

Petter Vejle Andersen *, Eva Veiseth-Kent, Jens Petter Wold

Nofima AS, Osloveien 1, 1430 Ås, Norway

ARTICLE INFO

Article history:
Received 3 June 2016
Received in revised form 30 September 2016
Accepted 10 November 2016
Available online 14 November 2016

Keywords:
Water-holding capacity
pH
Proteins
Vibrational spectroscopy
Fluorescence

ABSTRACT

The decline of pH and ultimate pH in meat postmortem greatly influences meat quality (e.g. water holding capacity). Four spectroscopic techniques, Raman, Fourier transform infrared (FT-IR), near infrared (NIR) and fluorescence spectroscopy, were used to study protein and amino acid modifications to determine pH-related changes in pork myofibril extracts at three different pH-levels, 5.3, 5.8 and 6.3. Protonation of side-chain carboxylic acids of aspartic and glutamic acid and changes in secondary structure, mainly the amide I–III peaks, were the most important features identified by Raman and FT-IR spectroscopy linked to changes in pH. Fluorescence spectroscopy identified tryptophan interaction with the molecular environment as the most important contributor to changes in the spectra. NIR spectroscopy gave no significant contributions to interpreting protein structure related to pH. Results from our study are useful for interpreting spectroscopic data from meat where pH is an important variable.

1. Introduction

The postmortem pH-decline in meat has been studied extensively, and has been shown to affect overall quality of meat and meat products significantly (Fischer, 2007). The main motivations for measuring pH in meat is that it is closely related to water-holding capacity (WHC) (Schafer, Rosenvold, Purslow, Andersen, & Henckel, 2002), it impacts the potential for proteolysis postmortem and subsequent changes in protein structure (Huff-Lonergan & Lonergan, 2005), and it influences shelf-life of meat (Blixt & Borch, 2002). WHC is an important quality parameter for meat as it influences total salable weight, eating quality (e.g. juiciness (Lawrie, 1985)) and nutritional value of meat (Savage, Warriss, & Jolley, 1990). Poor WHC causes high amounts of liquid exuding from the meat, which starts forming when muscles are contracting during the rigor mortis process postmortem, and continues for several days and weeks afterwards. The amount of drip formed is dependent on several factors, such as antemortem handling at the slaughterhouse (Henckel, Karlsson, Oksbjerg, & Soholm Petersen, 2000), rate of pH decline and ultimate pH postmortem (Bee, Anderson, Lonergan, & Huff-Lonergan, 2007), enzyme activity (Davis, Sebranek, Huff-Lonergan, & Lonergan, 2004), genetic predisposition and temperature during conditioning and storage (Cheng & Sun, 2008). Many of these factors are interconnected, and this signifies that WHC is a very complex quality trait in meat. Thus, there is a need for more knowledge about which mechanisms influence WHC in a significant way, and there is a demand for a method to predict WHC in the slaughterhouse. Spectroscopic analyses are prime candidates to contribute to advancing the knowledge of both these topics, because they are rapid techniques suitable for on-line measurements that can give specific biochemical information of meat.

Two of the most promising spectroscopic techniques in this regard are Raman and Fourier transform infrared (FT-IR) spectroscopy. Using these techniques, it is possible to extract information about secondary structure of proteins, protein and amino acid interaction with the environment and protonation of amino acids (Tu, 1986), all of which may be subjected to modification as pH changes and the proteins can subsequently act as pH-probes. By following the pH decline in meat postmortem and simultaneously record Raman spectra, Nache, Scheier, Schmidt, and Hitzmann (2015) was able to predict pH with cross validated coefficient of determination (r^2_{cv})of 0.97 and cross-validated root mean square error (RMSECV) of 0.06 pH units. Raman measurements at the slaughter line has not yielded as good results for predicting pH, but are showing some promise, with an r^2_{cv} of 0.55 and RMSECV of 0.09 pH units for pH at 35 min. postmortem and an r^2_{cv} of 0.31 and RMSECV of 0.05 pH units for pH at 24 h. postmortem in a recent study (Scheier, Scheeder, & Schmidt, 2015). FT-IR and Raman spectroscopy are also showing promise as methods of predicting WHC. Using FT-IR, Pedersen et al. was able to predict WHC with an r^2 of 0.89 and RMSECV of 0.86% in a research setting and an r^2 of 0.79 and RMSECV of 1.06% in an industrial trial (Pedersen, Morel, Andersen, & Balling Engelsen, 2003). Raman spectroscopy performed at 60–120 min. postmortem in a cooling room achieved an r^2_{cv} of 0.73 and a RMSECV of 1.0% for drip loss (Scheier, Bauer, & Schmidt, 2014), while measurements at 30–60 min.

* Corresponding author.
E-mail addresses: petter.andersen@nofima.no (P.V. Andersen), eva.veiseth-kent@nofima.no (E. Veiseth-Kent), jens.petter.wold@nofima.no (J.P. Wold).

http://dx.doi.org/10.1016/j.meatsci.2016.11.005
0309-1740/

postmortem at the slaughter line achieved an r^2_{cv} of 0.52 and a RMSECV of 0.6% for drip loss (Scheier et al., 2015).

Near-infrared (NIR) spectroscopy has successfully been implemented in slaughterhouses to analyze main chemical composition of meat (Prieto, Roehe, Lavin, Batten, & Andres, 2009), and it has been investigated extensively as a method for predicting pH and WHC. In one recent study using a hyperspectral NIR spectroscopy laboratory set-up, Barbin, ElMasry, Sun, and Allen (2012) managed to predict pH with an r^2_{cv} of 0.86 and a RMSECV of 0.11 pH units and drip loss with an r^2_{cv} of 0.88 and a RMSECV of 0.73%. Another approach is to use an insertion probe NIR instrument, and Forrest et al. (2000) was able to predict drip loss with a correlation coefficient (r) of 0.84 and root mean square error of prediction (RMSEP) of 1.8% using such an instrument.

Fluorescence spectroscopy can give important information about the three amino acids phenylalanine (Phe), tyrosine (Tyr) and tryptophan (Trp) and their interactions with the molecular environment (Christensen, Norgaard, Bro, & Engelsen, 2006), thus giving a possible link between proteins and pH in meat. The research on fluorescence spectroscopy for measuring pH and WHC is not as thorough as for Raman, FT-IR and NIR, but there have been a few attempts to utilize this technique as well. An example is a study by Brondum et al. (2000), where drip loss was predicted with moderate success by laboratory fluorescence measurements giving an r of 0.68 and standard error of prediction (SEP) of 2.27%.

In many of the studies using Raman, FT-IR, NIR or fluorescence spectroscopy, the focus has been to predict pH and WHC, and the interpretation of the spectral features and what information the spectra can give about protein structure relevant for meat quality has not been emphasized. In meat samples, changes in α-helical secondary protein structure have been linked to changes pH for both Raman spectra (Scheier, Kohler, & Schmidt, 2014) and FT-IR spectra (Pedersen et al., 2003). In most studies with NIR and fluorescence related to pH and WHC an interpretation of the connection between spectra, protein structure and pH is lacking.

Thus, the aim of this study was to gain more detailed knowledge regarding the potential effects of pH on the spectroscopic properties of myofibrillar proteins. Since pH is known to influence WHC of meat, this knowledge may in the long run lay grounds for improved spectroscopic modelling/prediction of WHC. In order to avoid the influence of other chemical and physical features of muscle on the spectroscopic measurements, a myofibril model system, containing extracted myofibril proteins from pork meat, was used in this study to examine protein modifications at selected pH-levels relevant in postmortem meat by Raman, FT-IR, NIR and fluorescence spectroscopy. Similar model systems have been used by others to study the effect of e.g. proteolysis on muscle proteins (Koohmaraie, Schollmeyer, & Dutson, 1986) and the influence of protein oxidation on digestibility of meat proteins (Sante-Lhoutellier, Aubry, & Gatellier, 2007). By using myofibril extracts, it is possible to make samples with homogenous pH, obtain protein-specific spectroscopic influence and acquire a deeper understanding of protein-protein interactions related to pH in meat. This gives an opportunity to weight spectral channels in statistical models based on general protein characteristics related to pH, and it can give an important contribution to understanding some of the mechanisms of WHC in meat.

2. Materials and methods

2.1. Animals, myofibril isolation and sample preparation

Five pigs were slaughtered at a commercial abattoir in Tønsberg, Norway, following standard slaughtering procedures. The entire *M. longissimus dorsi* muscle was excised from the left side of each carcass approximately 24 h postmortem. The samples were stored at 4 °C and transported to Nofima AS, Ås, where the muscles were sliced, vacuum packed and stored at −20 °C.

A meat slice from each pig was thawed in room temperature prior to isolation. Connective tissue and fat was removed before ~20 g of each sample was sliced in small cubes and transferred to a 250 ml centrifuge tube. 160 ml pyrophosphate relaxing buffer (PRB) (2 mM $Na_4P_2O_7$, 2 mM $MgCl_2$, 2 mM triethylene glycol diamine tetraacetic acid, 10 mM Tris(hydroxymethyl)aminomethane maleate salt, 0.5 mM dithiothreitol, 0.1 mM phenylmethanesulfonyl fluoride, pH 6.8) was added to the tube and sample was homogenized using a polytron at a speed of 15,000 rpm for 30 s three times with a 30 s resting step in between. The homogenate was centrifuged at 1000*g* for 10 min at 4 °C. After centrifugation, the homogenate was washed as follows: discarded the supernatant, added 200 ml extraction buffer (PRB without $Na_4P_2O_7$ and PMSF), rigorously shaking the homogenate prior to centrifugation as described earlier. The supernatant was discarded, 200 ml extraction buffer was added and the homogenate was rigorously shaken, before the homogenate was filtered through a sieve (400-μm mask width for sample 1 to 4, 710-μm for sample 5) to remove connective tissue, and once more centrifuged as described earlier. After another step of washing, the supernatant was discarded and 200 ml of Triton X-100 buffer (extraction buffer supplemented with 0.02% w/v Triton X-100) was added, the sample was rigorously shaken and centrifuged as described earlier. The samples were washed three times and finally stored at −20 °C in 42.5% (v/v) glycerol in extraction buffer. Protein concentration in each of the myofibril extracts was measured by the Biuret method (Gornall, Bardawill, & David, 1949).

Myofibril extracts were thawed in room temperature, then transferred to a centrifuge tube and subsequently washed three times in extraction buffer (using the same volume of extraction buffer as sample volume after removal of the supernatant) to remove glycerol. Each sample was diluted to a protein concentration of ~20 mg/ml with extraction buffer. The diluted sample was distributed in three test tubes, each containing 15 ml. A Beckman Φ31 pH Meter (Brea, CA, USA) was used to measure and adjust pH in each tube to 5.3, 5.8 or 6.3 (±0.1) with 3 N HCl. The pH-adjusted samples were distributed in three new test tubes, each containing 5 ml sample, giving 45 samples all together. All samples were incubated for 2 h at 4 °C on a rotating test tube holder at 40 rpm. After measuring pH, all samples were analyzed by Raman, FT-IR, NIR and fluorescence spectroscopy. The experiment was conducted over three days, where samples from two pigs were prepared and analyzed day one and day two, and one pig on day three.

2.2. Spectroscopy and data analysis

2.2.1. Raman microspectroscopy

A droplet from each sample was placed on an aluminum plate with a plastic Pasteur pipette and left to dry for 2 h at room temperature prior to Raman spectroscopic analysis.

Raman spectra were recorded on a LabRam HR 800 Raman microscope (Horiba Scientific, France). The Raman system was equipped with a 785 nm laser used for excitation and was coupled confocally to a spectrograph with a focal length of 800 mm equipped with a grating of 600 g/mm. The laser light was tightly focused using a Fluotar ×50 objective (Leica, Germany, 0.55 NA). Scattered Raman photons from the sample were collected in the backscattered geometry by the same microscope objective and collected by the spectrometer. The confocal hole was set at 1000 μm. The spectrometer was equipped with an air-cooled deep depletion CCD array detector (1024 × 256 pixels). The laser power at the sample surface was approx. 90 mW, and for all samples an exposure time of 5 times 5 s was used in the range 300–1800 cm^{-1}. The spectra were calibrated to a standard silicon reference peak at 520.7 cm^{-1}. Three spectra were recorded from different locations on the dried droplet for each sample. Data acquisition and instrument control was carried out by using LabSpec software version 5.93.20 (HORIBA Jobin Yvon SAS).

2.2.2. FT-IR spectroscopy

Six microlitres of each sample were transferred onto 96-well IR-transparent Si-plates and kept to dry overnight in a desiccator. FT-IR-measurements were carried out with a High-Throughput Screening Extension (HTS-XT) coupled to a Tensor 27 spectrometer (Bruker Optics, Germany) taking 40 scans per sample. The spectra were recorded in transmission mode in the spectral region 400 to 4000 cm^{-1} with a resolution of 4 cm^{-1}, and an aperture of 6.0 mm. Prior to each sample measurement, background spectra of the Silicon substrate were collected to account for variation in water vapor and CO_2. All samples were measured in triplicate, and the spectra were averaged for each sample prior to analyses.

2.2.3. NIR spectroscopy

The sample (~1 ml) was transferred to a Gold Reflectance Cellkit 0.1 MM sample holder (4 cm i.d.), and placed in the spectrophotometer. All samples were scanned in liquid with an XDS Rapid content analyzer (FOSS Analytical, Hillerød, Denmark) measuring in the 400–2500 nm wavelength region at 0.5 nm intervals. Spectra were recorded as log(1/R) with FOSS NIRSystem Vision software. Three spectra from each sample were recorded, and the spectra were averaged for each sample prior to analyses.

2.2.4. Fluorescence spectroscopy

A subsample of 3 ml of each extract was filled in quarts cuvettes (10 mm ∗ 10 mm ∗ 5 mm). Fluorescence was measured in front face mode since the samples were thin slurries with high absorption and light scattering. Fluorescence excitation emission landscapes were collected for the excitation range 280–330 nm (10 nm step size) and the emission range 300–550 nm (4 nm step size). The measurements were carried out with a FluoroMax-4 (Horiba Scientific, Edison, NJ, USA). Close to completion of measurements it was discovered that a focusing lens in the front face set-up did not transmit sample emission wavelengths from below about 350 nm. The spectra were therefore cut-off below this wavelength.

2.3. Pre-processing and data analysis

2.3.1. Pre-processing of spectral data

Pre-processing of spectral data was done to give comparable spectra for further analysis, by reducing or removing the impact of noise, scatter effects and other undesirable alterations in the spectra.

Raman spectra were pre-processed by means of full extended multiplicative scattering correction (EMSC) (Afseth & Kohler, 2012) including 6th order polynomial. The three spectra from each sample were averaged and subsequently smoothed by applying a Savitzky-Golay filter with four smoothing points on each side in the second order.

Pre-processing of FT-IR spectra was done by first applying Savitzky–Golay 2nd derivative (DeNoyer & Dodd, 2001) with two polynomials and four smoothing points on each side in the region from 1800 to 600 cm^{-1}, followed by EMSC in the same region.

The NIR spectra were divided in three regions, the VIS region 400 to 700 cm^{-1}, 1100 to 1700 cm^{-1}, and 1700 to 2400 cm^{-1}, before EMSC was applied to each region separately.

Fluorescence spectra were subjected to standard normal variate (SNV) (Barnes, Dhanoa, & Lister, 1989) pre-processing for each excitation and emission spectrum recorded. One sample was removed prior to SNV due to low signal.

2.3.2. Data analysis

Principal component analysis (PCA) was used to reveal if there were inherent systematic patterns of variation between samples (Martens & Martens, 2001). PCA was used to verify that samples were grouped according to pH, meaning that changes to difference spectra are representative of the pH-related variation in the spectra. Partial least squares regression (PLSR) was used for determining relationship between pH measurements and spectroscopic data, where information important for explaining variation in pH gets emphasized (Martens & Martens, 2001). Both analyses were cross-validated using leave-one-out procedure. An uncertainty test was performed for the PLSR model to give information about important variables in the model. Reference measurements for PLSR were the measured pH in each sample after 2 h of incubation. Difference spectra for Raman and FT-IR spectroscopy was made by averaging all pre-processed spectra for each pH group, and subsequently calculating pH 5.8 minus pH 5.3 and pH 6.3 minus pH 5.8.

PCA, PLSR and difference spectra calculations (for Raman and FT-IR) was performed in the following spectral regions: Raman: 300 to 1800 cm^{-1}, FT-IR: from 600 to 1800 cm^{-1}, NIR: each of the spectral regions from EMSC separately and fluorescence: excitation at 290 and 330 nm and emission at 300 nm.

Data analysis was carried out using Open EMSC toolbox for MATLAB freely downloadable from http://nofimaspectroscopy.org in MATLAB version R2013b (The MathWorks, Natick, MA) and using The Unscrambler® X version 10.3 (CAMO Process AS, Norway).

3. Results and discussion

3.1. Myofibril extracts

A summary of measured pH in the myofibril extracts after incubation is shown in Table 1. There was some variation in each of the pH classes, but all samples in each class were still separated by at least 0.29 pH units from the samples in the other classes. Although some samples had lower pH than intended, they were all within the range of relevant pH for postmortem meat.

3.2. Raman spectroscopy

Raman spectra from all samples showed a similar structure in the entire recorded region, implying that the myofibrils in the different samples were comparable (Fig. 1). Assignment of Raman modes useful for interpretation of protein structure and modification was done according to published literature (Herrero, 2008; LiChan, 1996), and characteristic protein bands are shown in Fig. 1.

One region of special interest in the spectra (Fig. 1 inset) is 1390 to 1430 cm^{-1}, where the different pH-levels gave rise to systematic differences discernable without chemometric analysis. This region can be attributed to the ionized state of the COO^- group of aspartic (Asp) and glutamic (Glu) acids at approx. 1415 cm^{-1} (Lord & Yu, 1970). The number of COO^- groups should be higher at pH 6.3 than for pH 5.8, which again should be higher than for pH 5.3, thus giving a higher intensity for this peak at high pH. Another feature to note is that the amide I band was centered at 1654 cm^{-1}, indicating that the secondary structure of proteins mainly consist of α-helices (Krimm & Bandekar, 1986).

A PLSR model was calculated to predict the pH of myofibril extracts based on pre-processed Raman spectra in the range from 300 to 1800 cm^{-1}. The measured pH for each sample after incubation was used as reference measurement. A summary of performance for models from spectroscopic analysis can be seen in Table 2. The PLSR model for Raman spectroscopy and pH shows that there is a systematic variation in pH and spectra, and that there is a strong relationship between the two analyses.

Difference spectra from Raman spectroscopy (Fig. 2) show that the changes from pH 5.3 to 5.8 and 5.8 to 6.3 are fairly consistent for the major peaks. The four regions with most importance when considering

Table 1
Measured pH in myofibril extracts after incubation.

pH class	Median	Mean	Standard deviation	Min	Max
5.3 (n = 15)	5.22	5.23	0.05	5.14	5.29
5.8 (n = 15)	5.85	5.80	0.10	5.66	5.90
6.3 (n = 15)	6.31	6.30	0.05	6.19	6.36

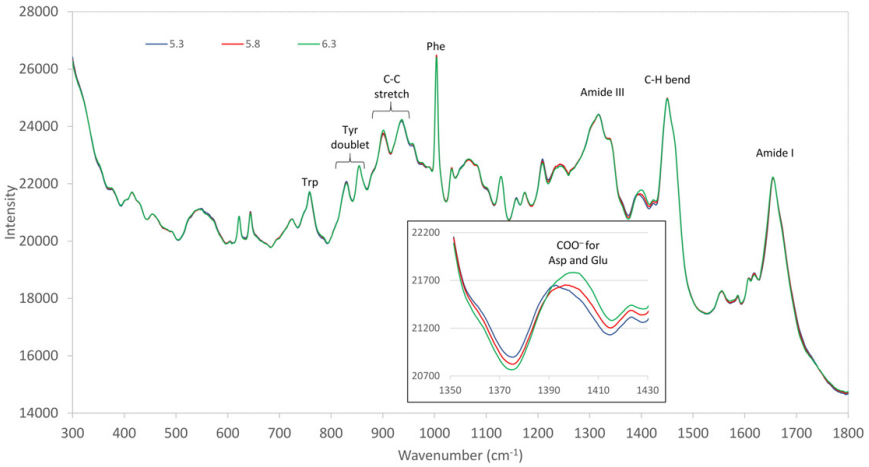

Fig. 1. Average Raman spectra for pH 5.3, 5.8 and 6.3 from all samples after EMSC, shown as blue, red and green lines respectively. Inset shows details in Raman spectra in the region from 1350 to 1430 cm^{-1}.

difference spectra and PLSR regression coefficients (not shown) related to change in pH were as follows: 1360 to 1373 cm^{-1} (peak at 1367 cm^{-1}), 1398 to 1412 cm^{-1} (peak at 1405 cm^{-1}), 1635 to 1644 cm^{-1} (peak at 1640 cm^{-1}) and 1699 to 1710 cm^{-1} (peak at approx. 1705 cm^{-1}).

The ratio of intensity, I_{1360}/I_{1340}, can be used to examine the hydrophobicity of Trp residues, where a high value for the ratio indicates hydrophobic interactions with the environment, Trp side chain is buried. Conversely, when the ratio is low, Trp is engaged in hydrophilic H-bonding with the environment (exposed Trp side chain) (Herrero, 2008). The intensity of the band at approx. 1360 cm^{-1} decreases as pH increases, while the intensity at approx. 1340 cm^{-1} stays unchanged, meaning that the ratio between these two bands decreases as pH increases. This indicates that Trp is gradually changing from hydrophilic to hydrophobic interactions as pH decreases towards 5.3, which may be explained by increased aggregation of protein at pH closer to the isoelectric point of meat proteins (approx. at pH 5.2 to 5.3) (Cheng & Sun, 2008).

The region from 1398 to 1412 cm^{-1} may originate from vibrations from COO^- group from Asp and Glu (Lord & Yu, 1970), as described above. At pH 6.3, the signal from the COO^- group should be stronger than for pH 5.3, as the amount of COO^- is higher at pH 6.3, and this could indeed be seen in both the Raman spectra (Figs. 1 and 2) and in the PLSR results. What further supports this finding is that the region at approx. 1700 cm^{-1}, which can be attributed to vibrations from the COOH group of Asp and Glu (Tu, 1986), gives an opposite contribution to the model and have negative values in both difference spectra.

Amide I, containing information about protein backbone structure, has a band centered between 1645 and 1685 cm^{-1} (Krimm & Bandekar, 1986). The region with the greatest change in the difference spectra was from 1635 to 1644 cm^{-1}, and this region is positioned on the slope just before the peak of amide I band. The amide I band width is expected to be wider when proteins unfold or denature (Lord & Yu, 1970), and in the case of myofibrils in liquid it can be hypothesized that the band changes width as a function of protein aggregation, giving higher intensities at high pH compared to low pH at a given wavelength in the amide I slope-region. This region also coincides with the broad band from H_2O, centered at approx. 1640 cm^{-1} (Socrates, 2001), where intensity of the signal from H_2O seem to be higher for high pH than for low pH. This may again be explained by increased aggregation of proteins at pH 5.3 compared to pH 6.3, where high pH may give more opportunity for protein-water interaction than low pH.

Table 2
Summary of performance for PLSR models. Only the best performing model from each spectroscopic method is shown.

Method	# factors in model	r^2	RMSECV
Raman	3	0.95	0.10
FT-IR	4	0.94	0.11
NIR	5	0.14	0.42
Fluorescence	2	0.84	0.18

One additional feature of the PLSR model is related to the peak at 1004 cm^{-1}, attributed to the breathing vibration of the Phe-ring, which is assumed to not change with conformation, but rather with protein concentration (Barrett, Peticolas, & Robson, 1978). This peak gives relatively large β-coefficients in the PLSR model and it seems to decrease in intensity with increased pH (Fig. 2), but it does not contribute significantly to the predictive power of the model, supporting the assumption that this peak gives information about protein concentration rather than conformational changes.

One factor that may have affected the results from Raman analysis was that the measurements were done on dried samples, which could have caused increased aggregation and cross-linking of proteins, the end result being a modification in the spectra when comparing them to spectra recorded from samples with higher water content (e.g. fresh meat). This implies that the results from dried myofibril extracts can be difficult to transfer directly to fresh meat analysis in the slaughterhouse. Raman spectroscopy can be applied to samples with high water content without any pre-treatment of the samples, and the reason for drying the samples in our study was to ensure high enough protein concentration for successful recording of spectra.

Current models for measuring pHu with Raman spectroscopy are often dependent on protonation of phosphates, and most phosphates are protonated at pH 5.5 (Scheier & Schmidt, 2013), meaning that measurements below 5.5 are uncertain with a model greatly reliable on phosphates. Consequently, protein structure and protonation of carboxylic acids can be very useful to take into account when analyzing samples with pHu below 5.5, because protein modifications still take place at pH lower than 5.5. This means that a model with both proteins and phosphates could perform better than one on each separately.

Studies on meat has identified one of the most impactful wavenumbers for measuring early pH and predicting pH as changes in intensity at ~976 cm^{-1} (Nache et al., 2015; Scheier et al., 2015),

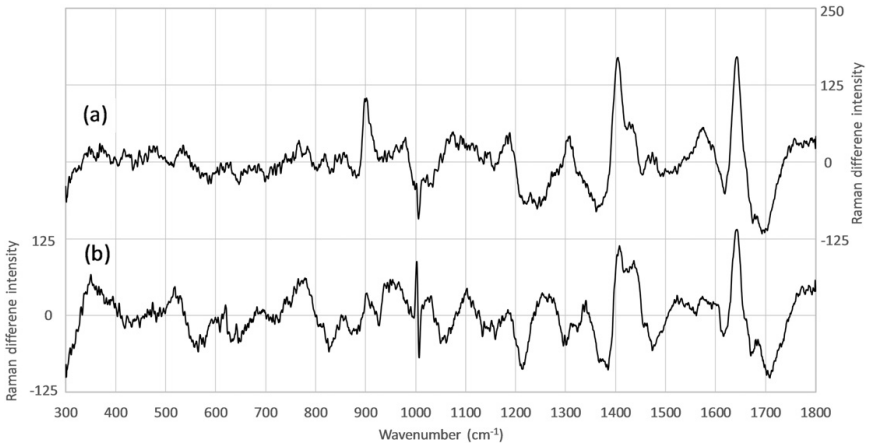

Fig. 2. Difference Raman spectra using the average spectra for each pH-level of (a) pH 6.3 minus pH 5.8 and (b) pH 5.8 minus pH 5.3. Raman difference intensity is shown on the right (a) and left (b) y-axis.

which is assigned to the basic form of terminal phosphate moieties. In addition, when analyzing meat samples with Raman spectroscopy at an early stage (<60 min postmortem), aiming to predict pH, important wavelengths seems to be tied to molecules involved in metabolism (e.g. creatine and lactate) (Scheier & Schmidt, 2013). Phosphate and metabolic molecules were not identified as important contributors to the models in our study, and the reason for this may be that most of the molecules responsible for these spectroscopic responses were washed out in the myofibril isolation process. Important wavelengths that overlap between our study and Nache et al. (2015) are the peaks at approx. 1410 and 1715 cm^{-1}, where both can be attributed to protonation state of carboxylic acid, in addition to a peak at approx. 1650 cm^{-1} attributed to amide I.

3.3. FT-IR spectroscopy

FT-IR spectra from all myofibril samples and pH-levels had similar structure (Fig. 3). Important regions for interpretation of FT-IR spectra are indicated in the figure (Barth, 2007). There seem to be systematic intensity differences in the amide I and II peaks related to pH, as well as the region from 1200 and 1280 cm^{-1} for amide III, which may be caused by aggregation of proteins, resulting in decreased intensity in the amide peaks at low pH. There also seem to be a tendency for the region corresponding to COO^- for Asp and Glu to follow pH as well, both at approx. 1400 and 1570 cm^{-1} (Barth, 2000), and the intensity is higher for high pH, which is similar to the results from Raman spectroscopy. The amide I and amide II band, centered at 1548 and 1652 cm^{-1} respectively, are both indicative of α-helix structure (Sengupta & Krimm, 1985).

PLSR results from FT-IR were similar to those for Raman, except the FT-IR model used one more factor to achieve comparable levels of prediction error in the model (Table 2). The PLSR model for FT-IR spectroscopy and pH showed that there was a systematic variation in pH and spectra, and that there was a strong relationship between the two analyses.

Difference spectra from FT-IR spectroscopy (Fig. 4) show that the changes from pH 5.3 to 5.8 and 5.8 to 6.3 are fairly consistent in

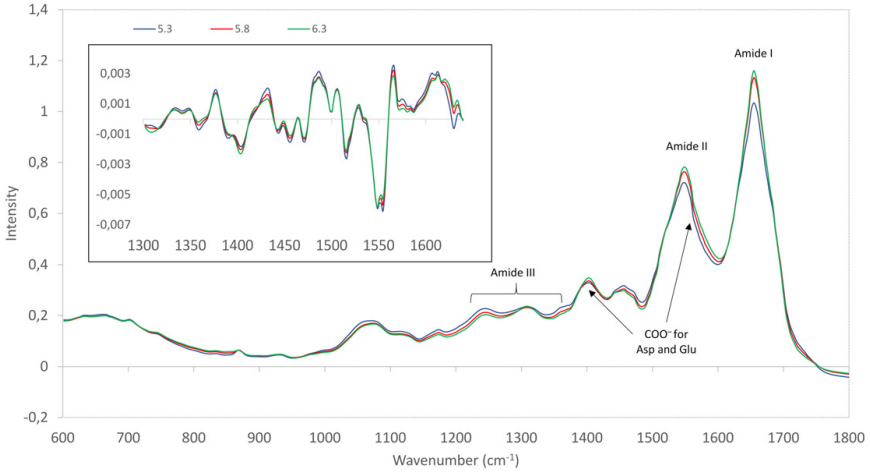

Fig. 3. Average FT-IR spectra for pH 5.3, 5.8 and 6.3 from all samples after EMSC, shown as blue, red and green lines respectively in the region from 600 to 1800 cm^{-1}. Inset shows 2nd derivative FT-IR spectra in the region from 1300 to 1640 cm^{-1}.

placement of the major peaks, but the difference intensity of the amide I and II peaks are much greater for pH 5.3 to 5.8 than for 5.8 to 6.3. The four regions with most importance when considering change in spectral intensity and PLSR regression coefficients (not shown) related to change in pH were as follows: 1398 to 1407 cm^{-1} (peak at 1402 cm^{-1}), 1552 to 1556 cm^{-1} (peak at 1554 cm^{-1}), 1562 to 1577 cm^{-1} (peak at 1566 and 1573 cm^{-1}) and 1650 to 1660 cm^{-1} (peak at 1654 cm^{-1}). The second derivative spectra of the most important peaks for the PLSR analysis are shown in the inset in Fig. 3.

One region of particular interest is the region from 1398 to 1407 cm^{-1}, and this can be attributed to the COO^- group for Asp and Glu (Barth, 2000), as this confirms the findings from both Raman spectroscopy and manual inspection of the FT-IR spectra.

The region from 1552 to 1577 cm^{-1} can in general be attributed to amide II of the protein backbone structure (Barth, 2007), but the area from 1556 to 1560 cm^{-1} and the area from 1574 to 1579 cm^{-1} can also be attributed to COO^- of Glu and Asp respectively (Rahmelow, Hubner, & Ackermann, 1998; Venyaminov & Kalnin, 1990). The majority of changes in this region seem to originate from changes in secondary structure seen in the broad peak in the difference spectra, but the important changes for the PLSR model seems to be within the narrow regions attributed to the amino acids. This underlines one of the difficulties when interpreting FT-IR and Raman spectra of proteins, namely that contribution from amino acid side chains and protein backbone features overlap in the spectra. Nonetheless, this further solidifies the importance of protein secondary structure and protonation of amino acids as important factors for pH-measurements.

The last region of interest, from 1650 to 1660 cm^{-1}, is attributed to α-helix structures within the amide I band (Sengupta & Krimm, 1985). The increase in average intensity as pH increased is obvious in the difference spectra, indicating an increase in α-helices as pH increases, where the greatest change happens when pH increases from 5.3 to 5.8. This peak was not as important in the PLSR analysis, meaning that it did not vary systematically with pH or there was large variations in intensity within each pH-group. In addition, FT-IR analysis of pork tissue sections has linked an increase in aggregated β-sheet structures (1619, 1628 and 1693 cm^{-1}) with low pH (Bocker, Ofstad, Bertram, Egelandsdal, & Kohler, 2006), which influenced the model significantly in our experiment as well, even though they were not among the most important wavenumbers for modelling pH. This further confirms that secondary structure of myofibril proteins seem to undergo modification following changes in pH, but it is challenging to determine the exact nature of these modifications based on data from this experiment.

FT-IR analysis was performed on dried myofibril samples and the same considerations as for Raman spectroscopy relating to sample properties applies here. One difference is that FT-IR is not suitable for samples with high water content, because water has a high absorption in IR (Pelton & McLean, 2000), and this may be the reason for the limited number of studies regarding FT-IR and meat quality as an online method in the slaughterhouse.

When comparing our results with an industry trial, it is evident that the protonation state of carboxylic acids is important for relating FT-IR to WHC in meat because of the inherent relationship between pH and WHC (Pedersen et al., 2003).

3.4. NIR spectroscopy

The NIR spectra did not vary systematically with pH in the regions investigated, and spectra from the different pH-levels seem to overlap (Fig. 5). PCA models gave no apparent grouping of samples based on design variables (results not shown). The best PLSR model was in the spectral region from 1100 to 1700 nm (Table 2), but this model is far from satisfactory to interpret the impact of pH on the NIR spectra from the myofibril extracts.

Contrary to Raman and FT-IR spectroscopy, NIR spectroscopy was measured on liquid samples. These samples had a very high water concentration, and this was likely to have a significant effect on the results from NIR analysis, because water has a strong absorption in the NIR spectrum. NIR spectroscopy does not seem to be specific enough to detect changes in proteins when the concentration is as low as in our study, and it follows that any comparison with real samples is pointless. There is no known direct link between NIR spectroscopy and pH or WHC in meat, so there has to be a correlation between these parameters and other parameters that NIR can measure, e.g. chemical composition or color (Prieto et al., 2009).

3.5. Fluorescence spectroscopy

From the fluorescence landscapes, the emission spectrum for excitation at 290 nm contained the most information about changes in pH and this was used for further analysis. Only wavelengths longer than the peak at 370 nm are shown because of the unintended cut-off in the instrument at about 350 nm (Fig. 6). In retrospect, measurements were done on a few remaining model samples without the lens causing the cut-off. A clear and broad peak was then seen at approximately 326 nm. The peak is assigned to Trp emission, as this is the amino acid

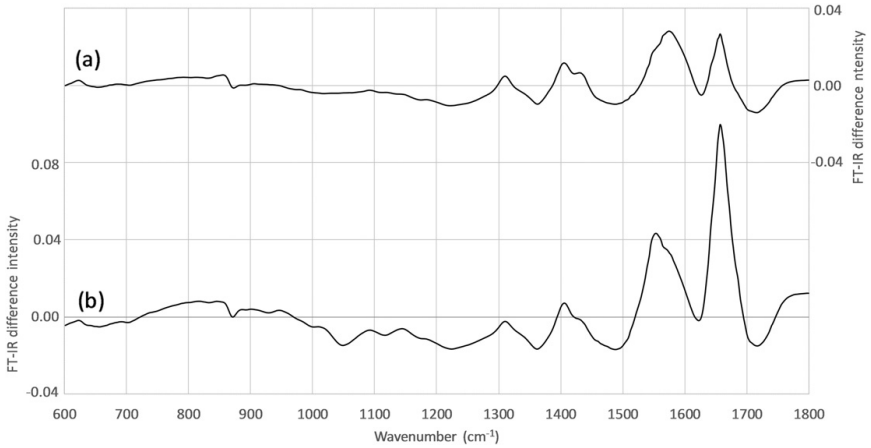

Fig. 4. Difference FT-IR spectra using the average spectra for each pH-level of (a) pH 6.3 minus pH 5.8 and (b) pH 5.8 minus pH 5.3. FT-IR difference intensity is shown on the right (a) and left (b) y-axis.

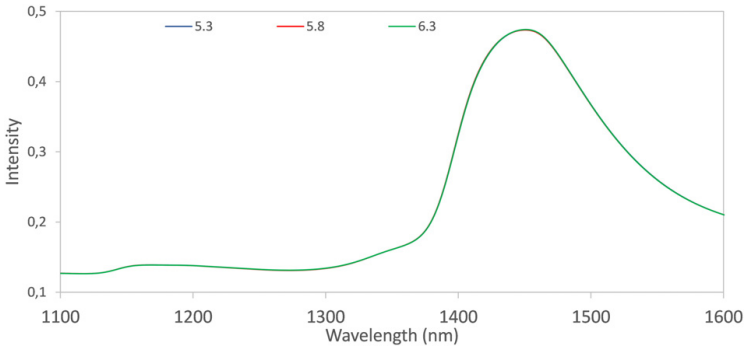

Fig. 5. Average NIR spectra for pH 5.3, 5.8 and 6.3 from all samples after EMSC, shown as blue, red and green lines respectively in the region from 1100 to 1700 nm.

with highest degree of excitation and emission at these wavelengths (Christensen et al., 2006). One characteristic of the fluorescence spectra to notice is that there was a shift in intensity linked to pH. Samples with low pH had the lowest intensity from 372 to 380 nm, followed by a small section with similar intensity for all pH-levels, and ending in a stretch from 396 to 430 nm where low pH had the highest intensity. The shift in fluorescence at higher wavelengths was highly correlated to variation in pH, although the predictive power of fluorescence spectroscopy was weaker than for Raman and FT-IR spectroscopy (Table 2). From the few measurements done without the cut-off lens, it could be seen that the shift observed in Fig. 6 corresponded with a shift of the peak at 326 nm, so the unintended cut-off did probably not cause loss of additional spectral information.

Trp and Tyr give stable fluorescence signals in the pH range of approx. 4 to 8 and 5 to 9, respectively (White, 1959), meaning that changes in fluorescence intensity attributed to these amino acids is not likely to vary much, and that changes in emission spectra are likely to arise from protein conformational changes. The molecular environment can introduce a shift in the fluorescence spectra, where changes in protein structure, pH and temperature can influence these shifts (Christensen et al., 2006). Pinpointing the exact mechanism for the shift in our experiment is difficult, as Trp emission can change because of many other factors (e.g. quenching and changes in quantum yield) (Ghisaidoobe & Chung, 2014). Evidence from Raman and FT-IR spectroscopy in our study suggests that the proteins are more tightly packed at lower pH, possibly lowering the distance between fluorescent amino acids in the samples with low pH, leading to higher degree of energy transfer between excited and non-excited amino acids, the end result being relatively higher intensities at longer wavelengths in samples with low pH.

As for NIR spectroscopy, the samples for fluorescence spectroscopy were analyzed in liquid form. Since fluorescence is very sensitive and specific, and the influence from water is negligible, this analysis was able to overcome the obstacle of low protein concentration in the solution.

Fluorescence spectra from meat has key fluorophores not present in our study, namely NADH, fatty and connective tissue (Brondum et al., 2000), but Trp-features detected in the model system could be relevant for intact meat. It may be important to analyze very lean meat to single out the effect found in our study.

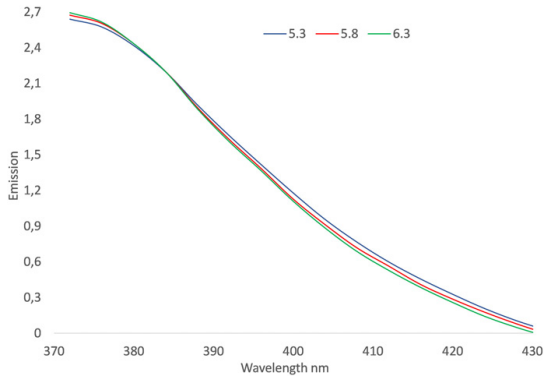

Fig. 6. Average fluorescence spectra for pH 5.3, 5.8 and 6.3 from all samples after SNV, shown as blue, red and green lines respectively from emission spectrum (excitation at 290 nm).

4. General discussion

Important regions associated with secondary structure and protonation state of carboxylic acid detected in Raman and FT-IR spectroscopy was consistent between the two methods (Table 3). Both methods demonstrated an increase in α-helix and a decrease in β-sheets as pH increases, indicating that the myofibrils is more aggregated in the form of β-sheets at low pH. The methods also show the same tendency for protonation of carboxylic acid, where there is an increase in deprotonated carboxylic acid at high pH.

When comparing the four spectroscopic methods included in our study, it is evident that Raman and fluorescence spectroscopy are the two methods that show most promise for implementation in slaughterhouses. Raman spectroscopy has shown promise in earlier studies by others, but has not been able to give satisfactory results in on-line applications. This could be caused by sampling issues, because of connective tissue and fat overshadowing the signal from proteins, or when

Table 3
Overview of changes in protein structure and carboxylic acid properties detected by Raman and FT-IR spectroscopy. Arrows refer to changes in intensity as pH increases from 5.3 to 6.3, and the corresponding wavenumber for each response is noted in parentheses.

Structure	Raman (approx. wavenumber (cm^{-1}))		FT-IR (approx. wavenumber (cm^{-1}))	
α-Helix	↑	(1653[a], 901[a])	↑	(1653[a], 1584[a], 1544[a])
β-Sheets	↓	(1669[a])	↓	(1694[a], 1284[a])
COO^-	↑	(1415[b])	↑	(1401[a])
COOH	↓	(1700–1755[c])	↓	(1700–1755[c])

[a] (Bocker et al., 2007).
[b] (Lord & Yu, 1970).
[c] (Socrates, 2001).

predicting pH, samples may be affected differently by other factors (e.g. temperature and meat chemical composition). Another important factor is the measuring spot size of the laser, which is usually very small for Raman instruments, requiring several measurements to get a representative selection from one sample. Raman spectroscopy can also be subject to strong fluorescence (Pelton & McLean, 2000), which makes robust pre-treatment and selection of valid spectra a must for successful analysis. Fluorescence spectroscopy has many of the same difficulties regarding sampling, but it may be easier to get a representative measuring area because it can be larger than what is common in Raman instruments.

FT-IR shows promise in our study, but may not be easy to implement on-line because of the strong water absorption. NIR spectroscopy has been implemented as an on-line method in slaughterhouses, but did not perform well within our experimental setting, meaning that NIR spectroscopy procedures needs improvement in experimental conditions to be able to assess the usefulness in analyzing pH in proteins, mainly by reducing water content in samples.

The effects seen in our study should in principle be transferable to whole meat, as proteins from meat was analyzed, meaning that the amino acid profile is close to the one found in meat. Still many other factors need attention to get a complete picture of spectroscopic analyses of meat, such as the impact of other meat constituents (e.g. fat, connective tissue and metabolites) and inherent heterogeneity of meat.

5. Conclusion

By using a myofibril model system and spectroscopic analyses it is possible to identify components in proteins that are affected by changes in pH. Both Raman and FT-IR spectroscopy identified COO^- group vibrations, most likely from Asp and Glu carboxylic acid, as the components that influenced prediction models the most. Other important components in proteins affected by pH were $COOH^-$ group of Asp and Glu, Trp, amide I, amide III. The results from the present study should be kept in mind when interpreting spectroscopy data from meat where pH is an important variable. However, because of inherent limitations of a model system (e.g. loss of structural integrity, removal of fatty and connective tissue), caution is advised when transferring our conclusions to studies on animal muscle.

Acknowledgements

We thank Bjørg Narum for technical assistance during sampling and in the analyses and Drs. Nils Kristian Afseth and Ulrike Böcker for critical comments on the manuscript. This work was supported by the Norwegian Levy on Agricultural Products and the Agricultural Agreement Research Fund of Norway.

References

Afseth, N. K., & Kohler, A. (2012). Extended multiplicative signal correction in vibrational spectroscopy, a tutorial. *Chemometrics and Intelligent Laboratory Systems*, *117*, 92–99. http://dx.doi.org/10.1016/j.chemolab.2012.03.004.

Barbin, D. F., ElMasry, G., Sun, D. W., & Allen, P. (2012). Predicting quality and sensory attributes of pork using near-infrared hyperspectral imaging. *Analytica Chimica Acta*, *719*, 30–42. http://dx.doi.org/10.1016/j.aca.2012.01.004.

Barnes, R. J., Dhanoa, M. S., & Lister, S. J. (1989). Standard normal variate transformation and de-trending of near-infrared diffuse reflectance spectra. *Applied Spectroscopy*, *43*(5), 772–777. http://dx.doi.org/10.1366/0003702894202201.

Barrett, T. W., Peticolas, W. L., & Robson, R. M. (1978). Laser Raman light-scattering observations of conformational changes in myosin induced by inorganic salts. *Biophysical Journal*, *23*(3), 349–358. http://dx.doi.org/10.1016/S0006-3495(78)85454-X.

Barth, A. (2000). The infrared absorption of amino acid side chains. *Progress in Biophysics and Molecular Biology*, *74*(3–5), 141–173.

Barth, A. (2007). Infrared spectroscopy of proteins. *Biochimica et Biophysica Acta*, *1767*(9), 1073–1101. http://dx.doi.org/10.1016/j.bbabio.2007.06.004.

Bee, G., Anderson, A. L., Lonergan, S. M., & Huff-Lonergan, E. (2007). Rate and extent of pH decline affect proteolysis of cytoskeletal proteins and water-holding capacity in pork. *Meat Science*, *76*(2), 359–365. http://dx.doi.org/10.1016/j.meatsci.2006.12.004.

Blixt, Y., & Borch, E. (2002). Comparison of shelf life of vacuum-packed pork and beef. *Meat Science*, *60*(4), 371–378. http://dx.doi.org/10.1016/S0309-1740(01)00145-0.

Bocker, U., Ofstad, R., Bertram, H. C., Egelandsdal, B., & Kohler, A. (2006). Salt-induced changes in pork myofibrillar tissue investigated by FT-IR microspectroscopy and light microscopy. *Journal of Agricultural and Food Chemistry*, *54*(18), 6733–6740. http://dx.doi.org/10.1021/jf060178q.

Bocker, U., Ofstad, R., Wu, Z., Bertram, H. C., Sockalingum, G. D., Manfait, M., ... Kohler, A. (2007). Revealing covariance structures in fourier transform infrared and Raman microspectroscopy spectra: A study on pork muscle fiber tissue subjected to different processing parameters. *Applied Spectroscopy*, *61*(10), 1032–1039. http://dx.doi.org/10.1366/000370207782217707.

Brondum, J., Munck, L., Henckel, P., Karlsson, A., Tornberg, E., & Engelsen, S. B. (2000). Prediction of water-holding capacity and composition of porcine meat by comparative spectroscopy. *Meat Science*, *55*(2), 177–185.

Cheng, Q., & Sun, D. W. (2008). Factors affecting the water holding capacity of red meat products: A review of recent research advances. *Critical Reviews in Food Science and Nutrition*, *48*(2), 137–159. http://dx.doi.org/10.1080/10408390601177647.

Christensen, J., Norgaard, L., Bro, R., & Engelsen, S. B. (2006). Multivariate autofluorescence of intact food systems. *Chemical Reviews*, *106*(6), 1979–1994. http://dx.doi.org/10.1021/cr050019q.

Davis, K. J., Sebranek, J. G., Huff-Lonergan, E., & Lonergan, S. M. (2004). The effects of aging on moisture-enhanced pork loins. *Meat Science*, *66*(3), 519–524. http://dx.doi.org/10.1016/S0309-1740(03)00154-2.

DeNoyer, L. K., & Dodd, J. K. (2001). Smoothing and derivatives in spectroscopy. In J. M. Chalmers, & P. R. Griffiths (Eds.), *Handbook of vibrational spectroscopy. Vol. 3.* (pp. 2173–2183). Chichester, U.K.: John Wiley & Sons Ltd.

Fischer, K. (2007). Drip loss in pork: Influencing factors and relation to further meat quality traits. *Journal of Animal Breeding and Genetics*, *124*(Suppl. 1), 12–18. http://dx.doi.org/10.1111/j.1439-0388.2007.00682.x.

Forrest, J. C., Morgan, M. T., Borggaard, C., Rasmussen, A. J., Jespersen, B. L., & Andersen, J. R. (2000). Development of technology for the early post mortem prediction of water holding capacity and drip loss in fresh pork. *Meat Science*, *55*(1), 115–122.

Ghisaidoobe, A. B., & Chung, S. J. (2014). Intrinsic tryptophan fluorescence in the detection and analysis of proteins: A focus on Forster resonance energy transfer techniques. *International Journal of Molecular Sciences*, *15*(12), 22518–22538. http://dx.doi.org/10.3390/ijms151222518.

Gornall, A. G., Bardawill, C. J., & David, M. M. (1949). Determination of serum proteins by means of the biuret reaction. *Journal of Biological Chemistry*, *177*(2), 751–766.

Henckel, P., Karlsson, A., Oksbjerg, N., & Soholm Petersen, J. (2000). Control of post mortem pH decrease in pig muscles: Experimental design and testing of animal models. *Meat Science*, *55*(1), 131–138.

Herrero, A. M. (2008). Raman spectroscopy a promising technique for quality assessment of meat and fish: A review. *Food Chemistry*, *107*(4), 1642–1651. http://dx.doi.org/10.1016/j.foodchem.2007.10.014.

Huff-Lonergan, E., & Lonergan, S. M. (2005). Mechanisms of water-holding capacity of meat: The role of postmortem biochemical and structural changes. *Meat Science*, *71*(1), 194–204. http://dx.doi.org/10.1016/j.meatsci.2005.04.022.

Koohmaraie, M., Schollmeyer, J. E., & Dutson, T. R. (1986). Effect of low-calcium-requiring calcium activated factor on myofibrils under varying pH and temperature conditions. *Journal of Food Science*, *51*(1), 28-&. http://dx.doi.org/10.1111/j.1365-2621.1986.tb10828.x.

Krimm, S., & Bandekar, J. (1986). Vibrational spectroscopy and conformation of peptides, polypeptides, and proteins. [Review] *Advances in Protein Chemistry*, *38*, 181–364. http://dx.doi.org/10.1016/s0065-3233(08)60528-8.

Lawrie, R. A. (1985). Chapter 10 - the eating quality of meat. *Meat science* (pp. 169–207) (4th ed.). Oxford, England: Pergamon Press Ltd (Pergamon).

LiChan, E. C. Y. (1996). The applications of Raman spectroscopy in food science. [Article] *Trends in Food Science & Technology*, *7*(11), 361–370. http://dx.doi.org/10.1016/s0924-2244(96)10037-6.

Lord, R. C., & Yu, N. T. (1970). Laser-excited Raman spectroscopy of biomolecules. I. Native lysozyme and its constituent amino acids. *Journal of Molecular Biology*, *50*(2), 509–524.

Martens, H., & Martens, M. (2001). *Introduction to multivariate data analysis for understanding quality*. Chichester, U.K.: John Wiley & Sons Ltd.

Nache, M., Scheier, R., Schmidt, H., & Hitzmann, B. (2015). Non-invasive lactate- and pH-monitoring in porcine meat using Raman spectroscopy and chemometrics. *Chemometrics and Intelligent Laboratory Systems*, *142*, 197–205. http://dx.doi.org/10.1016/j.chemolab.2015.02.002.

Pedersen, D. K., Morel, S., Andersen, H. J., & Balling Engelsen, S. (2003). Early prediction of water-holding capacity in meat by multivariate vibrational spectroscopy. *Meat Science*, *65*(1), 581–592. http://dx.doi.org/10.1016/S0309-1740(02)00251-6.

Pelton, J. T., & McLean, L. R. (2000). Spectroscopic methods for analysis of protein secondary structure. *Analytical Biochemistry*, *277*(2), 167–176. http://dx.doi.org/10.1006/abio.1999.4320.

Prieto, N., Roehe, R., Lavin, P., Batten, G., & Andres, S. (2009). Application of near infrared reflectance spectroscopy to predict meat and meat products quality: A review. *Meat Science*, *83*(2), 175–186. http://dx.doi.org/10.1016/j.meatsci.2009.04.016.

Rahmelow, K., Hubner, W., & Ackermann, T. (1998). Infrared absorbances of protein side chains. *Analytical Biochemistry*, *257*(1), 1–11. http://dx.doi.org/10.1006/abio.1997.2502.

Sante-Lhoutellier, V., Aubry, L., & Gatellier, P. (2007). Effect of oxidation on in vitro digestibility of skeletal muscle myofibrillar proteins. *Journal of Agricultural and Food Chemistry*, *55*(13), 5343–5348. http://dx.doi.org/10.1021/Jf070252k.

Savage, A. W., Warriss, P. D., & Jolley, P. D. (1990). The amount and composition of the proteins in drip from stored pig meat. *Meat Science*, *27*(4), 289–303. http://dx.doi.org/10.1016/0309-1740(90)90067-G.

Schafer, A., Rosenvold, K., Purslow, P. P., Andersen, H. J., & Henckel, P. (2002). Physiological and structural events post mortem of importance for drip loss in pork. *Meat Science*, *61*(4), 355–366.

Scheier, R., & Schmidt, H. (2013). Measurement of the pH value in pork meat early postmortem by Raman spectroscopy. *Applied Physics B: Lasers and Optics*, *111*(2), 289–297. http://dx.doi.org/10.1007/s00340-012-5332-y.

Scheier, R., Bauer, A., & Schmidt, H. (2014b). Early postmortem prediction of meat quality traits of porcine semimembranosus muscles using a portable Raman system. *Food and Bioprocess Technology*, *7*(9), 2732–2741. http://dx.doi.org/10.1007/s11947-013-1240-3.

Scheier, R., Kohler, J., & Schmidt, H. (2014a). Identification of the early postmortem metabolic state of porcine *M. semimembranosus* using Raman spectroscopy. *Vibrational Spectroscopy*, *70*, 12–17. http://dx.doi.org/10.1016/j.vibspec.2013.10.001.

Scheier, R., Scheeder, M., & Schmidt, H. (2015). Prediction of pork quality at the slaughter line using a portable Raman device. *Meat Science*, *103*, 96–103. http://dx.doi.org/10.1016/j.meatsci.2015.01.009.

Sengupta, P. K., & Krimm, S. (1985). Vibrational analysis of peptides, polypeptides, and proteins. XXXII. alpha-Poly(L-glutamic acid). *Biopolymers*, *24*(8), 1479–1491. http://dx.doi.org/10.1002/bip.360240805.

Socrates, G. (2001). Infrared and Raman characteristic group frequencies. *Tables and charts* (3rd ed.). Chichester, U.K.: John Wiley & Sons Ltd.

Tu, A. T. (1986). *Spectroscopy of biological systems*. Wiley.

Venyaminov, S., & Kalnin, N. N. (1990). Quantitative IR spectrophotometry of peptide compounds in water (H2O) solutions. I. Spectral parameters of amino acid residue absorption bands. *Biopolymers*, *30*(13–14), 1243–1257. http://dx.doi.org/10.1002/bip.360301309.

White, A. (1959). Effect of pH on fluorescence of tyrosine, tryptophan and related compounds. *The Biochemical Journal*, *71*(2), 217–220.

PAPER II

Analyzing μ-Calpain induced proteolysis in a myofibril model system with vibrational and fluorescence spectroscopy

Petter Vejle Andersen [a]*, Jens Petter Wold [a], Eva Veiseth-Kent [a]

[a] Nofima AS, Osloveien 1, 1430 Ås, Norway

E-mail adresses:

Petter Vejle Andersen: petter.andersen@nofima.no

Jens Petter Wold: jens.petter.wold@nofima.no

Eva Veiseth-Kent: eva.veiseth-kent@nofima.no

*Corresponding author at: Nofima AS, Osloveien 1, 1430 Ås, Norway. Tel.: +47 64 97 04 90.

Manuscript submitted to Meat Science

ABSTRACT

Degree of post-mortem proteolysis influences overall meat quality (e.g. tenderness and water holding capacity). Degradation of isolated pork myofibril proteins by μ-Calpain for 0, 15 or 45 min was analyzed using four spectroscopic techniques; Raman, Fourier transform infrared (FT-IR), near infrared (NIR) and fluorescence spectroscopy. Sodium dodecyl sulfate polyacrylamide gel electrophoresis was used to determine degree of proteolysis. The main changes detected by FT-IR and Raman spectroscopy were degradation of myofibril protein backbone manifested in the spectra as an increase in terminal carboxylic acid vibrations, a decrease in CN vibration, as well as an increase in skeletal vibrations. A reduction in β-sheet secondary structures was also detected, while α-helix secondary structure seemed to stay relatively unchanged. NIR and fluorescence were not suited to analyze degree of proteolysis in this model system.

Keywords

Myofibrils; proteolysis; proteins; vibrational spectroscopy; fluorescence

1. INTRODUCTION

The degree of post-mortem proteolysis in meat has been linked to important quality parameters of fresh meat, such as water holding capacity (Calvo, Toldra, Aristoy, Lopez-Bote, & Rey, 2016; Huff-Lonergan & Lonergan, 2005; Hughes, Oiseth, Purslow, & Warner, 2014; Kristensen & Purslow, 2001; Melody et al., 2004) and tenderness (Huff Lonergan, Zhang, & Lonergan, 2010; Koohmaraie, 1992; Moczkowska, Poltorak, & Wierzbicka, 2017; Taylor, Geesink, Thompson, Koohmaraie, & Goll, 1995; Veiseth-Kent, Hollung, Ofstad, Aass, & Hildrum, 2010). It is therefore of interest to analyze the degree of proteolysis in intact meat rapidly, without the use of invasive and time-consuming chemical approaches, to elucidate the relationship between proteolysis and other quality parameters and to contribute towards the measurement and prediction of meat quality.

One ubiquitous proteolytic system playing a major role in muscle tissue is the calpain system, mainly consisting of the Ca^{2+} requiring cysteine proteases μ-Calpain and m-Calpain, and the calpain-specific inhibitor Calpastatin (Goll, Thompson, Li, Wei, & Cong, 2003). The calpain system has been identified and shown to be active in post-mortem porcine muscles (Ouali & Talmant, 1990), additionally, μ-Calpain has been shown to be active under post-mortem conditions (i.e. pH 5.5 and 4°C) (Koohmaraie, Schollmeyer, & Dutson, 1986). Substrates for μ-Calpain in muscle tissue are many, and some important ones for meat quality includes troponin-T, actin, myosin heavy chain and myosin light chain proteins (Lametsch, Roepstorff, Moller, & Bendixen, 2004).

During proteolysis, proteins are degraded by cleavage of the C-N bond in the protein backbone, resulting in the formation of new terminal amino and carboxylate groups, which is a process that can potentially be followed using spectroscopic techniques. Another consequence of proteolysis is the disruption of protein structure, in particular secondary structure, of which both Raman and Fourier-transform infrared (FT-IR) spectroscopy are well suited to analyze (Barth, 2007a; Krimm & Bandekar, 1986). Recent studies have shown promise for FT-IR spectroscopy to predict protein and peptide size in laboratory scale enzymatic hydrolysis of meat by-products (Bocker, Wubshet, Lindberg, & Afseth, 2017; Wubshet et al., 2017). However, there is a limited number of studies investigating the relationship between Raman and FT-IR spectroscopy and proteolysis in meat, and most of these focus on determining degree of proteolysis in various dry-cured ham products (e.g. Moller, Parolari, Gabba, Christensen, & Skibsted, 2003; Prevolnik et al., 2011) or bulk changes in spectra following ageing (e.g. Beattie, Bell, Borggaard, & Moss, 2008). Near infrared (NIR) and fluorescence spectroscopy do not contain as much information about protein structure as Raman or FT-IR spectroscopy, but both methods are sensitive to some features of proteins. For instance, NIR spectroscopy contain absorption bands from amide I and amide II protein structures (Li-Chan, Ismail, Sedman, & van de Voort, 2002), while fluorescence spectroscopy contains information about certain

amino acids microenvironment (Christensen, Norgaard, Bro, & Engelsen, 2006), both of which can contribute to analysis of proteolysis in meat.

The aim of this study was to investigate opportunities for spectroscopic analysis to determine degree of proteolysis in meat. To achieve this, we used four different spectroscopic techniques; FT-IR, Raman, NIR and fluorescence, to analyze changes in a myofibril model system, containing isolated myofibril proteins from pig muscle, incubated with μ-Calpain and Ca^{2+}. Using a model system allows for a targeted analysis of the muscle constituents that are predominantly altered during conversion from muscle to meat, specifically the myofibrillar proteins. In addition, the model system has the benefit of being relatively homogenous and experimental parameters can more easily be controlled. On the other hand, there are some drawbacks concerning e.g. the loss of muscle structure and other muscle components that will affect the spectroscopic results in real meat tissue.

2. MATERIALS AND METHODS

2.1 Animals, myofibril isolation and sample preparation

Myofibril isolates were prepared from five pigs as described by Andersen, Veiseth-Kent, and Wold (2017). In short, *Longissimus thoracis et lumborum* was excised and approx. 20 g was homogenized, washed in buffers and passed through a sieve to remove fat and connective tissue, before glycerol was added and samples were stored in a freezer at -20°C until further use. Samples were thawed and washed before they were used in the experiment.

Each sample was diluted to a protein concentration of ~30 mg/ml in elution buffer. Three ml was transferred to 5 ml sample tubes in nine parallels; three were used for controls, three for intermediate proteolysis and three for extended proteolysis. 300 μl 100 mM $CaCl_2$, 200 μl 300 mM EDTA (pH 7.6) and 8 μl Calpain-1 (Calbiochem, cat. no. 208712) was added to the control samples, and they were subsequently vortex mixed and stored at 4°C. 300 μl 100 mM $CaCl_2$ and 8 μl Calpain-1 was added to the intermediate and extended samples, before they were vortex mixed and incubated, while rotating, at 25°C. After 15 min incubation, 200 μl 300 mM EDTA was added to the intermediate samples before they were vortex mixed and stored at 4°C. The same procedure was applied to the remaining samples after 45 min. The experiment was conducted over three days, where samples from one pig was analyzed day one and samples from two pigs each of the two following days.

2.2 Sodium Dodecyl Sulfate Polyacrylamide Gel Electrophoresis (SDS-PAGE) and Liquid chromatography tandem-mass spectrometry (LC-MSMS)

From each sample, 200 μl was transferred to an Eppendorf tube and 200 μl treatment buffer (0.125 M Tris(hydroxymethyl)aminomethane, 4% sodium dodecyl sulfate, 20% glycerol) was added, before

the sample was vortex mixed and incubated at 95°C for 5 min, mixed by pipetting and incubated at 95°C a final time for 5 min. Samples were subsequently centrifuged at 13000 rpm at 4°C for 20 min, the supernatant was transferred to a fresh Eppendorf tube and stored at –20°C. Protein concentration was measured using Bio-Rad Protein Assay (Bio-Rad, California, USA) microplate procedure, and protein concentration in each sample was adjusted to 1 mg/ml by mixing thawed sample and treatment buffer with DTT (0.2 M) and bromophenol blue (0.04%). 20 µg protein was loaded in each well when running SDS-PAGE gel electrophoresis (NuPage 12% Bis-Tris 12 well, Invitrogen).

The gels were transferred to a small container, 50 ml Coomassie blue (0.1% Coomassie Brilliant Blue G-250 dissolved in 50% methanol and 7% acetic acid) was added and they were incubated with shaking for one hour. After this incubation, the gels were washed with dH_2O and finally 100 ml of destaining buffer (20% methanol and 7% acetic acid) was added. The gels were subsequently incubated for 2 hours with shaking, and stored in dH_2O afterwards. The gels were scanned, lanes were aligned using Progenesis SameSpots version 4.5 (Nonlinear Dynamics, Newcastle upon Tyne, UK), and profiles were extracted using ImageQuant TL 1D version 7.0 (GE Healthcare, Chicago, Ill, USA).

The five most prominent protein bands that showed systematic changes between the 0 and 45 min incubations were excised from a SDS-PAGE gel. Proteins in the gel pieces were reduced (10 mM DTT) and alkylated (55 mM IAA), prior to digestion with Trypsin/Lys-C at 37 °C overnight, and finally peptide extraction was accomplished by sonication. The peptide extracts were purified and concentrated using a StageTip, C18 material filled in 200 µl pipette tips, according to Rappsilber, Mann, and Ishihama (2007) and Yu, Smith, and Pieper (2014). Peptides were eluted with 50 µl 70 % acetonitrile (ACN) and dried completely with a speed-vac (Thermo Fisher Scientific, USA). The dried peptides were dissolved in loading solution (0.05 % TFA, 2% ACN in water) loaded on to a trap column (Acclaim PepMap 100, C18, 5µm, 100Å, 300µm i.d. x 5 mm) and then backflushed onto a 50 cm x 75 µm analytical column (Acclaim PepMap RSLC C18, 2 µm, 100 Å, 75 µm i.d. x 50 cm, nanoViper). The gradient profile used for peptide separation was from 4 to 45 % solution B (80 % CAN, 0.1 % formic acid) in 56 min at a flow rate of 300 nL/ min. The Q-Exactive mass spectrometer was set up as follows: a full scan (300-1600 m/z) at R = 70000 was followed by (up to) 10 MS2 scans at R=35000 using an NCE setting of 28. Singly charged precursors were excluded for MS/MS as were precursors with z > 5. Dynamic exclusion was set at 20 sec. Thermo raw files were converted to .mgf format using the msconvert module of ProteoWizard (http://proteowizard.sourceforge.net/), and used to search a SwissProt database (*Taxonomy other Mammalia*) on an in-house Mascot server (version 2.4). Search parameters were: i) 10 ppm/20 mamu tolerance for MS and MS/MS,

respectively; ii) trypsin, allowing up to 2 missed cleavages, iii) fixed modification cysteine carbamidomethylation and variable modification methionine oxidation. The Mascot result (.dat) files were used as input for the Scaffold software (http://www.proteomesoftware.com/products/scaffold/), for convenient result visualization and validation.

2.3 Spectroscopic analysis

Spectroscopic analysis was carried out as described by Andersen et al. (2017) with the following changes:

Raman spectroscopy: 200 µl aliquots was placed on an aluminum plate and left to dry overnight in a desiccator. Confocal hole was set to 500 µm. Exposure time was set to 6 times 10 s in the range from 500 to 1800 cm^{-1}.

FT-IR spectroscopy: Two µl of sample transferred to the plate.

NIR spectroscopy: No change for measuring liquid samples. Dried samples were measured using the same instrument settings, but a spot size of 10 mm. The samples were the same as for the Raman measurements. The aluminum plate was placed in the spectrophotometer upside down, with the dried droplet sample placed in center over the sampling window of the module. Three spectra from each sample were recorded for both analyses, and the spectra were averaged for each sample prior to analyses.

Fluorescence spectroscopy: Excitation only at 292 nm in the emission range 300 – 500 nm (2 nm step size).

2.4 Pre-processing and data analysis

2.4.1 Pre-processing of spectral data and gel profiles

Pre-processing of spectral data and gel lane profiles was done to give comparable spectra for further analysis, by reducing or removing the impact of noise, scatter effects and other undesirable alterations in the spectra.

Gel lane profiles were normalized using standard normal variate (SNV) (Barnes, Dhanoa, & Lister, 1989), before correlation optimized warping with a segment size of 90 and a slack of 10 was applied to align peaks.

The FT-IR spectra were subjected to Extended Multiplicative Signal Correction (Martens & Stark, 1991) (EMSC) with replicate correction (Kohler et al., 2009) to reduce the effects of changes in light intensity and scattering, and day to day variation in the measurements. EMSC is a model based pre-processing approach which handles additive polynomial baselines (6^{th} order was used) as well as multiplicative effects in a single model. Replicate correction finds common variation across sets of

replicates using singular value decomposition of EMSC corrected spectra, i.e. batches of measurements from individual days. The dominant common variation is reintroduced into the EMSC model as interferent spectra to perform a final combined modelling and correction. One sample was excluded from FT-IR analysis because of too high absorption.

Raman spectra were pre-processed by means of full extended multiplicative scattering correction (EMSC) including 6th order polynomial (Liland, Kohler, & Afseth, 2016). Five spectra from each sample were averaged and subsequently smoothed by applying a Savitzky-Golay filter with four smoothing points on each side in the second order. Two samples were excluded from Raman analysis because of changes in confocal hole diameter, giving too dissimilar spectra to compare with the others. Reason for changes to confocal hole was saturation of the detector in one sample and too little signal for the detector for the other sample.

The NIR spectra from Gold Reflectance Cellkit were divided into three regions, 400 to 900 nm, 1100 to 1700 nm, and 1700 to 2350 nm, before EMSC was applied to each region separately. NIR spectra from dried samples were subjected to EMSC in the entire recorded region from 1100 to 2500 nm.

Fluorescence spectra were pre-processed only by SNV.

2.4.2 Data analysis

Principal component analysis (PCA) was utilized to verify that samples were grouped according to degree of proteolysis, meaning that changes in spectra is representative of the proteolysis-related variation in the spectra. Partial least squares regression (PLSR) was used for determining relationship between proteolysis and spectroscopic data, the procedure included an uncertainty test for revealing important variables in the model. Both analyses were cross-validated using leave-one-out procedure. FT-IR and Raman used only the important variables from uncertainty test to make the models in table 2, while NIR and fluorescence used all variables. Reference measurements for PLSR were SDS-PAGE PCA scores for principal component 1 for each sample, which represents a relative value for degree of proteolysis within the current experiment.

PCA and PLSR was performed in the following spectral regions: Raman: 500 to 1800 cm^{-1}, FT-IR: from 800 to 1800 cm^{-1}, NIR: each of the spectral regions from EMSC separately and fluorescence: excitation at 292 nm and emission 306 – 412 nm.

Data analysis was carried out using Open EMSC toolbox for MATLAB freely downloadable from http://nofimaspectroscopy.org in MATLAB version R2013b (The MathWorks, Natick, MA) and using The Unscrambler® X version 10.4 (CAMO Process AS, Norway).

3. RESULTS AND DISCUSSION

3.1 SDS-PAGE

Inspection of average lane profiles from SDS-PAGE and Coomassie staining reveals a time-dependent degradation of certain proteins (Fig. 1). Degradation of myosin heavy chain (MHC) is the most prominent, as evidenced by the decrease in the MHC band and an increase in the amount of fragmented MHC in all LC-MSMS analyzed bands. Significant degradation of MHC in isolated myofibrils has been documented before (Lametsch et al., 2004), but the degradation is limited in intact meat (Lametsch, Roepstorff, & Bendixen, 2002), meaning that potential responses in spectroscopy from MHC degradation are questionable when transferring these results to analysis of intact meat. According to the LC-MSMS analysis the concentration of intact actin decreases as incubation time increases, but the peak in the lane profile shows the opposite relation and is probably a result of the increase in MHC fragments. Degradation of troponin-T follows the same pattern as MHC, with highest concentration of the intact protein at the onset of the experiment, which gradually decreases as incubation time increases, and the reverse pattern was identified for the degradation product. Degradation of troponin-T in post-mortem meat is thoroughly documented (Huff Lonergan et al., 2010; Moczkowska et al., 2017), and the intensity of the 32 kDa degradation product can be used as a marker of overall proteolysis in meat (Olson, Parrish, Dayton, & Goll, 1977).

A PCA was performed to investigate if the differences in gel lane profiles were consistent over all samples and incubation times, and what parts of the gel lanes were the most important for separating the different incubation times. Fig. 2 shows that there was a separation along PC-1 in accordance with the three incubation times, hence, the scores from PC-1 can be used to quantify the degree of proteolysis. Samples incubated for 15 and 45 min were more similar than samples incubated for 0 and 15 min, evidenced by the overlap of samples for 15 and 45 min and no overlap between 0 and 15 min for PC-1. This indicates that the proteolytic activity decreases after 15 min of incubation. Loadings from PCA for PC-1 (results not shown) reveals that the most important part of the gel profiles for separating degree of proteolysis was the amount of intact and degradation product from MHC, and to a lesser degree, troponin-T.

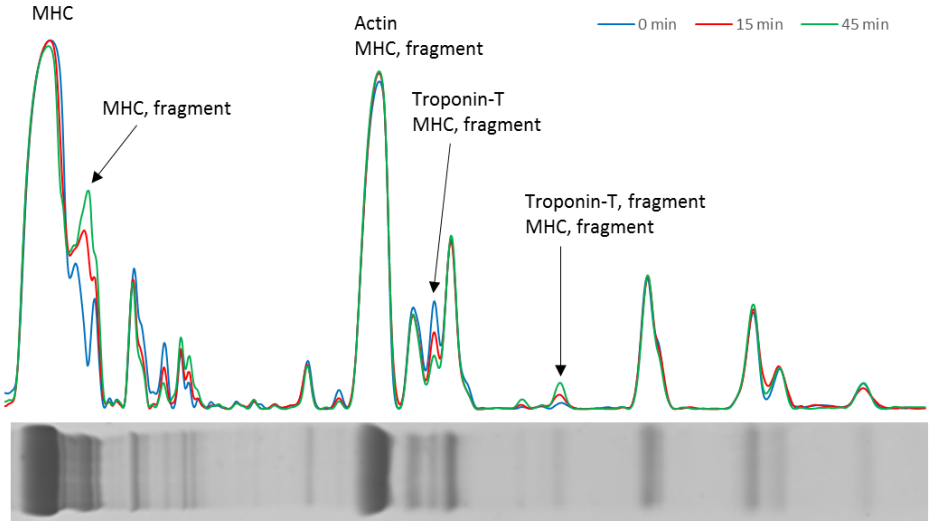

Figure 1. Average lane profiles after incubation for 0, 15 and 45 min. from SDS-PAGE analysis. The horizontal gel-lane underneath the graph is a representative sample after 45 min incubation. Full-length proteins and protein fragments with concentration changes following incubation is marked in the figure, the proteins was identified by LC-MSMS.

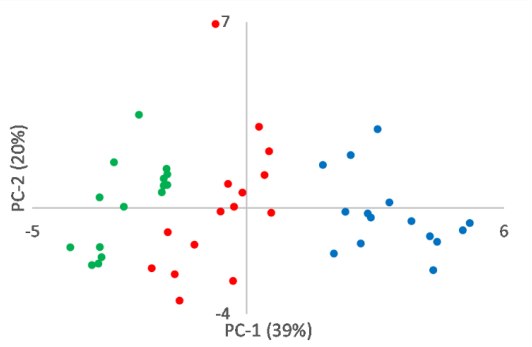

Figure 2. PCA scores plot from lane profiles. Blue dots = 0 min, red dots = 15 min and green dots = 45 min.

3.2 FT-IR spectroscopy

The FT-IR spectra had a strong protein signature, where the amide I and II peaks were prominent (Fig. 3). The center of the peaks for both amide I and amide II suggest that the protein secondary structure were predominantly α-helices (Bocker et al., 2007). To identify regions in the spectrum that were important for determining degree of proteolysis both the native spectrum and the difference

spectrum (Fig. 3) were analyzed. There was a systematic change in the spectra from 0 to 15 min and 15 to 45 min, and the change is more pronounced from 0 to 15 min than for 15 to 45 min, which was in correspondence with results from SDS-PAGE.

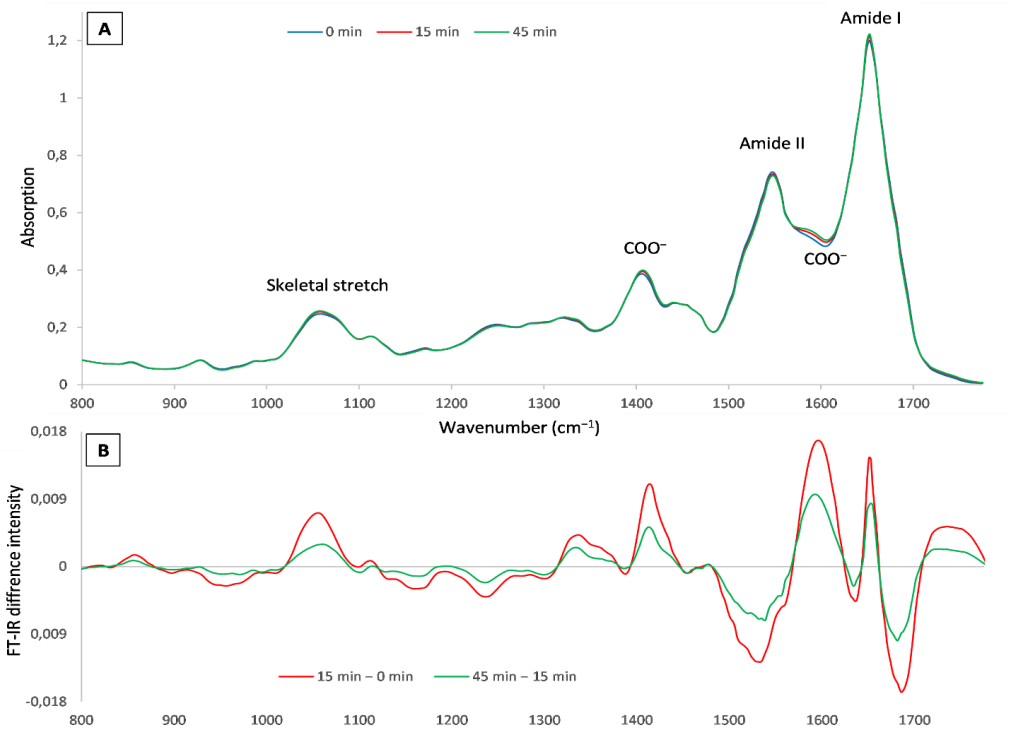

Figure 3. (A) Average spectra from FT-IR from four myofibril isolates. Peaks important for analyzing degree of proteolysis are noted in the figure. ***(B)*** Difference spectra for average FT-IR spectra for each incubation time, where 15 min – 0 min and 45 min – 15 min corresponds to green and red lines, respectively.

In the difference spectra there were six peaks clearly related to protein modifications following proteolysis (Table 1). The same peaks were the most important for differentiating between proteolysis times in a PCA, resulting in a grouping along PC1 in the PCA scores plot (Fig. 4). To explore the link between spectroscopy and proteolysis a PLSR model was calculated (Table 2), which showed that FT-IR can predict degree of proteolysis in the model system very well (r_{cv}^2=0.92 and RMSECV = 0.78). The spectroscopic changes could be split into two categories, first, there were direct changes following cleavage of peptide bonds, and secondly, there were secondary structure changes.

Table 1. *Overview of important spectroscopic responses detected by FT-IR spectroscopy related to degree of proteolysis in the current study. Arrows denote changes in intensity as a function of degree of proteolysis.*

Wavenumber (cm^{-1})	Absorbance change	Structure
1685	↓	Amide I, β-sheet, C=O [a]
1650	↑	Amide I, α-helix/disordered, C=O [b]
1595	↑	COO^- (antisymmetric) [c]
1533	↓	Amide II, β-sheet, CN [a]
1414	↑	COO^- (symmetric) [c]
1055	↑	Skeletal stretch [d]

[a] (Bocker et al., 2007), [b] (Barth, 2007a), [c] (Guler, Dzafic, Vorob'ev, Vogel, & Mantele, 2011), [d] (Barth, 2007b)

Table 2. *Summary of performance for cross-validated PLSR models from spectroscopy vs. PC1 scores from PCA of SDS lane profiles. Only the best performing model from each spectroscopic method is shown.*

Method	n	# factors in model	r^2	RMSECV
FT-IR	36	6	0.92	0.78
Raman	27	4	0.83	1.07
NIR (dried)	43*	10	0.74	1.42
NIR (liquid)[¤]	45	4	0.10	2.61
Fluorescence	43*	2	0.25	2.27

*Two samples were removed from NIR (dried) and fluorescence PLSR because of extreme residual values.
[¤] Spectral range from 1700 nm to 2350 nm used in the model.

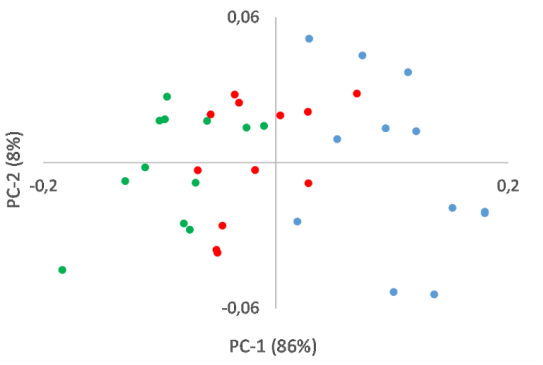

Figure 4. PCA scores plot from FT-IR spectroscopy. Blue dots = 0 min, red dots = 15 min and green dots = 45 min.

Peptide bond cleavage is manifested in the spectra by an increase in absorption of carboxylate, at 1595 cm^{-1} and 1414 cm^{-1} (Guler et al., 2011), and by reduced absorption of CN in the amide II region (Barth, 2007a). Changes in secondary structure seem to be in the form of a reduction in β-sheets and a simultaneous increase in α-helix and/or disordered structures. Reduction in β-sheet absorbance is evident in the amide I peak, at 1685 and 1635 cm^{-1}, and the amide II peak, at 1533 cm^{-1}. The changes to α-helix absorption were contradictory, as there is an increase in absorption at 1650 cm^{-1} for amide I and a decrease at 1544 cm^{-1} for amide II. An explanation for the increased absorbance at 1650 cm^{-1} can be an increase in disordered secondary structures accompanied by an increase in solute exposed α-helices (Barth, 2007a), caused by calpain recognition and digestion of disordered protein structures (Tompa et al., 2004). Decrease of absorption in the amide II region was most likely a consequence of major decrease in CN absorption, influencing all other features in the amide II peak. The reason for a reduction in β-sheet absorbance might be that these structures are more prone to destabilization, compared to α-helices, when the overall integrity of the protein is compromised. Skeletal stretch in proteins are generally found in the region from 1200-880 cm^{-1}(Barth, 2007b), and the absorption of the peak at 1055 cm^{-1} can be attributed to changes in secondary structure, where an increase in disordered structures at the expense of ordered structures could be causing the increase in absorption. Bocker et al. (2017) identified the skeletal stretch as a region inversely correlating to the degree of hydrolysis of different muscle hydrolysates, which is opposite of the response in the current study. This can be attributed to differences in the constituents of the analyzed samples. In the current study, a representative volume of the whole sample was used for FT-IR, while Bocker et al. (2017) used a filtered sample from the peptide-rich water phase. Meaning that Bocker et al. (2017) analyzed increasing amounts of smaller peptides, while the current study analyzes a mix of peptides and more intact proteins and protein structures, possibly causing the inverse relation between FT-IR and proteolysis in the two studies. Overall, this indicates that the skeletal stretch was an important region for analyzing degree of proteolysis.

3.3 Raman spectroscopy

Analyzing differences in Raman spectra reveal many of the same responses following proteolysis as the FT-IR analysis, including the relative difference in intensity between incubation times (Fig. 5 and Table 3). PCA revealed the same areas of importance as for the difference spectra, but they were not as distinct as for FT-IR. The PLSR model from Raman was less good than for FT-IR, but shows that there was a reasonable link between Raman and degree of proteolysis in the model system. In short, there seem to be a decrease in β-sheet vibrations, with a simultaneous increase in carboxylic acid and skeletal/α-helix vibrations. Decrease in β-sheets following proteolysis was evident in both the amide I and III peak, with a respective decrease in intensity at 1673 and 1246 cm^{-1} (Krimm &

Bandekar, 1986). Intensity for COO^- at 1405 cm^{-1} and for COOH at 1720 cm^{-1} increases, reinforcing the notion that the amount of C-terminal carboxylic acid increases (Tu, 1986). Increase at 915 cm^{-1} in the skeletal stretch region can indicate an increase in α-helix structures (Tu, 1986), and may be explained by a relative increase in α-helices compared to other secondary structures as the amount of β-sheets were reduced. In addition, the intensity of amino acid side chain ring vibrations of phenylalanine (Phe) at 1003 cm^{-1} imply a decrease in protein concentration in the analyzed samples with increasing degree of proteolysis, but does not contain any conformational information (Barrett, Peticolas, & Robson, 1978).

Table 3*. Overview of important spectroscopic responses detected by Raman spectroscopy related to degree of proteolysis in the current study. Arrows denote changes in intensity as a function of degree of proteolysis.*

Approx. wavenumber (cm^{-1})	Absorbance change	Structure
915	↑	Skeletal stretch, CC, α-helix [a, b, c]
1003	↓	Phe [a, b, c]
1245	↓	Amide III, CN and NH, β-sheet/random coil [a ,b, c]
1405	↑	COO^- [a, c]
1673	↓	Amide I, β-sheet [a, b, c]

[a] (Herrero, 2008), [b] (Rygula et al., 2013), [c] (Tu, 1986).

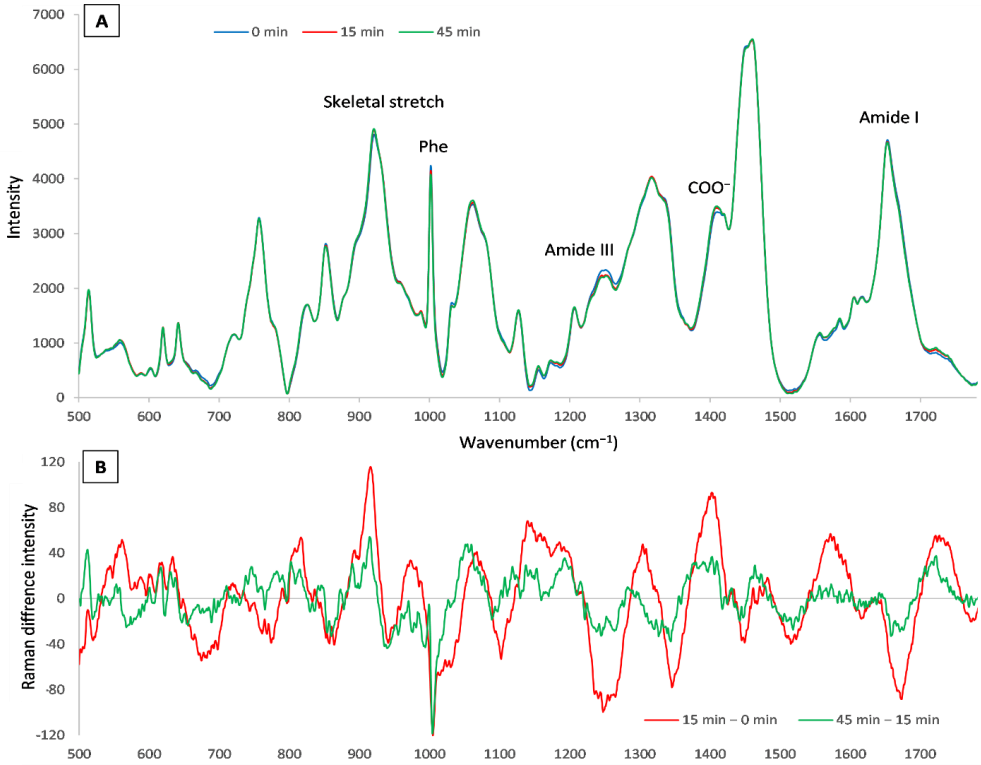

Figure 5. (A) Average Raman spectra for each incubation time from three samples in the wavenumber range from 500 to 1800 cm^{-1}. Peaks important for analyzing degree of proteolysis are noted in the figure. ***(B)*** Difference spectra for average Raman spectra for each incubation time where 15 min – 0 min and 45 min – 15 min corresponds to red and green lines, respectively.

3.4 NIR spectroscopy

NIR spectroscopy of dried samples showed some promise when examining the spectra (Fig. 6), PCA and PLSR (Table 2). This means that there was possibly enough information in the NIR spectra to distinguish larger differences in degree of proteolysis of dried samples. PCA reveals that the peak at approx. 1940 nm explains almost all of the variation in the spectra related to degree of proteolysis, and this peak is attributed to water (Buning-Pfaue, 2003). The higher absorption for lesser degree of proteolysis can be because of a higher concentration of bound water in more intact myofibrils or it could be because of changes in the conditions surrounding the water molecules, e.g. gelation properties or the size of proteins (Buning-Pfaue, 2003). This makes it difficult to pin-point the mechanism behind the NIR response.

NIR spectroscopy of liquid samples yielded poor results for all methods of investigating the spectra. It did not reveal any distinct spectral differences, PCA grouping or any good PLSR models (Table 2) related to degree of proteolysis.

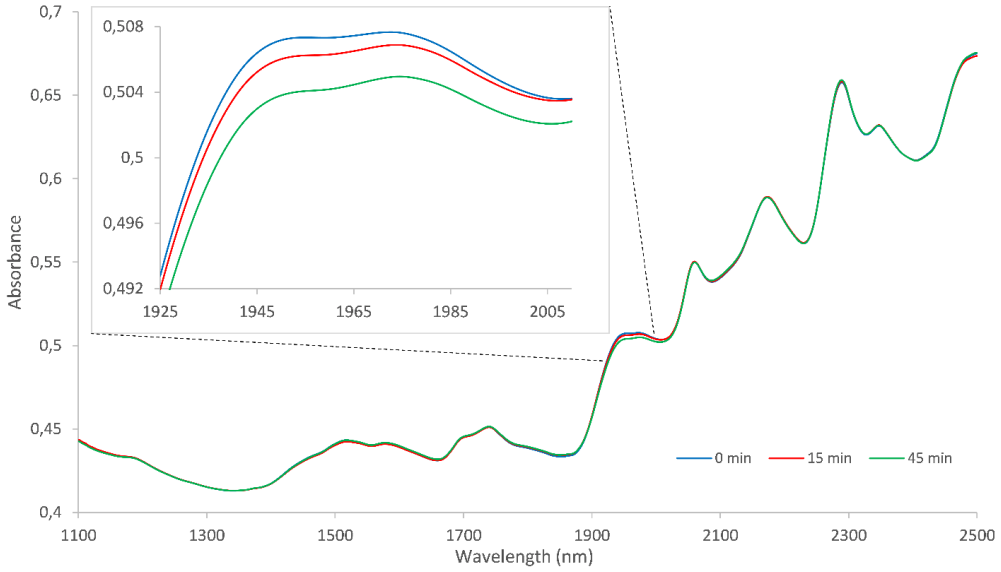

Figure 6. Average NIR spectra from dried samples after incubation for 0 min, 15 min and 45 min in the wavelength range from 1100 to 2500 nm. Inset shows the peak at approx. 1950 nm.

3.5 Fluorescence spectroscopy

Fluorescence spectra of liquid samples (Fig. 7) seems to differentiate between degraded and non-degraded samples, manifested as a slight shift in the emission maximum peak to higher wavelengths for degraded samples. Furthermore, spectra from degraded samples were overlapping at different wavelengths throughout the main peak, reinforcing the impression that fluorescence spectroscopy is not sensitive to protein degradation beyond the major changes before 15 min in the current experiment. This trend was present in PCA (not shown), but the shift to higher wavelengths was not consistent for all samples, giving a high degree of overlap in the scores plot. Results from PLSR supports the notion that the correlation was weak, as the model was not reliable when predicting degree of proteolysis (Table 2). The fluorescence peak is attributed to tryptophan (Trp) emission, and changes in maximum emission peak position of Trp is often related to microenvironment changes (Christensen et al., 2006). Trp emission peak centers at longer wavelengths for less structured molecules, which can explain the observed change in emission peak, because the degraded proteins were less structured than their un-degraded counterparts.

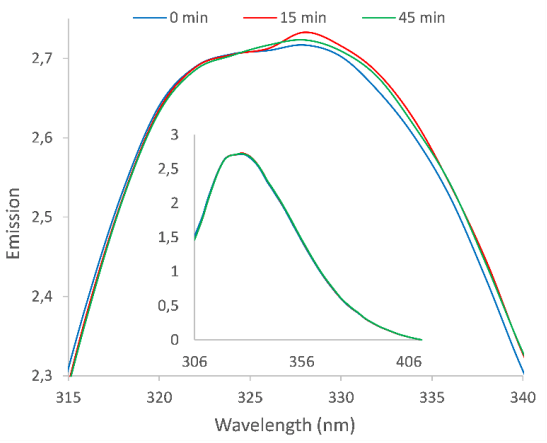

Figure 7. Average fluorescence emission spectra (excitation at 292 nm) from liquid samples for incubation at 0 min, 15 min and 45 min after SNV, shown as blue, red and green lines respectively. Inset shows entire spectra, while the main figure shows only the peak.

4. GENERAL DISCUSSION

From the current experiment, it was evident that FT-IR spectroscopy was capable of predicting degree proteolysis in myofibrils. However, there are some concerns regarding FT-IR if one was to integrate it in a meat processing plant, first one need to overcome the obstacle of high water absorption in FT-IR, and secondly one needs a constant atmosphere or vacuum when measuring. This can be solved by using attenuated total reflectance where the water peak at 1640 cm^{-1} is omitted in the spectra and the crystal is thoroughly cleaned between each measurement, which may be too much work to be a practical solution. However, FT-IR can potentially be used as tool to screen samples for degree of proteolysis by analyzing cryosections in the laboratory.

Raman spectroscopy did not perform as well as FT-IR in PCA or PLSR, but interpretation of spectroscopic differences were consistent with results from FT-IR, which makes us believe that Raman spectroscopy can perform on a similar level as FT-IR. The poorer performance for Raman spectroscopy in the current study may be caused by less standardized measurements (e.g. by manually focusing and acquiring Raman spectra) and fewer samples included in the analysis. Regardless, both FT-IR and Raman showed the same trend in intensity changes as the degree of proteolysis did, showing larger differences early in the degradation process than later, demonstrating that there is a possible quantitative association between spectroscopy and protein degradation. Another important consideration is how plausible it is for the spectroscopic method to be used in a meat processing plant, and in this case Raman spectroscopy has several advantages, most importantly that it is not very sensitive to water in the sample, it can be used in ambient conditions

and spectra can be recorded directly on the meat surface (Li-Chan, 1996). Sensitivity of Raman spectroscopy is also a subject to consider, as the Raman signal is relatively weak, and requires analyte concentration in the range of 2-20 mg/mL to get good signal using conventional Raman instruments (Li-Chan, 1996). Since the concentration of degraded proteins is relatively small compared to the total amount of proteins, and the spectroscopic response is universal in nature (not linked to specific proteins), it is possible that the specificity of Raman spectroscopy is not good enough for measurements of degree of proteolysis.

Models from NIR spectroscopy performed inferior to both Raman and FT-IR on dried samples, but still seems to contain important information regarding degree of proteolysis. The poorer performance may be caused by a higher degree of overlapping spectral features and less specific spectral information related to the important changes during protein degradation (e.g. protein secondary structure and CN vibration) in NIR spectra. Since the observed change in NIR spectra in the current study was believed to be caused by the condition of the dried samples, and not specific protein modifications, there is little reason to believe that these findings are transferrable to intact meat.

Even though Fluorescence spectroscopy is a very sensitive method, it did not perform well enough to give models of predictive value, indicating that fluorescence spectroscopy may not be suited for measuring degree of proteolysis.

As protein degradation progresses, the amount of peptide terminal groups increases, which causes a decrease in pH. This decrease in pH has been shown to not affect FT-IR spectroscopy of whey proteins (Poulsen et al., 2016), and the buffer used in the current experiment should keep pH stable, so this effect was considered negligible in the current experiment. Nevertheless, it is plausible that the spectroscopic contribution of C-terminal carboxylic acids (at approx. 1400 cm^{-1}), formed during proteolysis, will partially disappear or merge with contributions from the naturally occurring pH-decline post-mortem (Andersen et al., 2017).

5. CONCLUSION

FT-IR and Raman spectroscopy showed promise for measuring degree of proteolysis in myofibrils, with Raman spectroscopy as the front-runner for testing and possible implementation as a part of meat quality assessment in a meat processing plant. NIR and fluorescence spectroscopy showed little promise for measuring degree of proteolysis. It is important to point out that this study only indicates that spectroscopic techniques are viable for analyzing degree of proteolysis in model systems, and that more studies are needed to make any conclusions as to the viability for measuring proteolysis in intact meat.

Acknowledgements

We thank Bjørg Narum, Vibeke Høst and Dr. Morten Skaugen for technical assistance during sampling and in the analyses, Dr. Kristian Liland for assistance in pre-processing of spectroscopic data and Dr. Ulrike Böcker for critical comments on the manuscript and interpretation of spectroscopic results. This work was supported by the Foundation for Research Levy on Agricultural products and the Agricultural Agreement Research Fund of Norway.

6. REFERENCES

Andersen, P. V., Veiseth-Kent, E., & Wold, J. P. (2017). Analyzing pH-induced changes in a myofibril model system with vibrational and fluorescence spectroscopy. *Meat Sci, 125*, 1-9.

Barnes, R. J., Dhanoa, M. S., & Lister, S. J. (1989). Standard Normal Variate Transformation and De-Trending of near-Infrared Diffuse Reflectance Spectra. *Applied Spectroscopy, 43*(5), 772-777.

Barrett, T. W., Peticolas, W. L., & Robson, R. M. (1978). Laser Raman light-scattering observations of conformational changes in myosin induced by inorganic salts. *Biophys J, 23*(3), 349-358.

Barth, A. (2007a). Infrared spectroscopy of proteins. *Biochim Biophys Acta, 1767*(9), 1073-1101.

Barth, A. (2007b). *Methods in Protein Structure and Stability Analysis: Vibrational spectroscopy*: Nova Biomedical Books.

Beattie, J. R., Bell, S. E. J., Borggaard, C., & Moss, B. W. (2008). Preliminary investigations on the effects of ageing and cooking on the Raman spectra of porcine longissimus dorsi. *Meat Science, 80*(4), 1205-1211.

Bocker, U., Ofstad, R., Wu, Z., Bertram, H. C., Sockalingum, G. D., Manfait, M., Egelandsdal, B., & Kohler, A. (2007). Revealing covariance structures in fourier transform infrared and Raman microspectroscopy spectra: a study on pork muscle fiber tissue subjected to different processing parameters. *Appl Spectrosc, 61*(10), 1032-1039.

Bocker, U., Wubshet, S. G., Lindberg, D., & Afseth, N. K. (2017). Fourier-transform infrared spectroscopy for characterization of protein chain reductions in enzymatic reactions. *Analyst, 142*(15), 2812-2818.

Buning-Pfaue, H. (2003). Analysis of water in food by near infrared spectroscopy. *Food Chemistry, 82*(1), 107-115.

Calvo, L., Toldra, F., Aristoy, M. C., Lopez-Bote, C. J., & Rey, A. I. (2016). Effect of dietary organic selenium on muscle proteolytic activity and water-holding capacity in pork. *Meat Science, 121*, 1-11.

Christensen, J., Norgaard, L., Bro, R., & Engelsen, S. B. (2006). Multivariate autofluorescence of intact food systems. *Chem Rev, 106*(6), 1979-1994.

Goll, D. E., Thompson, V. F., Li, H., Wei, W., & Cong, J. (2003). The calpain system. *Physiol Rev, 83*(3), 731-801.

Guler, G., Dzafic, E., Vorob'ev, M. M., Vogel, V., & Mantele, W. (2011). Real time observation of proteolysis with Fourier transform infrared (FT-IR) and UV-circular dichroism spectroscopy: Watching a protease eat a protein. *Spectrochimica Acta Part a-Molecular and Biomolecular Spectroscopy, 79*(1), 104-111.

Herrero, A. M. (2008). Raman spectroscopy a promising technique for quality assessment of meat and fish: A review. *Food Chemistry, 107*(4), 1642-1651.

Huff-Lonergan, E., & Lonergan, S. M. (2005). Mechanisms of water-holding capacity of meat: The role of postmortem biochemical and structural changes. *Meat Sci, 71*(1), 194-204.

Huff Lonergan, E., Zhang, W., & Lonergan, S. M. (2010). Biochemistry of postmortem muscle - lessons on mechanisms of meat tenderization. *Meat Sci, 86*(1), 184-195.

Hughes, J. M., Oiseth, S. K., Purslow, P. P., & Warner, R. D. (2014). A structural approach to understanding the interactions between colour, water-holding capacity and tenderness. *Meat Science, 98*(3), 520-532.

Kohler, A., Bocker, U., Warringer, J., Blomberg, A., Omholt, S. W., Stark, E., & Martens, H. (2009). Reducing Inter-replicate Variation in Fourier Transform Infrared Spectroscopy by Extended Multiplicative Signal Correction. *Applied Spectroscopy, 63*(3), 296-305.

Koohmaraie, M. (1992). The Role of Ca-2+-Dependent Proteases (Calpains) in Postmortem Proteolysis and Meat Tenderness. *Biochimie, 74*(3), 239-245.

Koohmaraie, M., Schollmeyer, J. E., & Dutson, T. R. (1986). Effect of Low-Calcium-Requiring Calcium Activated Factor on Myofibrils under Varying Ph and Temperature Conditions. *Journal of Food Science, 51*(1), 28-&.

Krimm, S., & Bandekar, J. (1986). VIBRATIONAL SPECTROSCOPY AND CONFORMATION OF PEPTIDES, POLYPEPTIDES, AND PROTEINS. [Review]. *Advances in Protein Chemistry, 38*, 181-364.

Kristensen, L., & Purslow, P. P. (2001). The effect of ageing on the water-holding capacity of pork: role of cytoskeletal proteins. *Meat Science, 58*(1), 17-23.

Lametsch, R., Roepstorff, P., & Bendixen, E. (2002). Identification of protein degradation during post-mortem storage of pig meat. *J Agric Food Chem, 50*(20), 5508-5512.

Lametsch, R., Roepstorff, P., Moller, H. S., & Bendixen, E. (2004). Identification of myofibrillar substrates for mu-calpain. *Meat Sci, 68*(4), 515-521.

Li-Chan, E. C. Y. (1996). The applications of Raman spectroscopy in food science. *Trends in Food Science & Technology, 7*(11), 361-370.

Li-Chan, E. C. Y., Ismail, A. A., Sedman, J., & van de Voort, F. R. (2002). Vibrational Spectroscopy of Food and Food Products *Handbook of Vibrational Spectroscopy*: John Wiley & Sons, Ltd.

Liland, K. H., Kohler, A., & Afseth, N. K. (2016). Model-based pre-processing in Raman spectroscopy of biological samples. *Journal of Raman Spectroscopy, 47*(6), 643-650.

Martens, H., & Stark, E. (1991). Extended Multiplicative Signal Correction and Spectral Interference Subtraction - New Preprocessing Methods for near-Infrared Spectroscopy. *Journal of Pharmaceutical and Biomedical Analysis, 9*(8), 625-635.

Melody, J. L., Lonergan, S. M., Rowe, L. J., Huiatt, T. W., Mayes, M. S., & Huff-Lonergan, E. (2004). Early postmortem biochemical factors influence tenderness and water-holding capacity of three porcine muscles. *J Anim Sci, 82*(4), 1195-1205.

Moczkowska, M., Poltorak, A., & Wierzbicka, A. (2017). The effect of ageing on changes in myofibrillar protein in selected muscles in relation to the tenderness of meat obtained from cross-breed heifers. *International Journal of Food Science and Technology, 52*(6), 1375-1382.

Moller, J. K., Parolari, G., Gabba, L., Christensen, J., & Skibsted, L. H. (2003). Monitoring chemical changes of dry-cured Parma ham during processing by surface autofluorescence spectroscopy. *J Agric Food Chem, 51*(5), 1224-1230.

Olson, D. G., Parrish, F. C., Dayton, W. R., & Goll, D. E. (1977). Effect of Postmortem Storage and Calcium Activated Factor on Myofibrillar Proteins of Bovine Skeletal-Muscle. *Journal of Food Science, 42*(1), 117-124.

Ouali, A., & Talmant, A. (1990). Calpains and Calpastatin Distribution in Bovine, Porcine and Ovine Skeletal-Muscles. *Meat Science, 28*(4), 331-348.

Poulsen, N. A., Eskildsen, C. E., Akkerman, M., Johansen, L. B., Hansen, M. S., Hansen, P. W., Skov, T., & Larsen, L. B. (2016). Predicting hydrolysis of whey protein by mid-infrared spectroscopy. *International Dairy Journal, 61*, 44-50.

Prevolnik, M., Skrlep, M., Janes, L., Velikonja-Bolta, S., Skorjanc, D., & Candek-Potokar, M. (2011). Accuracy of near infrared spectroscopy for prediction of chemical composition, salt content and free amino acids in dry-cured ham. *Meat Sci, 88*(2), 299-304.

Rappsilber, J., Mann, M., & Ishihama, Y. (2007). Protocol for micro-purification, enrichment, pre-fractionation and storage of peptides for proteomics using StageTips. *Nature Protocols, 2*(8), 1896-1906.

Rygula, A., Majzner, K., Marzec, K. M., Kaczor, A., Pilarczyk, M., & Baranska, M. (2013). Raman spectroscopy of proteins: a review. *Journal of Raman Spectroscopy, 44*(8), 1061-1076.

Taylor, R. G., Geesink, G. H., Thompson, V. F., Koohmaraie, M., & Goll, D. E. (1995). Is Z-Disk Degradation Responsible for Postmortem Tenderization. *Journal of Animal Science, 73*(5), 1351-1367.

Tompa, P., Buzder-Lantos, P., Tantos, A., Farkas, A., Szilagyi, A., Banoczi, Z., Hudecz, F., & Friedrich, P. (2004). On the sequential determinants of calpain cleavage. *J Biol Chem, 279*(20), 20775-20785.

Tu, A. T. (1986). *Spectroscopy of Biological Systems*: Wiley.

Veiseth-Kent, E., Hollung, K., Ofstad, R., Aass, L., & Hildrum, K. I. (2010). Relationship between muscle microstructure, the calpain system, and shear force in bovine longissimus dorsi muscle. *Journal of Animal Science, 88*(10), 3445-3451.

Wubshet, S. G., Mage, I., Bocker, U., Lindberg, D., Knutsen, S. H., Rieder, A., Rodriguez, D. A., & Afseth, N. K. (2017). FTIR as a rapid tool for monitoring molecular

weight distribution during enzymatic protein hydrolysis of food processing by-products. [10.1039/C7AY00865A]. *Analytical Methods, 9*(29), 4247-4254.
Yu, Y., Smith, M., & Pieper, R. (2014). A spinnable and automatable StageTip for high throughput peptide desalting and proteomics.

PAPER III

Predicting post-mortem meat quality in porcine *longissimus lumborum* using Raman, Near Infrared and Fluorescence spectroscopy

Petter Vejle Andersen [a]*, Jens Petter Wold [a], Eli Gjerlaug-Enger[b], Eva Veiseth-Kent [a]

[a] Nofima, Osloveien 1, 1430 Ås, Norway

[b] Norsvin, Storhamargata 44, 2317 Hamar, Norway

E-mail adresses:

Petter Vejle Andersen: petter.andersen@nofima.no

Jens Petter Wold: jens.petter.wold@nofima.no

Eli Gjerlaug-Enger: eli.gjerlaug@norsvin.no

Eva Veiseth-Kent: eva.veiseth-kent@nofima.no

*Corresponding author at: Nofima, Osloveien 1, 1430 Ås, Norway. Tel.: +47 64 97 04 90.

Manuscript prepared for submission to Meat Science

ABSTRACT

Spectroscopic techniques can provide valuable information about post-mortem meat quality. In the current study, Raman, NIR and fluorescence spectroscopy was used to analyze pH, drip loss and intramuscular fat in pork *longissimus lumborum* (n = 122) at 4-5 days post-mortem. Results were promising for partial least squares regression (PLSR) from Raman spectroscopy, giving coefficients of determination from cross validation (r_{cv}^2) ranging from 0.41 to 0.73. Important regions in the PLSR models from Raman spectroscopy were attributed to changes in concentrations of post-mortem metabolites and modifications of protein secondary structure. Near infrared and fluorescence spectroscopy showed limited ability to analyze quality, with r_{cv}^2 ranging from 0.16 to 0.51 and 0.02 to 0.18, respectively. This study encourages further research on the subject of Raman spectroscopy as a technique for meat quality analysis.

Keywords

Water-holding capacity; pH; intra muscular fat; Raman spectroscopy; NIR spectroscopy; fluorescence spectroscopy

1. INTRODUCTION

One of the most important quality parameters for pork is water-holding capacity (WHC), affecting monetary value, processing properties (Torley, D'Arcy, & Trout, 2000) and eating quality (Hughes, Oiseth, Purslow, & Warner, 2014). There are many factors influencing WHC of meat, including rate of post-mortem pH decline and ultimate pH (pH_u) (Warriss & Brown, 1987), proteolysis (Huff-Lonergan & Lonergan, 2005) and chemical composition of meat (e.g. intramuscular fat (IMF)) (Lawrie, 1985), illustrating the complexity of this property. WHC of fresh meat is usually measured as amount drip formed from a standardized meat sample, e.g. the bag method (Honikel, 1998) and EZ-DripLoss method (Rasmussen & Andersson, 1996), which are invasive, labor- and time-consuming methods. Even the standard method for measuring pH requires a glass probe to be inserted into the meat and manually recording the pH-value. Development of rapid and non-invasive methods for meat quality assessment for on-line or at-line application is consequently of interest to the meat industry, for amongst others meat classification and optimization of production procedures. To this end, there have been many studies conducted utilizing spectroscopic techniques to analyze pH, WHC and chemical composition of meat. The most promising techniques for implementation in the abattoir are near infrared (NIR), Raman and fluorescence spectroscopy, because they are all non-invasive and rapid techniques.

There have been numerous studies conducted concerning NIR spectroscopy and meat quality, and the subject has been thoroughly reviewed within the last decade (Prieto, Pawluczyk, Dugan, & Aalhus, 2017; Prieto, Roehe, Lavin, Batten, & Andres, 2009; Weeranantanaphan, Downey, Allen, & Sun, 2011). To the best of our knowledge, the benchmark of performance for VIS-NIR spectroscopy performed on pork are as follows: pH: coefficient of determination (r_{cv}^2) = 0.82 and root mean square error of cross validation (RMSECV) = 0.10 (Liao, Fan, & Cheng, 2010); drip loss: r_p^2 = 0.76 and root mean square error of prediction (RMSEP) = 0.8% (Kapper, Klont, Verdonk, Williams, & Urlings, 2012); and IMF: r_{cv}^2 = 0.96 and RMSECV = 0.46% (Prevolnik et al., 2005). Although many studies have shown great promise, no NIR instruments for commercial use for prediction of pH and WHC have been developed.

Raman spectroscopy has gained some traction for pork quality analysis the last few years with the development of a handheld Raman instrument (Schmidt, Sowoidnich, & Kronfeldt, 2010), which subsequently has been used to analyze pork quality. Results for pH_u and drip loss predictions have been promising from Raman spectra acquired between 30 and 120 min post-mortem in the abattoir. Being able to predict pH_u with r_{cv}^2 = 0.68 and RMSECV = 0.09 and drip loss with r_{cv}^2 = 0.73 and RMSECV = 1.0% in one study (Scheier, Bauer, & Schmidt, 2014), and r_{cv}^2 = 0.31 and RMSECV = 0.05 and drip loss with r_{cv}^2 = 0.52 and RMSECV = 0.6% in a follow-up study (Scheier, Scheeder, & Schmidt,

2015). We are unaware of any studies on IMF in pork, but a study has been conducted for lamb meat, resulting in a r_{cv}^2 = 0.02 and RMSECV = 1.2% for IMF (Fowler, Ponnampalam, Schmidt, Wynn, & Hopkins, 2015).

Not many studies have been conducted using fluorescence spectroscopy to analyze fresh pork quality. One of the few studies analyzing fresh pork quality with fluorescence was carried out by Brondum et al. (2000), where drip loss was predicted with r^2 = 0.68 and SEP = 2.27% and IMF was predicted with r^2 = 0.57 and SEP = 1.09%. Fluorescence spectroscopy has also shown promise to analyze pH in a model system containing isolated myofibrils from pork (Andersen, Veiseth-Kent, & Wold, 2017), encouraging further research in this area.

The main aim of this work was to investigate the potential for Raman, NIR and fluorescence spectroscopy to predict drip loss and measure pH_u of fresh pork, with a secondary aim to measure IMF. Drip loss was measured by EZ-DripLoss method and drip formed during eight days of vacuum storage, giving two fundamentally different approaches for measurement of drip loss. Using three spectroscopic techniques on the same set of samples allows for comparison of spectroscopic techniques under similar conditions, possibly indicating which techniques should be the focus in future research.

2. MATERIALS AND METHODS

2.1 Animals and meat quality analyses

A selection of 122 Norwegian Landrace boars from an ongoing testing programme at Norsvin's boar test station in southeastern Norway were part of this study. The boars were fed ad libitum on conventional concentrates, and the average start and end weight at the test station was 35 to 120 kg live weight. The boars were slaughtered in eight batches at a commercial abattoir over a period of 9 months. The animals were stunned with 90 % CO2, followed by exsanguination, scalding and splitting within 30 min post-mortem. After 45 min the carcasses were transported through a cooling tunnel (-22 °C, air velocity 8-10 m/s). Following this, the carcasses were chilled in a cooler at 1 °C to 3 °C for 20 h until a core temperature of 7 °C was reached. Finally, the carcasses were transported to a partial dissection line at Animalia, the Norwegian Meat and Poultry Research Centre.

At 4 or 5 days postmortem, the loin muscle (LL – *Longissimus lumborum*) was dissected from the right side of the carcasses, trimmed for fat and used for assessment of multiple meat quality traits and spectroscopic measurements as described in the following. Ultimate pH was measured at the last rib curvature using an insertion pH electrode (WTW 82362, pH 330i, Welheim, Germany). A 5-cm slice of the muscle (positioned 2 cm anterior and 3 cm posterior to the last rib curvature) was homogenized by grinding for 30 s using a mixer (Robot Coupe r5a+, W 1100, Robot Coupe, USA, Inc.)

for subsequent measurement of IMF (FOSS, Denmark) as described by Gjerlaug-Enger, Aass, Odegard, and Vangen (2010).

Assessments of drip loss were performed using two different strategies, namely the EZ-DripLoss method and purge loss in vacuum packages. For the EZ-DripLoss measurement (Rasmussen & Andersson, 1996), two samples at fixed locations on a 2-cm slice (positioned 3 to 5 cm posterior to the last rib curvature) were cut using a circular knife (2.5 cm diameter). Samples were placed in drip loss containers (C. Christensen ApS, Denmark), and stored at 4 °C for 24 h, after which the weight of the drip loss was measured, and expressed as a percentage of the initial sample weight. For the purge loss measurement, a 5-cm thick slice (positioned 8 to 13 cm posterior to the last rib curvature) was weighed before being placed in a plastic bag and vacuum packed using 98% vacuum. The vacuum packed slices were placed in a single layer on a rack in a cooler (4 °C), and stored for 8 days, after which the bags were opened, and the meat gently dabbed with paper before weighing again. Purge was calculated as a percentage of the initial sample weight.

2.2 Spectroscopic analysis

A freshly cut slice of approx. 3 cm (positioned 5 to 8 cm posterior to the last rib curvature) from *LL* was used for spectroscopic analyses at 4-5 days post-mortem. All samples were analyzed with NIR spectroscopy first, followed by fluorescence spectroscopy and finally Raman spectroscopy.

2.2.1 NIR spectroscopy

The meat slice designated for spectroscopy was cut and mounted in a Rapid content module sample cell (FOSS Analytical, Hillerød, Denmark). A spectrum from a sample surface of 17.25 mm was recorded at eight different locations on the meat surface using an XDS Rapid content analyzer (FOSS Analytical, Hillerød, Denmark) measuring in the 400-2500 nm wavelength region at 0.5 nm intervals. Spectra were recorded as log(1/R) with FOSS NIRSystem Vision software. All spectra from one sample were averaged prior to further analysis.

2.2.2 Fluorescence spectroscopy

Fluorescence was measured in front face mode on the same sample surface as was measured with NIR. The measurements were carried out with a FluoroMax-4 (Horiba Scientific, Edison, NJ, USA) in front face mode via a FL-300/FM43000 bifurcated fiber-optic probe (Horiba Scientific). The distance between the probe head and sample was about 5 cm and created a circular measurement area of 40 mm diameter. Probe and sample were covered by a black shield to avoid ambient straylight. Emission spectra in the region from 300 to 500 nm (2 nm intervals) were recorded for excitation at 292 nm.

2.2.3 Raman spectroscopy

The sample was cut into three slices and one spectrum was recorded from the freshly cut surface of each slice using a Kaiser RamanRXN2™ Multi-channel Raman analyzer (Kaiser Optical Systems, Inc., Ann Arbor, MI, USA) equipped with a 785 nm laser and PhAT probe, measuring a spot size of 6 mm in diameter. The spectra were recorded with a laser power set to 400 mW in the range of 150-1890 cm^{-1} with 0.3 cm^{-1} intervals and exposure of 3 times 15 s was used for acquisition. Instrument set-up and experiment was controlled using iC Raman version X software (Mettler Toledo, Greifensee, Switzerland).

2.3 Pre-processing of spectra and data analysis

2.3.1 Pre-processing of spectra

Pre-processing of spectral data was done to give comparable spectra for further analysis, by reducing or removing the impact of noise, scatter effects and other undesirable alterations in the spectra.

The three Raman spectra from each sample were averaged, and the oxygen peak at 1555 cm^{-1} was removed from the spectra prior to further pre-processing in the range from 450 to 1775 cm^{-1}. Raman spectra were first base-line corrected and fluorescence background was removed (Lieber & Mahadevan-Jansen, 2003), before full extended multiplicative scattering correction was applied (EMSC) (Liland, Kohler, & Afseth, 2016). The NIR spectra were divided into two regions, 400 to 1850 nm and 780 to 1850 nm, before standard normal variate (SNV) algorithm (Barnes, Dhanoa, & Lister, 1989) was applied to each region separately. Fluorescence spectra were pre-processed by SNV.

2.3.2 Data analysis

Partial least squares regression (PLSR) was used for determining relationships between reference measurements and spectroscopic data. PLSR emphasizes information in the spectra that is important for explaining variation in the reference measurements when making models (H. Martens & Martens, 2001). PLSR models were cross-validated using leave-one-out procedure. An uncertainty test was performed for the PLSR models to give information about important variables in the models (H. Martens & Martens, 2000), and to use these variables to investigate if more reliable models could be constructed using only the important variables. The ratio of prediction to deviation (RPD) value gives a quick appraisal of a model, and is calculated as the standard deviation of the reference values divided by the models RMSECV, where a value larger than 2 is recommended for rough screening purposes (Williams, 2014).

PLSR was performed in the following spectral regions: Raman: 450 to 1800 cm^{-1}; NIR: for pH: 400 to 1850 nm, for drip loss and IMF: 780 to 1850 nm; fluorescence: emission from 306 to 412 nm.

Pre-processing of Raman spectra were carried out using Open EMSC toolbox for MATLAB freely downloadable from http://nofimaspectroscopy.org in MATLAB version R2013b (The MathWorks, Natick, MA). Data analysis was done with The Unscrambler® X version 10.4 (CAMO Process AS, Norway).

3. RESULTS AND DISCUSSION

3.1 Reference meat quality measurements

Results from reference analyses are summarized in **table 1** and correlations between reference measurements are shown in **table 2**. The reference measurements were conducted later than what is typical for studies regarding pork quality, 4-5 days post-mortem, as opposed to the more common 24 h (L. B. Christensen, 2003; Otto, Roehe, Looft, Thoelking, & Kalm, 2004). This could have affected some of the reference measurements, for instance, can drip loss be influenced by post-mortem proteolysis (Gardner, Huff Lonergan, & Lonergan, 2005). Nevertheless, the distribution of the reference measurements was sufficient for modelling purposes, since the standard deviation divided by range was 0.21 for all analyses. The reason for conducting analyses at 4-5 days post-mortem was that this is a procedure established by the collaborating pig-breeding association. They analyze thousands of pigs yearly, which have led to very standardized operating procedures for meat quality analysis.

Table 1. Mean value, minimum and maximum value, standard deviation (SD) and SD divided by range for reference measurements (n = 122, except for VD where n = 103).

	Mean	Min	Max	SD	SD/range
pH_u	5.46	5.29	5.66	0.08	0.21
EZ-drip %	7.9	3.9	12.4	1.8	0.21
VD %	6.3	3.7	8.8	1.1	0.21
IMF	1.1	0.8	1.6	0.17	0.21

Table 2. Correlation between the investigated quality traits
(n = 122, except for VD where n = 103). (* denotes significant correlation with $p < 0.05$).

	pH_u	EZ-drip %	VD %
EZ-drip %	-0.48*		
VD %	-0.30*	0.60*	
IMF	0.03	-0.30*	-0.22*

Of note when comparing the two drip loss measurements is that the EZ-DripLoss measurement had a larger range than the vacuum drip (VD), even though the measurement for EZ-DripLoss was conducted over a 24 h period, as opposed to 8 d for VD. This is likely caused by the more invasive procedure and larger surface area to volume of the EZ-DripLoss method and that the VD samples might have an upper limit of drip formation attributed to physical constraints of the vacuum bag. Another cause for lower drip loss in vacuum packed samples could be reabsorption of water during storage, as hypothesized by Kristensen and Purslow (2001). The correlation between the two measurements was 0.60, meaning that they most likely measure different phenomena related to drip formation, e.g. the impact of vacuum packing or the effect of sample morphology.

The correlation of pH and IMF with the drip measurements showed the same tendency for both drip methods, where low values for pH and IMF were significantly correlated with high drip. This correlation was stronger for EZ-DripLoss than for VD, even though their SD/range values were comparable. This implies that the EZ-DripLoss measurement could be closer related to physical attributes of the meat than the VD measurement, thus giving reason to believe that EZ-DripLoss measured more of the inherent meat characteristics while VD to a larger extent was also influenced by the methodological procedures. However, it is still of interest to investigate if VD can be predicted by spectroscopic techniques, as this is how meat is often presented to consumers. Additionally, there is no golden standard for measurement of drip loss in meat, meaning that the method of measuring drip loss needs to be tailored to the specific applications.

3.2 Spectroscopy

A summary of the performance for PLSR models from NIR, fluorescence and Raman spectroscopy and reference measurements is shown in **table 3**. What is evident is that models from Raman spectroscopy performed better than NIR and fluorescence for all reference measurements, and that NIR performed better than fluorescence. The RPD for each model ranged from 0.97 to 1.91, meaning that no model exceeded the recommended threshold for rough screening at 2.0 (Williams, 2014). Nevertheless, the models based on Raman spectroscopy seem to be suitable for rough sorting of samples in batches according to their predicted values (**Fig. 1**). For instance, there was a significant 2.2% ($p<0.001$) difference in average measured EZ-DripLoss between the 20% samples with highest predicted EZ-DripLoss compared to the remaining samples. Batches of meat with higher drip loss can be sorted from the rest and used in products where the inferior quality is accounted for, such as canned pork (Florowski et al., 2017), while simultaneously increasing the average quality of the remaining pork.

Model performance has to be considered in relation to the error of the reference analysis, which is difficult to obtain for drip loss measurements because it is impossible to analyze the same sample

twice. It is possible to estimate this error by measuring adjacent samples, but then it is important to acknowledge that there is an inherent difference in drip loss, both longitudinal and transversal, along the entire *longissimus thoracis et lumborum* (L. B. Christensen, 2003; Otto et al., 2004).

Table 3. Performance of PLSR models from Raman, NIR and fluorescence spectroscopy vs. reference measurements. EZ = EZ-DripLoss in %, VD = vacuum drip loss in % and IMF = intramuscular fat in %.

	Raman				NIR				Fluorescence			
	n	r_{cv}^2	*RMSECV*	*RPD*	*n*	r_{cv}^2	*RMSECV*	*RPD*	*n*	r_{cv}^2	*RMSECV*	*RPD*
EZ	121	0.51	1.2	1.45	119	0.27[b]	1.5	1.20	121	0.18	1.6	1.13
VD	103	0.41	0.82	1.29	101	0.16[b]	0.97	1.09	103	0.02	1.1	0.97
pH_u	122	0.49	0.06	1.42	120	0.29[a]	0.07	1.20	122	0.02	0.08	1.02
IMF	122	0.73	0.09	1.91	120	0.51[b]	0.12	1.42	122	0.12	0.17	1.05

[a] SNV 400-1850 nm, [b] SNV 780-1850 nm

When performing PLSR it was discovered that some samples could be considered as outliers. For EZ-DripLoss, one sample was poorly described by all spectroscopic methods, giving strong reason to believe that something went wrong when conducting the reference measurement. This happened for one of the sample batches for VD; therefore, the entire batch (19 samples) was left out when conducting both PLSR and correlation analyses between reference measurements. Manual inspection of NIR spectra revealed two severely deviating spectra, and these were consequently left out of all NIR PLSR models. It is also worth noting that the model performance improved much by removing a few samples with high residual sample calibration variance for reference measurements (Y-variance, results not shown), without changing the important variables in models, suggesting that some of the reference measurements or spectra might have been incompatible.

3.2.1 Raman spectroscopy

It is useful to identify which spectral regions are important for establishing the relationship between spectroscopy and reference measurements for elucidating the qualitative association to known changes in post-mortem meat. To evaluate which spectroscopic regions are important for the models, the weighted regression coefficients for the best models for each reference analysis were evaluated. The five most important regions for the PLSR models from Raman spectroscopy are summarized in **table 4**. The changes in spectra related to reference measurements of pH and drip loss can in general be categorized in two groups, one being related to post-mortem metabolism and the other being changes in protein secondary structure (**Fig. 2**).

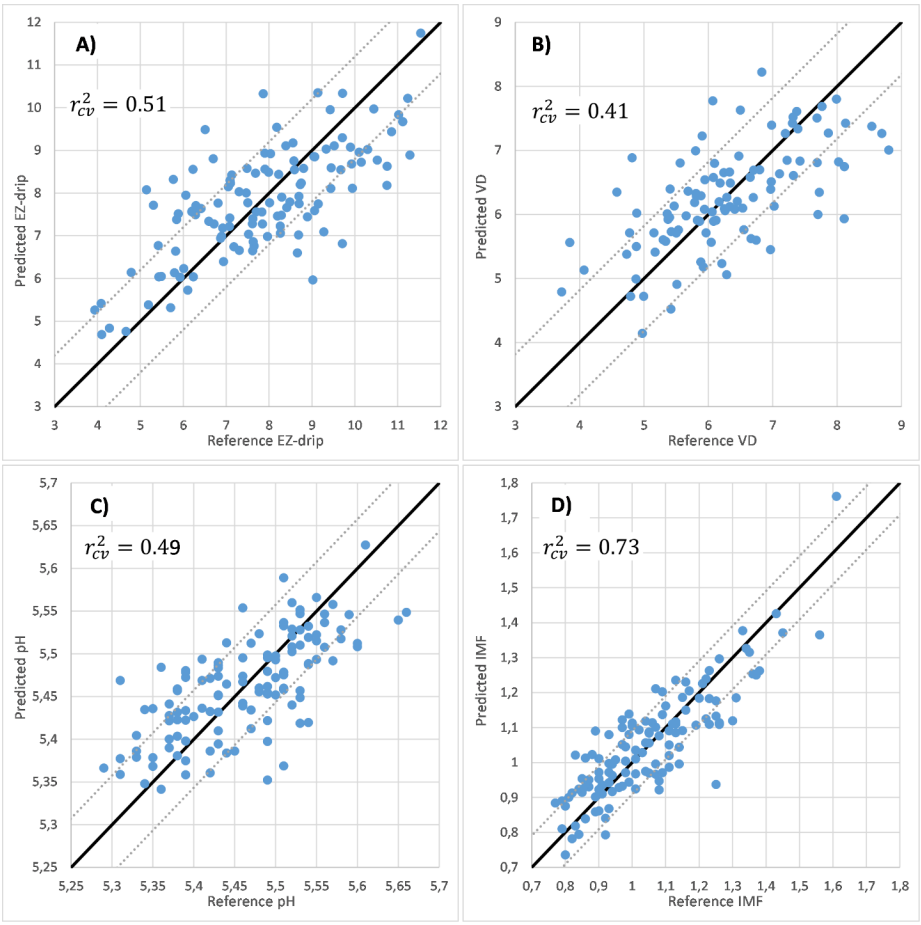

Figure 1. Predicted versus reference measurement plots showing results of PLSR from Raman spectroscopy, where target line is shown as a solid line and RMSECV for each model as dotted lines. A) EZ-DripLoss in %, B) Vacuum drip loss in %, C) pH and D) IMF in %.

Table 4. The most important wavenumber regions (in cm^{-1}) from PLSR of Raman spectroscopy and reference analyses, where sign of the coefficient is given in parenthesis. Regions are listed according to their importance in the model for each reference measurement.

Region	pH_u	EZ (%)	VD (%)	IMF
I	~973 (+)	~977 (−)	~978 (−)	~1635 (+)
II	~1635 (+)	~884 (+)	~1237 (+)	~1662 (−)
III	~1685 (−)	~1674 (+)	~1269 (−)	~1260 (−)
IV	~1269 (+)	~942 (−)	~1611 (+)	~1438 (+)
V	~1045 (−)	~1270 (−)	~1630 (+)	~802 (+)

For pH, the important regions related to metabolism are at 973 cm^{-1} and 1045 cm^{-1}, which have been assigned to the PO_3^{2-} stretching vibration of the phosphate moiety (Rimai, Cole, Parsons, Hickmott, & Carew, 1969) and creatine (Cr) or lactate in meat (Scheier, Kohler, & Schmidt, 2014), respectively. The phosphate signal at approx. 980 cm^{-1} is stronger under more basic conditions (Scheier & Schmidt, 2013), likely contributing to the positive correlation in the model. As concentration of lactate increases post-mortem, pH decreases, thus giving a negative correlation for the peak at 1045 cm^{-1}. For the EZ-DripLoss and VD models, the region at 977 cm^{-1} has an opposite sign compared to the pH model, most likely caused by the inverse relationship between pH and drip loss. The EZ-DripLoss model introduces contributions from another metabolism related molecule in the region at 884 cm^{-1}, attributed to the acidic form of inorganic phosphate (Scheier, Kohler, et al., 2014).

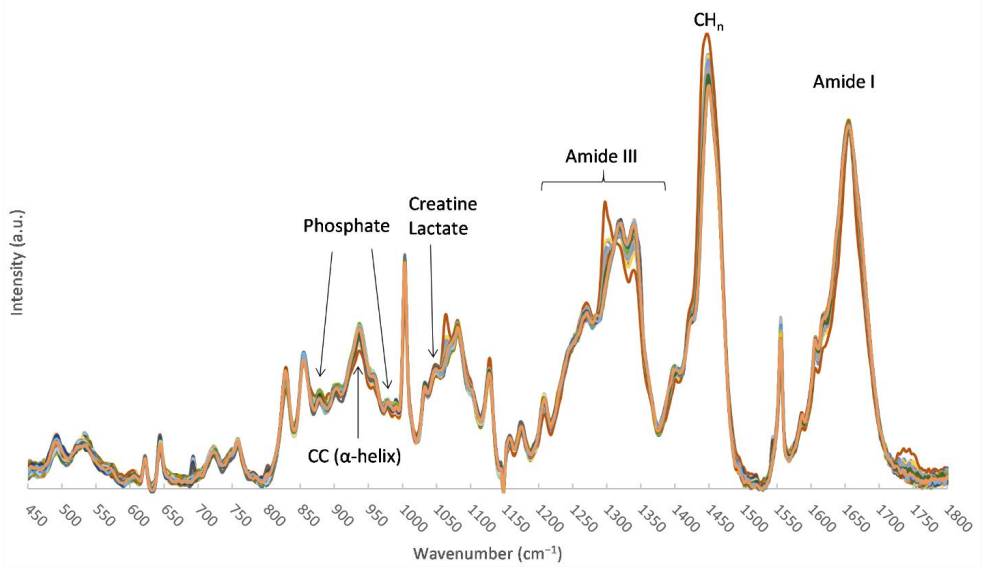

Figure 2. Pre-processed Raman spectra from all 122 samples, where some of the important regions for PLSR models are assigned.

Important regions related to protein secondary structure changes are in the amide I and amide III regions, where the bands at 1635 cm^{-1}, 1269 cm^{-1} and 942 cm^{-1} are assigned to α-helical structures and the bands at 1685 cm^{-1} and 1237 cm^{-1} are assigned to β-sheet structures (Krimm & Bandekar, 1986; Tu, 1986). Intensity of regions related to α-helical structures increases with increasing pH, while intensity of regions related to β-sheet structures decreases at high pH. As noted for metabolites, the relationship in the models is opposite for drip loss measurements. These changes might be caused because of the increased denaturation of proteins when pH declines rapidly post-

mortem (Joo, Kauffman, Kim, & Park, 1999), and similar changes to protein secondary structure have been shown to be a direct consequence of changes in pH (Andersen et al., 2017).

The important regions for the IMF model were all in close proximity to some of the characteristic peaks from pork adipose tissue, most prominent at 1296 cm^{-1}, 1438 cm^{-1} and 1655 cm^{-1} (Beattie, Bell, Borgaard, Fearon, & Moss, 2006), but some of the regions were also close to protein secondary structure regions (e.g. amide I). As IMF content was relatively low in the analyzed samples, and the characteristic fat peaks (at e.g. 1296 cm^{-1} and 1438 cm^{-1}) were only clearly visible in a few of the samples, it is plausible that the model relies on collinear regions from other molecular structures or the high correlation between fat and protein concentration in meat (Isaksson, Nilsen, Togersen, Hammond, & Hildrum, 1996). For improving the model for IMF predictions, effort should be put forth to make a model where samples with more variation in IMF are included.

The overlap of vibrations from fat and proteins highlights one of the difficulties when developing models for meat quality assessments, namely that it is difficult to distinguish the influence of one meat component from another. One of the traditionally limiting factors for Raman spectroscopy is the small sample area analyzed, which was improved in the current study by using a probe with a laser spot diameter of 6 mm. Conversely, the increased spot size comes at the cost of including strong scattering from IMF. Future studies are needed to investigate the impact of scattering from fat on the validity of models for other quality parameters from Raman spectroscopy concerning meat quality, as fat purposely have been avoided by others (Scheier, Bauer, et al., 2014; Scheier et al., 2015).

PLSR models developed in the current study performed on a comparable level to those developed by Scheier, Bauer, et al. (2014) and Scheier et al. (2015) for pH and drip loss predictions. Our results emphasize many of the same spectral regions as the two cited studies, thus strengthening the evidence for the importance of regions related to metabolites and protein secondary structure for predicting pH and drip loss. One important difference in the current study compared with the work of Scheier et al. (2014; 2015) is the time of measurement, where theirs were done on pre-rigor muscle at 30-120 min post-mortem, the analysis in the current study was performed on post-rigor muscle at 4-5 days post-mortem, making it harder to directly compare the results. Regarding estimation of IMF, results from the current study showed vastly improved model performance compared to a study on lamb (Fowler et al., 2015). This is most likely caused by the larger laser diameter in the current study (approx. 120 times increase in diameter), thus capturing a larger sample area.

3.2.2 NIR spectroscopy

Inspection of important regions of models from NIR spectroscopy is only meaningful for pH and IMF models, as the regression coefficients for drip loss did not reveal large enough stable regions and were rather noisy. The most important regions for the pH model were mainly in the visible part of the spectra, from 400 nm to 780 nm, likely caused by the correlation between color and pH (Joo et al., 1999), in addition to a stretch at 1410 nm to 1435 nm and a stretch from 1750 nm to 1850 nm. The stretch from 1410 nm to 1435 nm is attributed to water and it may be related to the strength of hydrogen bonds or the amount of water in the analyzed area (Segtnan, Sasic, Isaksson, & Ozaki, 2001). The longer stretch from 1750 nm to 1850 nm can be attributed to a mix of CH and OH vibrations (Li-Chan, Ismail, Sedman, & van de Voort, 2002). For the IMF model two regions were important, one from 1690 nm to 1708 nm, and a second from 1720 nm to 1735 nm, assigned to protein and fat, respectively (Williams & Norris, 2001). The model β-coefficients were positive for fat and negative for protein, once again emphasizing the inverse correlation between these parameters. This shows that some regions seem to have chemical information relevant for interpretation (e.g. 1720 nm to 1735 nm for IMF), while some important regions seem to rely on empirical correlations (e.g. 1750 nm to 1850 nm for pH).

The NIR models did not perform well compared to previous studies on fresh pork (Kapper et al., 2012; Liao et al., 2010; Prevolnik et al., 2005). A number of factors may have caused this discrepancy in the current study compared with others, including number of samples, relative time of measurements, total variation in the reference measurements and so forth. The reason for worse performing PLSR models than Raman spectroscopy might be that NIR spectroscopy exhibits relatively poor sensitivity and selectivity (Blanco & Villarroya, 2002).

3.2.3 Fluorescence spectroscopy

Fluorescence spectroscopy models did not perform particularly well for any of the reference measurements (**Table 3**). One of the reasons for this might be that samples were excited only at 292 nm, which may not be enough to capture the complexity of intact meat. It has been shown that excitations at longer wavelengths are optimal for fat and connective tissue, at 322 nm and 380 nm, respectively (Skjervold et al., 2003). The reason for choosing the wavelength used in the current experiment was that previous model system experiments have indicated a connection between a shift in the emission spectra from this excitation and changes in pH (Andersen et al., 2017), and it captures the emission from the most fluorescent amino acid, tryptophan, in proteins (J. Christensen, Norgaard, Bro, & Engelsen, 2006).

4. CONCLUSION

The current study reinforces the perception that Raman spectroscopy is a promising technique for analysis of pork quality. PLSR models for pH and drip loss relied largely on muscle metabolic state and protein structure, while the IMF model relied on characteristic regions for adipose tissue. The information provided in the Raman spectra seems to be appropriate to analyze complex biological systems, like that of meat, and may be applicable for other muscles and species because of the universal nature of post-mortem metabolism. NIR performed poorly in the current study, but has shown good ability to analyze meat quality in earlier studies, thus further research is still justified. Fluorescence spectroscopy did not show much promise for meat quality assessment, believed in part to be explained by only exciting the samples at one wavelength, thus, fluorescence spectroscopy cannot be ruled out as a possible future technique.

Before addressing the need for development of instruments applicable for testing in abattoir conditions, an effort should be put forth to improve upon the current experiment by for example analyzing the same sample with spectroscopy and the reference method and minimizing the delay between spectroscopic analysis and reference analysis. There is also a need to evaluate the optimal time of analysis post-mortem for a given parameter, both for improvement of models and for possible utilization of the results, which in a large part depends on the workflow in the abattoir. In conclusion, our results encourage further research focusing on the possible applications of Raman spectroscopy to assess meat quality.

Acknowledgements

We thank Bjørg Narum, Karen Wahlstrøm Sanden, Lene Øverby and Vibeke Høst for technical assistance during sampling and with the analyses. Prof. Tormod Næs for assistance in experimental design and data analysis and Dr. Kristian Liland for assistance in pre-processing of spectroscopic data. This work was supported by the Foundation for Research Levy on Agricultural products and the Agricultural Agreement Research Fund of Norway.

6. REFERENCES

Andersen, P. V., Veiseth-Kent, E., & Wold, J. P. (2017). Analyzing pH-induced changes in a myofibril model system with vibrational and fluorescence spectroscopy. *Meat Sci, 125*, 1-9.

Barnes, R. J., Dhanoa, M. S., & Lister, S. J. (1989). Standard Normal Variate Transformation and De-Trending of near-Infrared Diffuse Reflectance Spectra. *Applied Spectroscopy, 43*(5), 772-777.

Beattie, J. R., Bell, S. E. J., Borgaard, C., Fearon, A., & Moss, B. W. (2006). Prediction of adipose tissue composition using Raman spectroscopy: Average properties and individual fatty acids. *Lipids, 41*(3), 287-294.

Blanco, M., & Villarroya, I. (2002). NIR spectroscopy: a rapid-response analytical tool. *Trac-Trends in Analytical Chemistry, 21*(4), 240-250.

Brondum, J., Munck, L., Henckel, P., Karlsson, A., Tornberg, E., & Engelsen, S. B. (2000). Prediction of water-holding capacity and composition of porcine meat by comparative spectroscopy. *Meat Sci, 55*(2), 177-185.

Christensen, J., Norgaard, L., Bro, R., & Engelsen, S. B. (2006). Multivariate autofluorescence of intact food systems. *Chem Rev, 106*(6), 1979-1994.

Christensen, L. B. (2003). Drip loss sampling in porcine m. longissimus dorsi. *Meat Sci, 63*(4), 469-477.

Florowski, T., Florowska, A., Chmiel, M., Adamczak, L., Pietrzak, D., & Ruchlicka, M. (2017). The effect of pale, soft and exudative meat on the quality of canned pork in gravy. *Meat Science, 123*, 29-34.

Fowler, S. M., Ponnampalam, E. N., Schmidt, H., Wynn, P., & Hopkins, D. L. (2015). Prediction of intramuscular fat content and major fatty acid groups of lamb M. longissimus lumborum using Raman spectroscopy. *Meat Science, 110*, 70-75.

Gardner, M. A., Huff Lonergan, E., & Lonergan, S. M. (2005). *Prediction of fresh pork quality using indicators of protein degradation and calpain activation*. Paper presented at the 51st International Congress of Meat Science and Technology, Baltimaore, Maryland USA.

Gjerlaug-Enger, E., Aass, L., Odegard, J., & Vangen, O. (2010). Genetic parameters of meat quality traits in two pig breeds measured by rapid methods. *Animal, 4*(11), 1832-1843.

Honikel, K. O. (1998). Reference methods for the assessment of physical characteristics of meat. *Meat Sci, 49*(4), 447-457.

Huff-Lonergan, E., & Lonergan, S. M. (2005). Mechanisms of water-holding capacity of meat: The role of postmortem biochemical and structural changes. *Meat Sci, 71*(1), 194-204.

Hughes, J. M., Oiseth, S. K., Purslow, P. P., & Warner, R. D. (2014). A structural approach to understanding the interactions between colour, water-holding capacity and tenderness. *Meat Science, 98*(3), 520-532.

Isaksson, T., Nilsen, B. N., Togersen, G., Hammond, R. P., & Hildrum, K. I. (1996). On-line, proximate analysis of ground beef directly at a meat grinder outlet. *Meat Science, 43*(3-4), 245-253.

Joo, S. T., Kauffman, R. G., Kim, B. C., & Park, G. B. (1999). The relationship of sarcoplasmic and myofibrillar protein solubility to colour and water-holding capacity in porcine longissimus muscle. *Meat Sci, 52*(3), 291-297.

Kapper, C., Klont, R. E., Verdonk, J. M. A. J., Williams, P. C., & Urlings, H. A. P. (2012). Prediction of pork quality with near infrared spectroscopy (NIRS) 2. Feasibility and robustness of NIRS measurements under production plant conditions. *Meat Science, 91*(3), 300-305.

Krimm, S., & Bandekar, J. (1986). VIBRATIONAL SPECTROSCOPY AND CONFORMATION OF PEPTIDES, POLYPEPTIDES, AND PROTEINS. [Review]. *Advances in Protein Chemistry, 38*, 181-364.

Kristensen, L., & Purslow, P. P. (2001). The effect of ageing on the water-holding capacity of pork: role of cytoskeletal proteins. *Meat Science, 58*(1), 17-23.

Lawrie, R. A. (1985). CHAPTER 10 - THE EATING QUALITY OF MEAT *Meat Science (Fourth Edition)* (pp. 169-207): Pergamon.

Li-Chan, E. C. Y., Ismail, A. A., Sedman, J., & van de Voort, F. R. (2002). Vibrational Spectroscopy of Food and Food Products *Handbook of Vibrational Spectroscopy*: John Wiley & Sons, Ltd.

Liao, Y. T., Fan, Y. X., & Cheng, F. (2010). On-line prediction of fresh pork quality using visible/near-infrared reflectance spectroscopy. *Meat Science, 86*(4), 901-907.

Lieber, C. A., & Mahadevan-Jansen, A. (2003). Automated method for subtraction of fluorescence from biological Raman spectra. *Applied Spectroscopy, 57*(11), 1363-1367.

Liland, K. H., Kohler, A., & Afseth, N. K. (2016). Model-based pre-processing in Raman spectroscopy of biological samples. *Journal of Raman Spectroscopy, 47*(6), 643-650.

Martens, H., & Martens, M. (2000). Modified Jack-knife estimation of parameter uncertainty in bilinear modelling by partial least squares regression (PLSR). *Food Quality and Preference, 11*(1-2), 5-16.

Martens, H., & Martens, M. (2001). *Introduction to multivariate data analysis for understanding quality*. Chichester, U.K.: John Wiley & Sons Ltd.

Otto, G., Roehe, R., Looft, H., Thoelking, L., & Kalm, E. (2004). Comparison of different methods for determination of drip loss and their relationships to meat quality and carcass characteristics in pigs. *Meat Sci, 68*(3), 401-409.

Prevolnik, M., Candek-Potokar, M., Skorjanc, D., Velikonja-Bolta, S., Skrlep, M., Znidarsic, T., & Babnik, D. (2005). Predicting intramuscular fat content in pork and beef by near infrared spectroscopy. *Journal of near Infrared Spectroscopy, 13*(2), 77-85.

Prieto, N., Pawluczyk, O., Dugan, M. E. R., & Aalhus, J. L. (2017). A Review of the Principles and Applications of Near-Infrared Spectroscopy to Characterize Meat, Fat, and Meat Products. *Applied Spectroscopy, 71*(7), 1403-1426.

Prieto, N., Roehe, R., Lavin, P., Batten, G., & Andres, S. (2009). Application of near infrared reflectance spectroscopy to predict meat and meat products quality: A review. *Meat Science, 83*(2), 175-186.

Rasmussen, A. J., & Andersson, M. (1996, 1-6 September). *New method for determination of drip loss in pork muscles.* Paper presented at the In Proceedings 42nd international congress of meat science and technology, Lillehammer, Norway.

Rimai, L., Cole, T., Parsons, J. L., Hickmott, J. T., & Carew, E. B. (1969). Studies of Raman Spectra of Water Solutions of Adenosine Tri- Di- and Monophosphate and Some Related Compounds. *Biophysical Journal, 9*(3), 320-&.

Scheier, R., Bauer, A., & Schmidt, H. (2014). Early Postmortem Prediction of Meat Quality Traits of Porcine Semimembranosus Muscles Using a Portable Raman System. *Food and Bioprocess Technology, 7*(9), 2732-2741.

Scheier, R., Kohler, J., & Schmidt, H. (2014). Identification of the early postmortem metabolic state of porcine M. semimembranosus using Raman spectroscopy. *Vibrational Spectroscopy, 70*, 12-17.

Scheier, R., Scheeder, M., & Schmidt, H. (2015). Prediction of pork quality at the slaughter line using a portable Raman device. *Meat Sci, 103*, 96-103.

Scheier, R., & Schmidt, H. (2013). Measurement of the pH value in pork meat early postmortem by Raman spectroscopy. *Applied Physics B-Lasers and Optics, 111*(2), 289-297.

Schmidt, H., Sowoidnich, K., & Kronfeldt, H. D. (2010). A Prototype Hand-Held Raman Sensor for the in Situ Characterization of Meat Quality. *Applied Spectroscopy, 64*(8), 888-894.

Segtnan, V. H., Sasic, S., Isaksson, T., & Ozaki, Y. (2001). Studies on the structure of water using two-dimensional near-infrared correlation spectroscopy and principal component analysis. *Analytical Chemistry, 73*(13), 3153-3161.

Skjervold, P. O., Taylor, R. G., Wold, J. P., Berge, P., Abouelkaram, S., Culioli, J., & Dufour, E. (2003). Development of intrinsic fluorescent multispectral imagery specific for fat, connective tissue, and myofibers in meat. *Journal of Food Science, 68*(4), 1161-1168.

Torley, P. J., D'Arcy, B. R., & Trout, G. R. (2000). The effect of ionic strength, polyphosphates type, pH, cooking temperature and preblending on the functional properties of normal and pale, soft, exudative (PSE) pork. *Meat Science, 55*(4), 451-462.

Tu, A. T. (1986). *Spectroscopy of Biological Systems*: Wiley.

Warriss, P. D., & Brown, S. N. (1987). The relationships between initial pH, reflectance and exudation in pig muscle. *Meat Sci, 20*(1), 65-74.

Weeranantanaphan, J., Downey, G., Allen, P., & Sun, D. W. (2011). A review of near infrared spectroscopy in muscle food analysis: 2005-2010. *Journal of near Infrared Spectroscopy, 19*(2), 61-104.

Williams, P. (2014). The RPD Statistic: A Tutorial Note. *NIR news, 25*(1), 22-26.

Williams, P., & Norris, K. H. (2001). *Near-infrared Technology: In the Agricultural and Food Industries*: American Association of Cereal Chemists.

ISBN: 978-82-575-1493-8
ISSN: 1894-6402

Norwegian University
of Life Sciences

Postboks 5003
NO-1432 Ås, Norway
+47 67 23 00 00
www.nmbu.no